1127-11

JUL 20 1960

BROWN BOVERI REVIEW

140
RECEIVED
JUL 14 1960
INSTITUTE OF THE
AERONAUTICAL SCIENCES

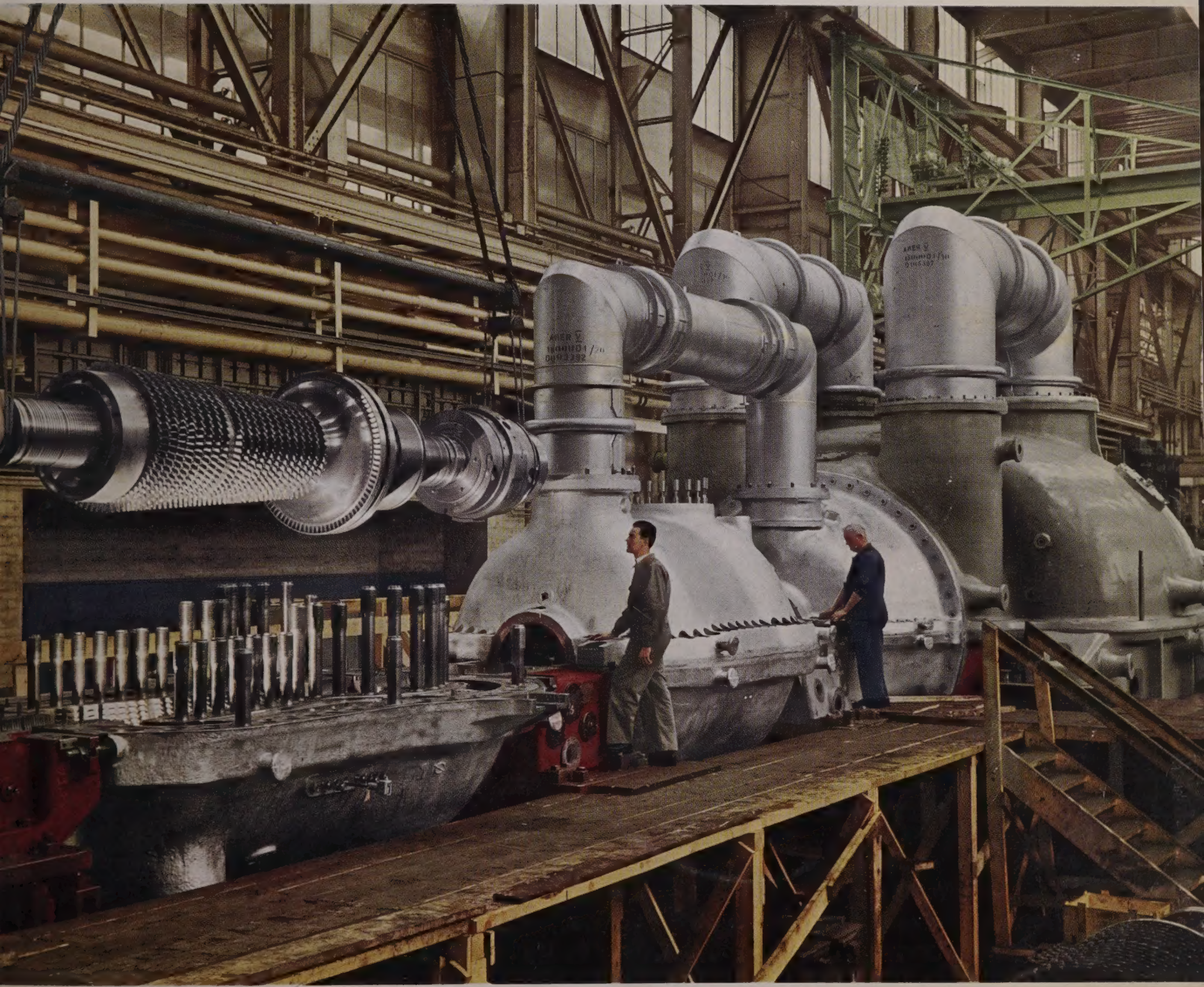

The largest steam turbine so far built by Brown Boveri, with an output of 175 MW at a speed of 3000 rev/min, for the Amer power station of the Provinciale Noordbrabantsche Electriciteits Maatschappij, Geertruidenberg, Holland. The machine is seen on the factory test-bed, with the h.p cylinder open to receive the associated part of the rotor and the inner part of the thrust bearing.

N BOVERI REV. VOL. 47 No. 1/2 p. 1–116 BADEN, JANUARY/FEBRUARY 1960

Printed in Switzerland

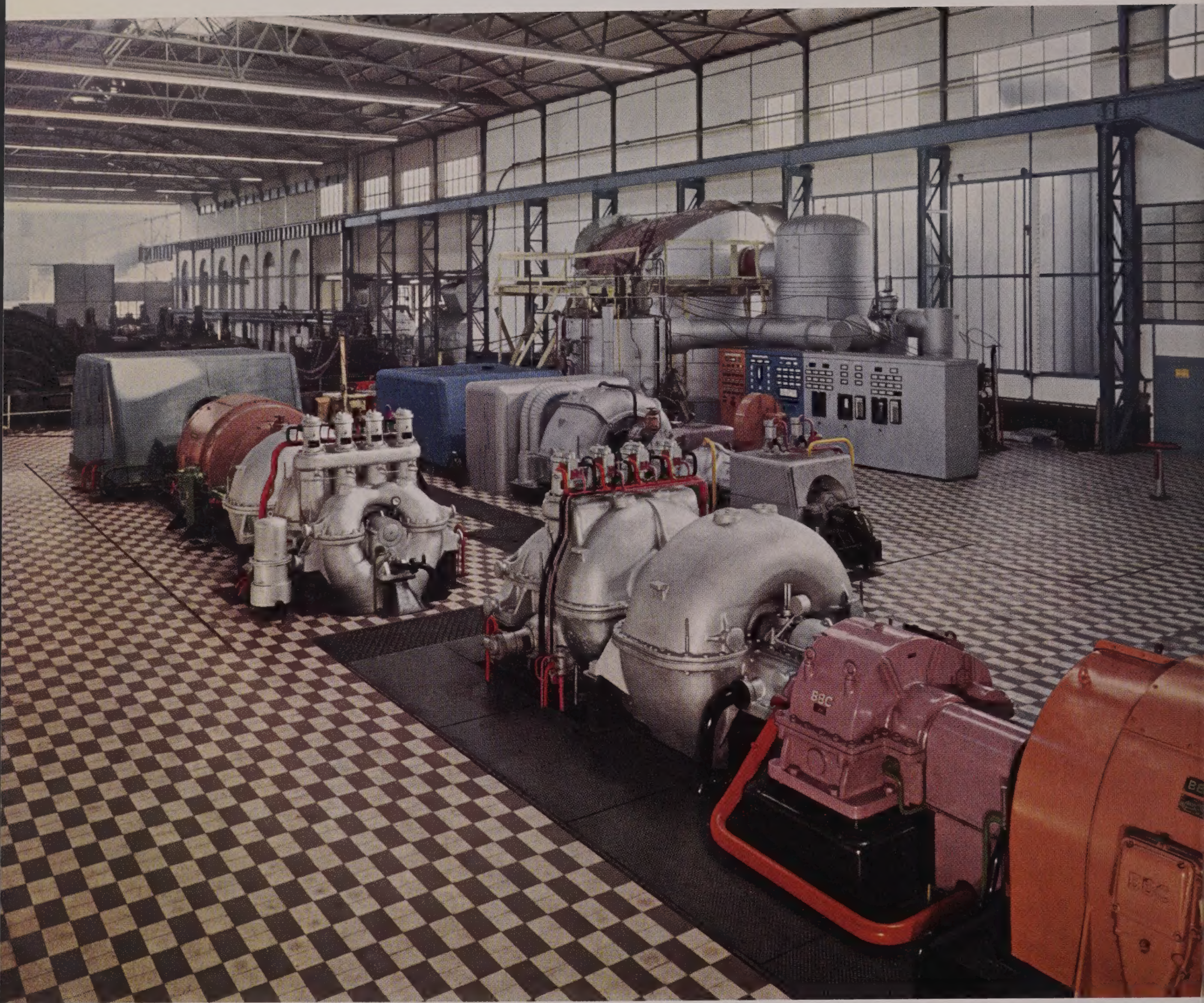

Gas-turbine set rated 5820 kW at the steelworks of Niederrheinische Hütte AG., Duisburg, Germany. In the foreground is a motor-driven blast blower, to the left of which is the low-pressure gas turbine with generator and blast blower and, to the right of that, the high-pressure line comprising the gas turbine, air compressor, gear, starting motor and compressor for the blast-furnace gas used as fuel. In the background is the combustion chamber and gas inlet pipe, air and gas pre-heaters, with the switchboard standing in front. The latter is in three parts: one for the thermal machines, one for the electrical system and the third for the auxiliaries and blast blower.

THE BROWN BOVERI REVIEW

ISSUED BY BROWN, BOVERI & COMPANY, LIMITED, BADEN (SWITZERLAND)

VOL. 47 JANUARY/FEBRUARY 1960 No. 1/2

The Brown Boveri Review appears monthly — Reproduction of articles or illustrations is permitted subject to full acknowledgement

CONTENTS:

	Page
C. SEIPPEL and G. OPLATKA: Criteria Governing the Economical Design of Thermal Generating Plants	3
P. HUMMEL and R. NOSER: Large Turbosets for the United States	6
A. OBERLE: Full-Load Throw-Off Tests with a Reheat Turbine	17
F. WEEHUIZEN: The Control of a Reheat Turbine with a Bypass	19
E. KOHLMANN: The Cooling-Water Supply for the Daragaç Power Station in Turkey	28
H. PFENNINGER: Brown Boveri Gas Turbines for an Inlet Temperature of 750 °C	35
W. P. AUER: Manama Gas-Turbine Power Station, Bahrain	65
R. SCHMIED: The World's Largest Gas-Turbine Power Station—Port Mann in Canada	67
G. GYSSLER: Investigations into the Exhaust Process of Pressure-Charged Two-Stroke Diesel Engines	73
R. SCHULTEN and E. JANTSCH: The Brown Boveri-Krupp High-Temperature Gas-Cooled Reactor	88
E. JANTSCH: The Trawsfynydd Nuclear Power Station from the Technical Point of View	97
E. JANTSCH: Thermal Problems of Atomic Power Stations (IV)	106
Publications by Brown Boveri Authors in Other Journals	112

CRITERIA GOVERNING THE ECONOMICAL DESIGN OF THERMAL GENERATING PLANTS

62.001.2.003

THIS ISSUE of the Review contains a number of articles dealing with thermal machines used in the generation of power. In arranging the various subjects, greater stress has been laid on topicality than on following a definite plan. This introduction deals with a subject common to all parts of such installations, one which brings them to a common denominator, so to speak: namely, the economic efficiency.

When an undertaking wishes to build a plant to generate a certain amount of energy and invites various manufacturers to tender, the price is naturally not considered alone, but also the quality and, above all, the efficiency of the equipment offered. But customers differ widely in their approach to this matter. One compares the annual cost of capital outlay and operation, based on a utilization programme, another may study the yield of the capital invested, while yet a third, working to certain principles, capitalizes the advantages which a better machine has to offer and corrects the prices offered accordingly.

The machine manufacturer, however, must know what economic stipulations the customer is going to make, in order to provide a truly economical plant. It is therefore necessary to resolve to a uniform basis these different outlooks which, though quite correct in themselves, are not always exactly equivalent. Naturally it would considerably ease matters if a large number of customers were to adopt the same approach. Mutual understanding would be reached more rapidly and misapprehensions avoided. A very important gain, however, for manufacturer and purchaser alike, would be that all parts of a plant would be designed to a uniform economic criterion which, as will be explained, is essential if optimum performance is to be achieved by the plant as a whole.

In the electrical trade it is standard practice to capitalize the losses in machines, the losses being reckoned as a sum of money per kilowatt added to the price of the machine. When dealing with steam turbines, on the other hand, it is more usual to state the sum of money a purchaser is prepared to offset against a difference of 1 kcal/kWh in the heat consumption of two tenders. Here it should be pointed out that this amount is proportional to the output of the machine, all other conditions being equal. Suppose a station has a 125-MW machine and a 250-MW machine, the evaluation in "Francs per kcal" is in the ratio 1:2. This figure is therefore not suitable for the necessary coordination of all parts of the installation, in particular for the electrical equipment.

The following procedure is therefore recommended:

1. Differences in efficiency are capitalized with reference to the time of ordering, as in the two examples above.
2. A figure A (Fr./kW) is determined which defines the parity between additional investment and equivalent improvement in the plant.
3. The improvement in the plant is expressed by the increase in the power output ΔP_Q to the system, resulting from unchanged heat input Q.

If the thermal efficiency η or the specific heat consumption w at rated load P are given, the increase in output is calculated as follows:

$$\Delta P_Q = P \frac{\Delta \eta}{\eta}$$

or

$$\Delta P_Q = - P \frac{\Delta w}{w}$$

The symbol Δ is always assumed to refer to relatively small differences.

To determine the parity factor A it is necessary to study the annual income and expenditure of the plant. The cost of additional capital is

$$K_1 = c \Delta C$$

in which c represents the annual factor for capital service, as given by the rate of interest and the period allowed for amortization, as shown in Table I. ΔC is the difference in purchase price.

The evaluation of the improvement in thermal efficiency is immediately clear if the heat input is really equal for both alternatives. The differences in efficiency then appear as differences between the terminal outputs which—provided consumption is assured—brings the following yield:

$$K_2 = h p \Delta P_Q$$

where h is the annual utilization factor (energy actually generated, divided by the rated output) and p is the price obtained for additional kWh. (This may be the actual production cost or, depending on the circumstances, a lower marginal value at which the additional energy can be disposed of.) Parity exists when the terms K_1 and K_2 are equal and consequently:

$$A = \left(\frac{\Delta C}{\Delta P_Q} \right)_{K_1 = K_2} = \frac{h \cdot p}{c}$$

TABLE I

Annual redemption rate 100 c of a liability of 100 Fr. over a period of n years and at an interest rate of k %

$$\text{With } q = \left(1 + \frac{k}{100}\right), \; c = \frac{q^n (q-1)}{q^n - 1}$$

k	n							
	3	4	5	10	15	20	25	30
3	35·35	26·90	21·84	11·72	8·38	6·72	5·74	5·10
3½	35·69	27·23	22·15	12·02	8·68	7·04	6·07	5·44
4	36·03	27·55	22·46	12·33	8·99	7·36	6·40	5·78
4½	36·38	27·87	22·78	12·64	9·31	7·69	6·74	6·14
5	36·72	28·20	23·10	12·95	9·63	8·02	7·10	6·51
6	37·41	28·86	23·74	13·59	10·30	8·72	7·82	7·27
7	38·11	29·52	24·39	14·24	10·98	9·44	8·58	8·06
8	38·80	30·19	25·05	14·90	11·68	10·19	9·37	8·88

Conditions are quite different though when a definite invariable maximum output is stipulated. Then the difference in efficiency only makes itself felt in the cost of fuel. For the price per kWh in this case only the fraction representing fuel costs must be substituted.

From the above it will be seen that the decision whether one variant shall be preferred to another will largely depend on whether the attainable output remains the same or not. Therefore it is expedient to base the economic comparison on the following extended expression:

$$\Delta V = -\Delta C + a \Delta P_Q + b \Delta P \qquad (1)$$

where

ΔV = Difference in economic performance

$\Delta C = C_2 - C_1$ = Difference in purchase price

ΔP_Q = Difference in output, assuming equal fuel input, $\Delta P_Q = P \frac{\Delta \eta}{\eta}$

a = Capitalized value of saving on fuel corresponding to a gain of 1 kW; $a = \frac{hp_Q}{c}$

p_Q = Share of fuel costs in the cost of generating 1 kWh

ΔP = Total difference in output at the busbars

b = Price one is prepared to pay to increase the output by 1 kW, regardless of any change in efficiency

The differences denoted by Δ must be consistently alternative 2 subtracted from 1.

When $\Delta V = 0$ in equation (1), parity exists, i.e. both alternatives are equivalent. For $\Delta V > 0$ alternative 2 is more economical, for $\Delta V < 0$ alternative 1.

If there are more than two alternatives, all proposals must be compared in the light of equation (1), in order that the optimum may be selected.

When an improvement in efficiency is effected by a means which does not change the heat input—such as may be obtained with any improvement to the turbine or condenser, for instance, considering the steam-raising unit as invariable—the output capacity of the plant then increases by precisely $\Delta P = \Delta P_Q$, and $\Delta V = -\Delta C + (a+b)\Delta P_Q$, in which $(a+b)$ is the parity value of the output obtained, as introduced earlier.

Formula (1) affords the most scope as far as individual allowance for special economic circumstances is concerned. The user may desire to amortize the plant over a long period, e.g. 20 years, but he may prefer to amortize any additional investment for improving the efficiency over a shorter period, say 5 years. The valuation b of the output can be made zero if there is no point in increasing the output, or, in contrast, the full price per installed kW can be substituted. In some plants allowance must be made for the fact that the initial outlay for the equipment does not increase proportionally with the output. The marginal figure for an additional kW is therefore smaller than the mean cost of generation, e.g. only half if the price is proportional to the square-root of the output.

No matter what aspects the purchaser may take into consideration, the result ought always to be given to the manufacturer in the form of two numbers a and b, from which the latter knows exactly how to attain the optimum design. Table II gives some approximate values of a and b. This table was published in 1950[1] but with only a very brief explanation.

TABLE II

	S.Fr./kW		
	a	b	$a+b$
Large plant for base load	600	400	1000
Plant for base load, capital limited, fuel relatively cheap	250	250	500
Typical standby plant	100	150	250

Naturally a and b can be converted into the currency in which the business is conducted.[2]

In most cases equation (1) decides the choice of discrete graduated standard elements. If a continuous multiplicity is involved, such as the rate of flow of cooling water through a standardized condenser, or the diameter of a very large pipe welded from plate, for which there are no standards, equation (1) has to be converted into a differential equation

$$-\mathrm{d}C + a\cdot\mathrm{d}P_Q + b\cdot\mathrm{d}P = 0$$

which yields the optimum.

The optimum for the whole plant is attained when optimum conditions have been achieved for all elements with the aid of uniform parity factors a and b. Exceptions are naturally elements with utilization factor different to that of the main machine, such as standby pumps, blow-down pipes, and the like.

It is possible to go a stage further and take into account the anticipated structure of the loading of the machine, by weighting the various loads according to the frequency with which they occur. Moreover there is a simple method which may be recommended, based on the fact that the fuel consumption of a thermal plant can usually be represented by the sum of the no-load quota proportional to the load. For a machine running most of the time below its full rated load it is perfectly permissible to assess the saving in no-load losses with a higher parity factor (a_1) than the saving in losses dependent on the load (a_2). In the expression $a = \frac{h p_Q}{c}$, for example, h can be the actual time in service in the first case and the time at rated load in the second. In this connection it is worth mentioning the efforts which are being made to reduce the consumption of cooling-water pumps when the plant is lightly loaded.

---

[1] C. SEIPPEL: The Energy Economy of Steam Power Plants. Brown Boveri Rev. 1950, Vol. 37, No. 10, p. 342–56; see page 354.

[2] The objection has been raised that the parity values defined herein are not non-dimensional. For definite transactions this is quite negligible. But if large-scale studies were to be undertaken with their aid, the results of which would be required over a long period, it would be more expedient if they were made non-dimensional by substituting a price index per kWh for the currency unit. Moreover, a and b would have to be divided by a unit of time, e.g. the total operating time until fully amortized. In fact, the technically correct conception of an installation is largely dependent on this period and on the relationship between the market value of the machines and the market value of the energy.

This article concludes with an appeal to customers always to provide the designer with complete information regarding the economic assumptions which will be adopted when planning a thermal plant. How they do this is not vitally important. The designer will convert the information provided into the parity factors defined herein and, with their aid, will design the most economical plant possible.

(KME) C. SEIPPEL
G. OPLATKA

LARGE TURBOSETS FOR THE UNITED STATES

621.165:621.313.322 (73)

This article describes the two 230-MW single-shaft turbosets ordered by the City of Los Angeles and a 500-MW cross-compound unit for the Tennessee Valley Authority. In addition to giving the technical data, the article explains the design selected.

EARLY in March 1959 Brown Boveri received the order from the Department of Water and Power of the City of Los Angeles for two 230-MW steam turbosets to be installed in their new Haynes power station at Long Beach, California. This order for, at the time, the largest units ever ordered from the Brown Boveri concern, was only secured after a fierce battle with American and European competitors. Since it was not possible to claim any experience of operating machines of this size, the technical conception of the Brown Boveri offer was examined into the smallest detail. It is therefore most gratifying that, despite this added hazard, the advantages of the design submitted, though differing appreciably from most American arrangements, succeeded in convincing the customer. A deciding factor was that we were able to offer the most economical machine with a very good heat consumption. The advantages of our welded turbine rotors, an accident to which has never once led to complete destruction of the turbine, were duly appreciated in America. It was also established, to our great satisfaction, that all requirements relating to the control system, arising out of standard American practice, could be fulfilled with our flexible hydraulic control system, not only with ease, but with a number of additional advantages. The first set is due to come into operation in the summer of 1962.

During August 1959 a still more spectacular order was received. The Tennessee Valley Authority (TVA), the largest electricity undertaking in America, ordered a 500-MW turboset for an as yet unnamed station. Here, too, the same reasons which led to the previous order were responsible for the Brown Boveri offer being preferred in this case. This set is due to be commissioned in the summer of 1963.

The Turbosets for Los Angeles

Steam Turbines

The single-shaft (tandem-compound) turbosets are designed for a normal output of 200 MW and a maximum continuous rating of 230 MW at 3600 rev per min. The turbines are supplied with live steam at 2000 psig, 1000 °F, the steam being reheated to 1000 °F, with a back pressure of 1·5 in. Hg. As can

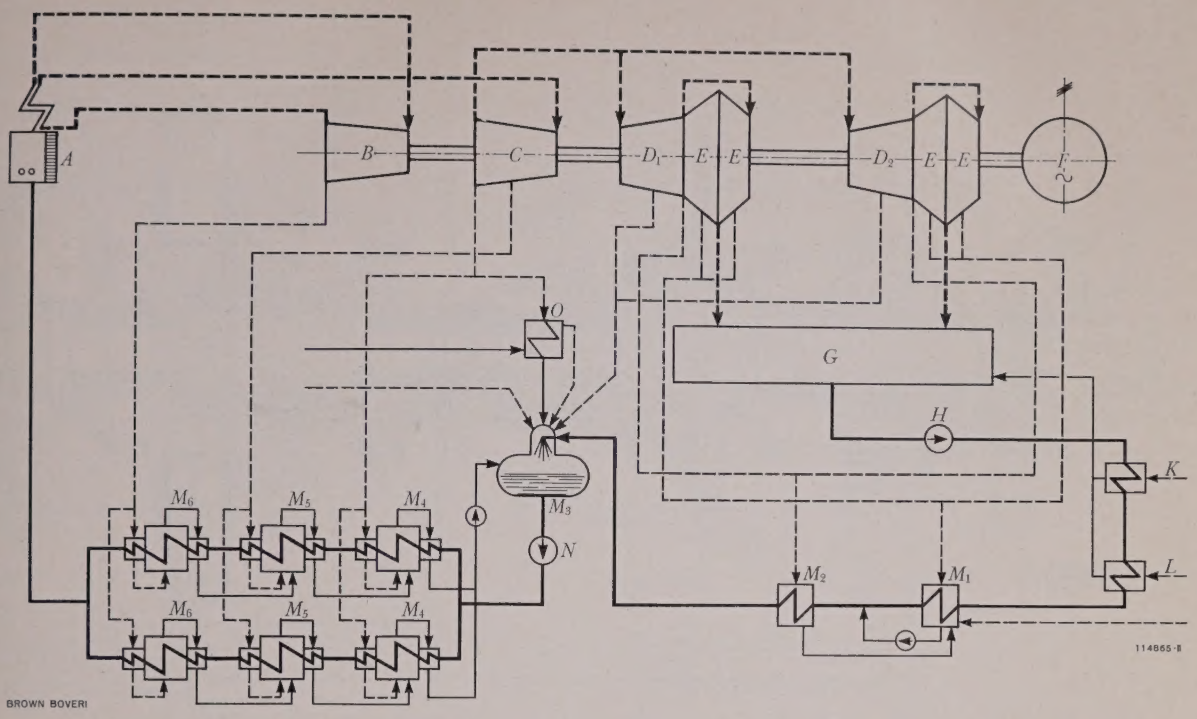

Fig. 1. – Thermal circuit diagram of the 230-MW turbosets for Los Angeles

A = Boiler
B = High-pressure cylinder
C = First intermediate-pressure cylinder
D_1, D_2 = Second i.p. sets of blading
E = Low-pressure blading
F = Generator
G = Condenser
H = Condensate pump
K = Gland-steam condenser
L = Condenser for steam from steam-jet air ejector
M_1–M_6 = Feedwater heaters
N = Feedwater pump
O = Evaporator for make-up water

be seen from the thermal circuit diagram (Fig. 1), six feed-heating stages are provided, in which the feedwater is heated to 475 °F at 230 MW. The third feed-heater is designed as a de-aerating mixing heater. The waste heat from the steam-jet air ejectors and the gland-steam condenser is recovered.

The turbine (Fig. 2) has four cylinders: a high-pressure (h.p.) cylinder exhausting into the reheater, an intermediate-pressure high-temperature cylinder (first i.p.) following the reheater, and two combined intermediate and low-pressure (i.p./l.p.) cylinders. From two valve chests, mounted on the left and right of the turbine and each containing an emergency stop valve and two regulating valves, the live steam flows to the h.p. cylinder through four pipes and enters the four sets of nozzles via inlet pipes sealed with piston rings.

A new feature of this design is the arrangement of the four sets of nozzles in a one-piece ring. Before inserting the rotor into the cylinder, this ring is placed in position over the rotor. Thus, at full load, the steam strikes practically the whole of the single row of regulating blading, thereby avoiding losses due to filling and emptying effects. It also improves the flow to the nozzles, thus considerably reducing friction losses.

The subsequent inner shell, which carries the stationary reaction blading, is split vertically in half. This prevents the pressure difference across the inner shell at the inlet end from becoming too great, because this would have necessitated unduly large flanges and bolts. All internal parts, such as the balancing pistons, nozzle ring and inner shell, are free to move on expansion inside the outer shell, a well-known Brown Boveri principle [1].[1] All elements, especially the labyrinths, piston rings, and

---

[1] The figures in brackets refer to the bibliography on p. 17.

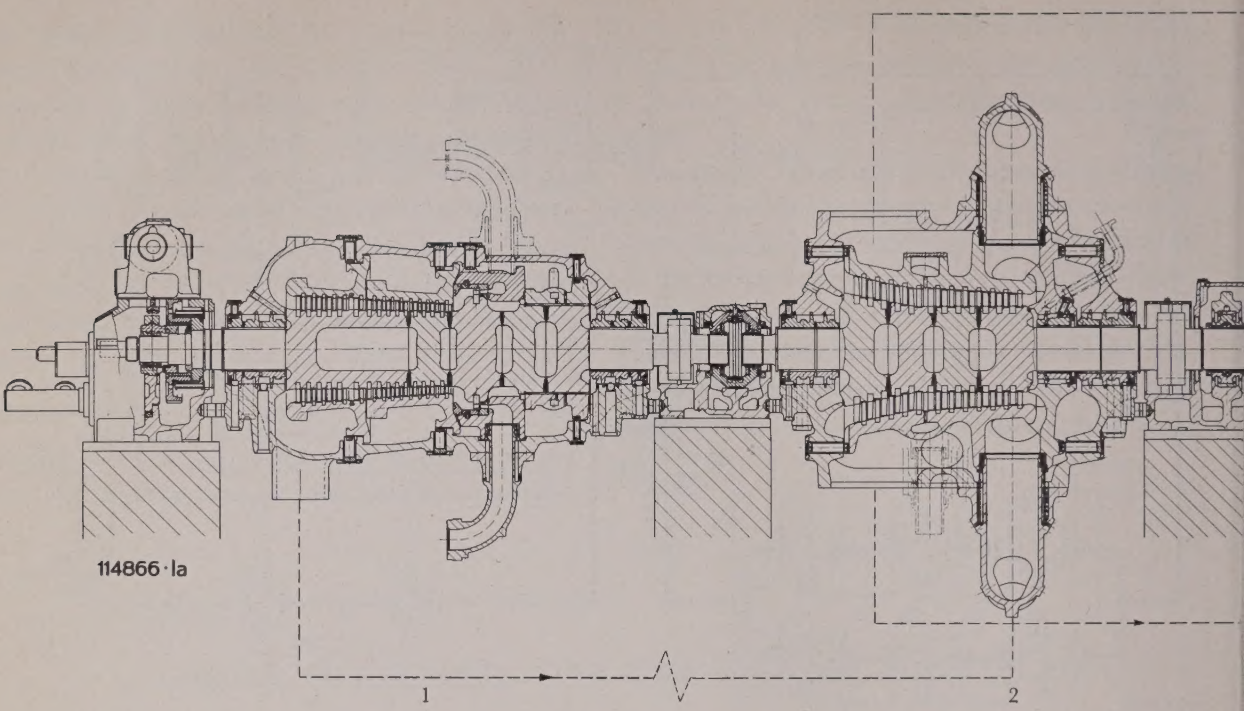

Fig. 2. – Sectional elevation of a 230-MW steam turbine for Los Angeles

Speed 3600 rev/min
Live steam at 2000 psig, 1000 °F
Reheat to 1000 °F
Vacuum 1·5 in. Hg

1 = High-pressure cylinder
2 = First i.p. cylinder
3, 4 = Combined i.p./h.p. cylinders

so on, have already been tested in service or by endurance tests. An exception is the nozzle ring which, although specially developed for this installation, will be a normal component of all turbines over 125 MW with single-stage impulse wheel.

In this respect the question arose whether the construction of such large turbines for a frequency of 60 c/s, instead of for the usual European figure of 50 c/s, would give rise to any special problems. For the h.p. and the first i.p. cylinders the increase in speed is definitely favourable. The heat drop per stage can be increased and the rotors accordingly shortened; since the power output and, in consequence, also the quantity of steam is very large, the blades are sufficiently long to permit the attainment of very high efficiencies. The increased centrifugal force resulting from the higher speed is compensated by appropriate reinforcement of the rotating parts, so that the same safety factors are attained as with turbines for 3000 rev/min. With the welded rotor design this is easily achieved by making the individual shaft sections thicker.

The effect of the higher speed on the l.p. cylinders is not so favourable. The annular area of the last row of blades determines the losses between them and the condenser and there is no point in accepting increased losses at higher speed. With the same blade dimensions, however, the centrifugal force increases as the square of the speed, so that much heavier blades and more robust means of fixing are required, which exert a marked influence on the manufacturing costs. The most favourable solution proved to be the division of the outlet area into four parallel flows. It has been clearly established that this method yields the lowest costs, an important factor again being the reduction in the length of the rotors due to the increased heat drop per stage. This discovery that, for a given outlet area, the division of the flow leads to a reduction in the manufacturing costs, is of a general nature. It is merely necessary to determine the most economical combination from one case to another, obviously taking into account the length of the machine. For instance, the present division would not have been economical for a 50-c/s turbine.

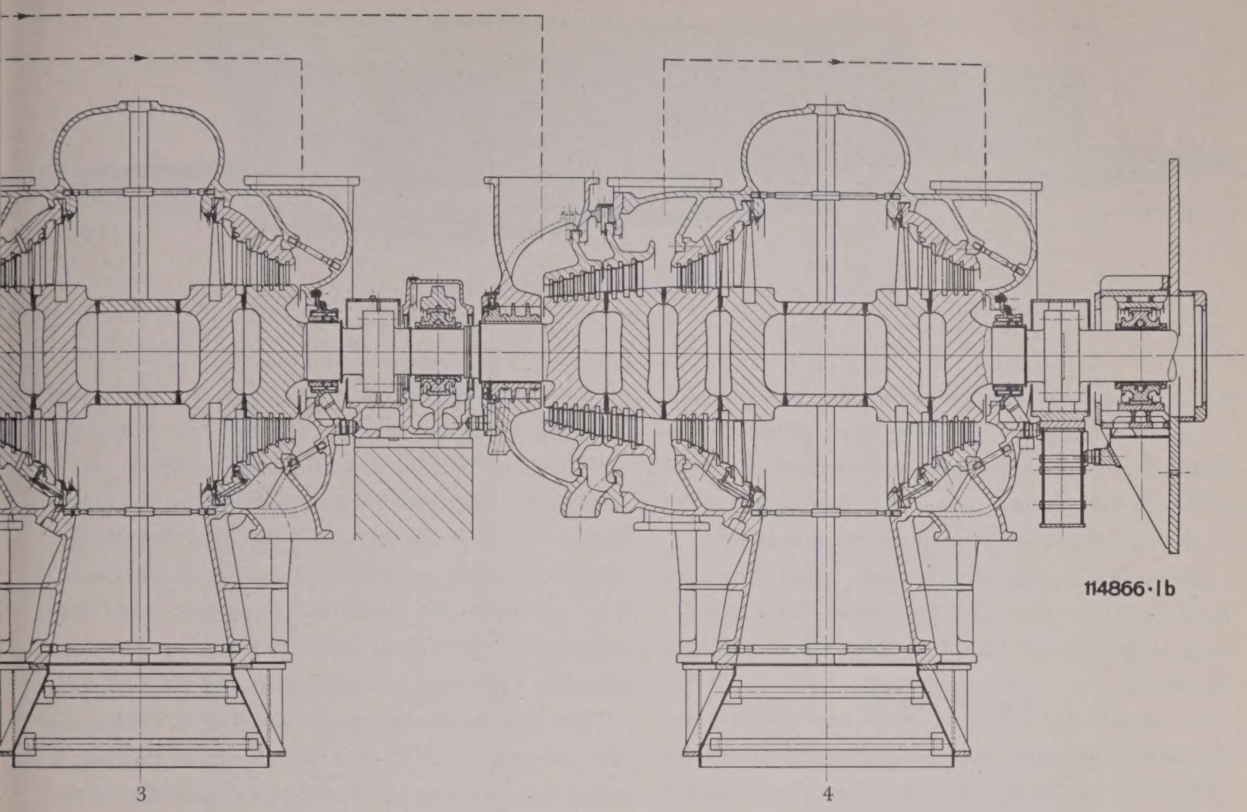

A further advantage is the relatively short length of the final rows of blades and the resultant reduction in their centrifugal force. The peripheral speed at the tips of short blades is also less, thereby reducing the risk of erosion by water. Admittedly this argument does not carry much weight with reheat turbines in which the wetness of the steam is very low.

Following reheat the steam flows through four parallel interceptor valves into the first i.p. cylinder. The chests are mounted in pairs to left and right of the machine, each containing an emergency stop valve and a regulating valve. A new feature is that not only the stop valves but also the interceptor valves can be fully closed for testing in service, and this is easily performed with the hydraulic control system fitted to the turbines. The reason for this requirement is that the turbines are intended for almost permanent full-load operation, during which the interceptor valves are seldom called upon to operate, therefore facilities for a functional test while the turbine is running are most desirable.

The first i.p. cylinder is of the normal double-shell design and does not contain anything which is fundamentally new. The steam is conveyed to the No. 1 and No. 2 i.p./l.p. cylinders through a pair of interconnecting pipes. In each cylinder the steam passes from the i.p. blading to a double-flow l.p. section.

With this arrangement there was no difficulty in overcoming the axial thrusts. As in all Brown Boveri reheat turbines the h.p. rotor is inherently balanced by means of the balancing piston. The first i.p. rotor counteracts the sum of the thrusts from the i.p. sections of the two i.p./l.p. rotors.

The No. 1 and No. 2 i.p./l.p. cylinders are firmly attached to the foundations through the base-plate. The thrust from the No. 1 i.p./l.p. cylinder is taken up axially by the first i.p. cylinder through intermediate pieces in contact with the cylinder claw supports and, on expansion pushes the thrust-bearing pedestal and the h.p. cylinder forwards (i.e. to the left in Fig. 2); all the other bearing pedestals are rigidly fixed to the foundations. Thus, as experience has proved, the smooth running of the turbine can be appreciably improved. Relieving the bearing pedestals of axial thrust is also a pronounced advantage.

For the individual components the tried, normal designs which have been previously described in various articles in the Brown Boveri Review are

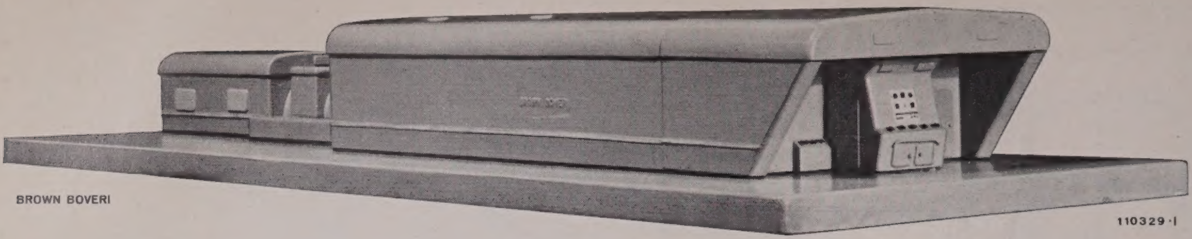

Fig. 3. – Model of a 230-MW outdoor turboset

employed in these turbines. Only the continuous barring gear exhibits one improvement on the former system, in that it can now be switched on while the turbine is still running and is therefore ideal for the remote-controlled power stations of the future.

All blades are of stainless steel; great care was also taken not to exceed the safety factor usually adopted for 3000-rev/min machines when designing the blading.

The steam conditions for these two turbines are quite normal, therefore the conventional, well-known materials could be used, and these were immediately accepted by the customer. Since the turbosets will stand in the open, their enclosure had to be designed accordingly. Fig. 3 shows the model of the complete turbine; the enclosure can be entered, providing access to all external parts of the turbine without having to be dismantled.

Generators

The generators are designed for the following data: Output 270 MVA at a hydrogen pressure of 45 psig, 18 kV, 8670 A, power factor 0·85, 3600 rev/min.

The copper of both rotor and stator windings is cooled direct. The rotor conductors are of drawn hollow section through which the cooling gas flows [2]. Fig. 4 shows the arrangement of a slot. To extend the cooling surface of the coil-ends of the rotor winding, they are made of shaped copper sections and are cooled by a separate powerful stream of gas. The body of the rotor itself conforms to standard Brown Boveri practice and is composed of separate sections pressed together by a central draw-bolt. In view of the considerable torque, the diameter of the coupling flange becomes quite large, in fact it is larger than the inside diameter of the end-bell disc. Since the latter is of a different material to the body of the rotor when this is forged in one piece, the coupling then has to be shrunk on. With the sectional method of construction, however, it is possible to insert the end-bell discs before the whole body is pressed together, and the coupling flanges can be forged in one piece with the shaft extensions. The end-bells are "floating", i.e. they are only attached to the body of the rotor and there is a considerable clearance between them and the shaft [3].

The copper of the stator winding is cooled by low-viscosity oil. Fig. 5 shows a section through a stator slot. Between the individual conductors of the Roebel bar are six hollow conductors, also transposed, through which the cooling oil flows [2, 4]. Special care was taken with the layout of the oil circuit in order to prevent contamination or silting. In the outer system the oil is always at a pressure in excess of atmospheric, thus preventing oxygen from entering. This is achieved by providing a cushion of inert gas at a slight excess pressure in the oil expansion vessel, where the oil pressure is lowest. Inside the generator the hydrogen pressure is everywhere higher than that in the oil system. Thus no oil can enter the generator frame in the event of a slight leakage.

The generator is excited by an exciter driven through gearing by the generator shaft. A magnetic amplifier regulator with a high-speed booster as output stage, inserted in series with the shunt field winding of the main exciter, controls the voltage of the generator. In accordance with American practice, a variable resistance in the same circuit is employed for setting the excitation by hand. In normal service this resistance is automatically adjusted so that the mean booster voltage is zero, permitting a change-over to manual control at any time without causing a surge.

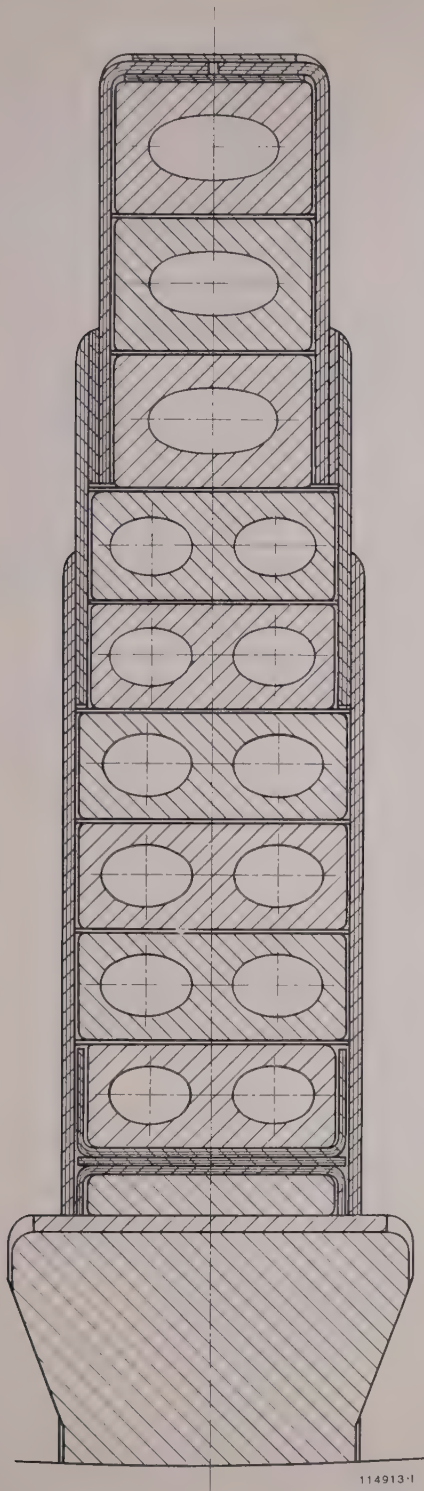

Fig. 4. – Section through a rotor slot of the generators for Los Angeles

Fig. 5. – Section through a stator slot of the generators for Los Angeles

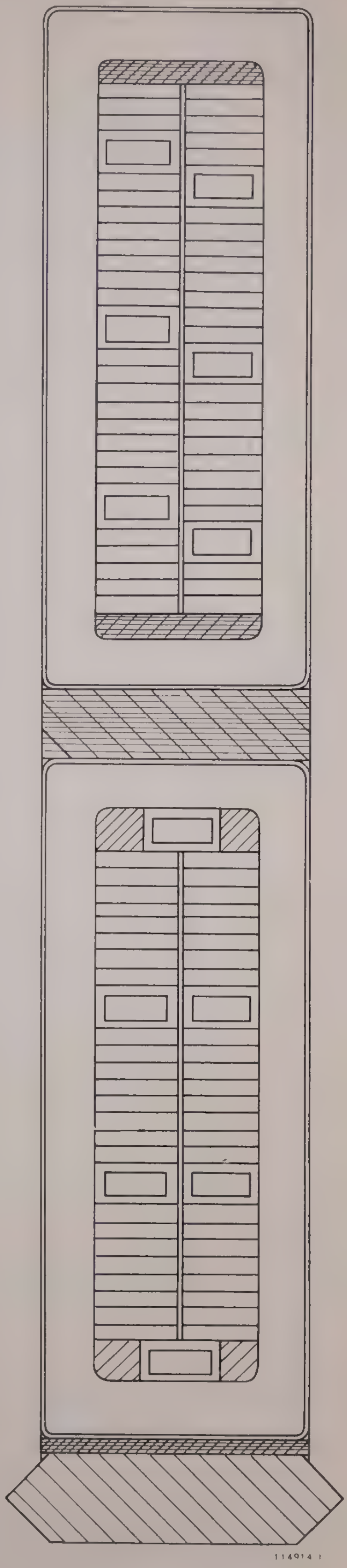

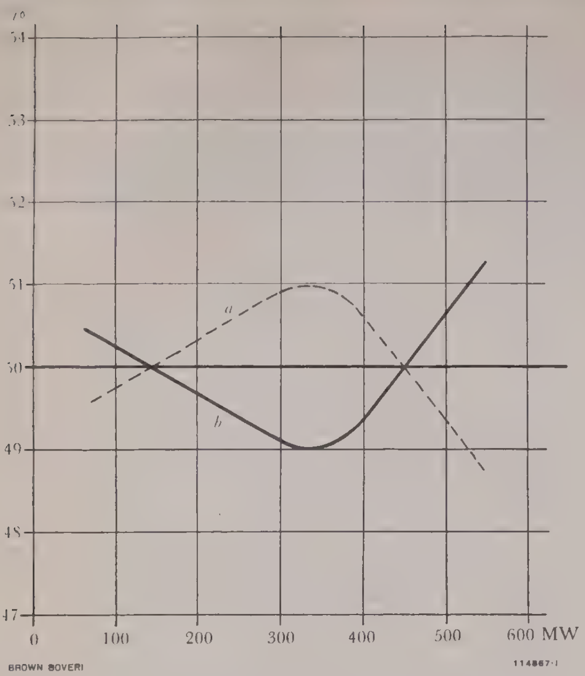

Fig. 6. – Percentage distribution of the load between the two shafts of the 500-MW turboset, in terms of full load

a = Power of No. I (h.p.) line
b = Power of No. II (l.p.) line

Ordinates: Ratio of shaft power to total output in %
Abscissae: Total terminal output in MW

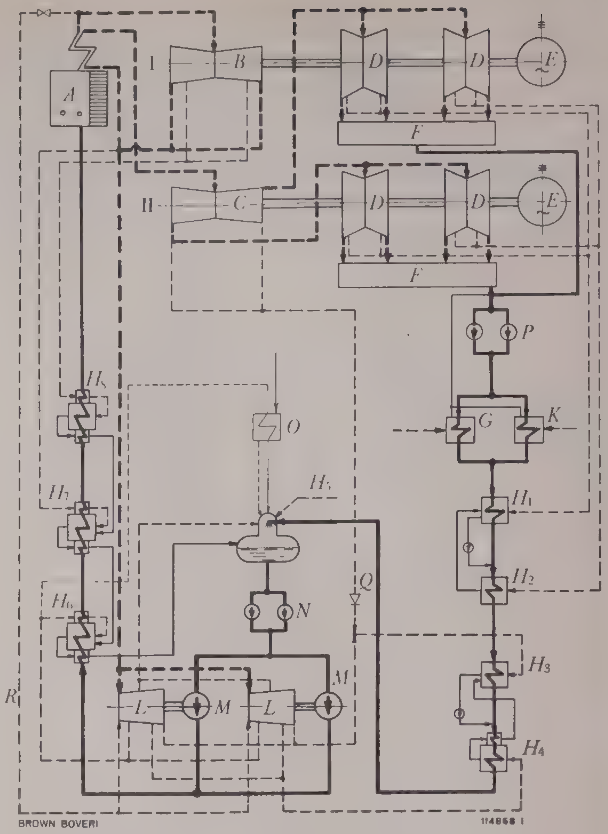

Fig. 7. – Thermal circuit diagram for the 500-MW turboset for TVA

A = Boiler
B = High-pressure cylinder
C = Intermediate-pressure cylinder
D = Low-pressure cylinders
E = Generators
F = Condensers
G = Gland-steam condenser
H_1–H_8 = Feedwater heaters
K = Condenser for steam from steam-jet air ejector
L = Auxiliary turbines driving feedwater pumps
M = Feedwater pumps
N = Booster pumps
O = Evaporator for make-up water
P = Condensate pumps
Q = Non-return flap
R = Supplementary live steam for auxiliary turbines
I = Line I (h.p.)
II = Line II (l.p.)

Turboset for TVA (Tennessee Valley Authority)

Steam Turbine

This turbine will produce a normal output of 500 MW; but since it has to achieve this output with about twice the normal back pressure and with about 3% make-up water, the maximum sustained output under normal circumstances is in the region of 550 MW. The live-steam conditions are 2400 psig, 1050 °F, with reheat to 1000 °F. The enormous amount of steam, 1700 tons per hour, required to produce this output, can naturally not be handled in a single-shaft turbine with a back pressure of 1·5 in. Hg. Therefore a two-shaft (cross-compound) arrangement was selected, but it was decided that both lines would run at 3600 rev/min, since investigations proved that l.p. shafts for 1800 rev/min would have been much more expensive and, furthermore, two quite different generators would have been required. Since the two lines develop roughly the same power, two identical generators can be built for 3600 rev/min. The load distribution between the two lines is plotted as a function of the total load in Fig. 6.

The thermal circuit diagram (Fig. 7) conforms to normal TVA practice. But since it deviates appreciably from European practice, it will be interesting to explain some of the principal features. A total of eight heating stages are provided which,

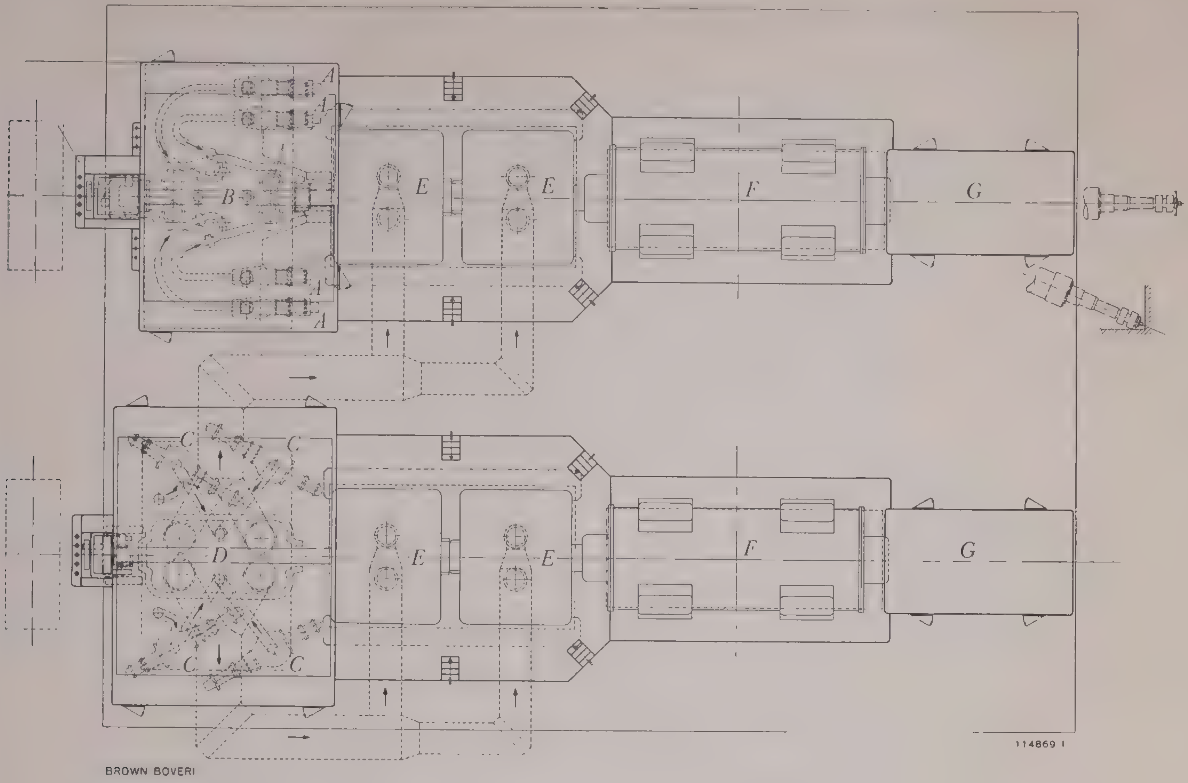

Fig. 8. – Plan view of the cross-compound 500-MW turboset for TVA, both lines running at 3600 rev/min

A = High-pressure admission valves
B = High-pressure cylinder
C = Interceptor valves
D = Intermediate-pressure cylinder
E = Low-pressure cylinders
F = Generators
G = Exciters

at 550 MW, raise the feedwater to about 525 °F. The fifth heater is designed as a mixing de-aerating heater. The two feedwater pumps are each driven by an auxiliary steam turbine, the combined output of which, for a natural-circulation boiler at full load, amounts to about 12 MW. The auxiliary turbines, which are also included in the Brown Boveri contract, are fed with steam bled from the exhaust of the h.p. cylinder. Their exhaust steam is conveyed to feed-heater H_3. Below three-quarter load only one pump is kept running. In this case, due to the severe reduction in the heat drop through the auxiliary turbine, h.p. exhaust steam alone is no longer sufficient and it has to be augmented by live steam. The steam for heater H_4, mixing heater H_5 and heater H_6 is not obtained from the main turbine but from the auxiliary turbines. Since the exhaust steam from the two auxiliary turbines is insufficient to feed the third heater, a certain amount of exhaust steam from first i.p. cylinder has to be added at all loads.

The advantages of this arrangement are, firstly, that at full load the auxiliary turbines do not consume any valuable live steam at a poorer efficiency than the main turbine, and secondly, that no bled steam at an unnecessarily high temperature is used and there is consequently no devaluation of the heat.

A non-return flap in the pipe connecting the exhaust of the i.p. cylinder with the heater H_3 prevents steam from flowing back into the main turbine under abnormal operating conditions. The steam for evaporating the make-up water is also taken from the auxiliary turbines.

Fig. 8 shows a plan view of the machine set, Fig. 9 the sectional elevation of the two turbines. Line I comprises the h.p. cylinder and two l.p. cylinders, all double-flow, while line II has the i.p. cylinder and two l.p. cylinders, again all double-flow. The great advantage of this arrangement is that it is much easier to spread the load evenly over the two lines. If, for instance, all four l.p. cylinders were on one shaft, the distribution would be largely depend-

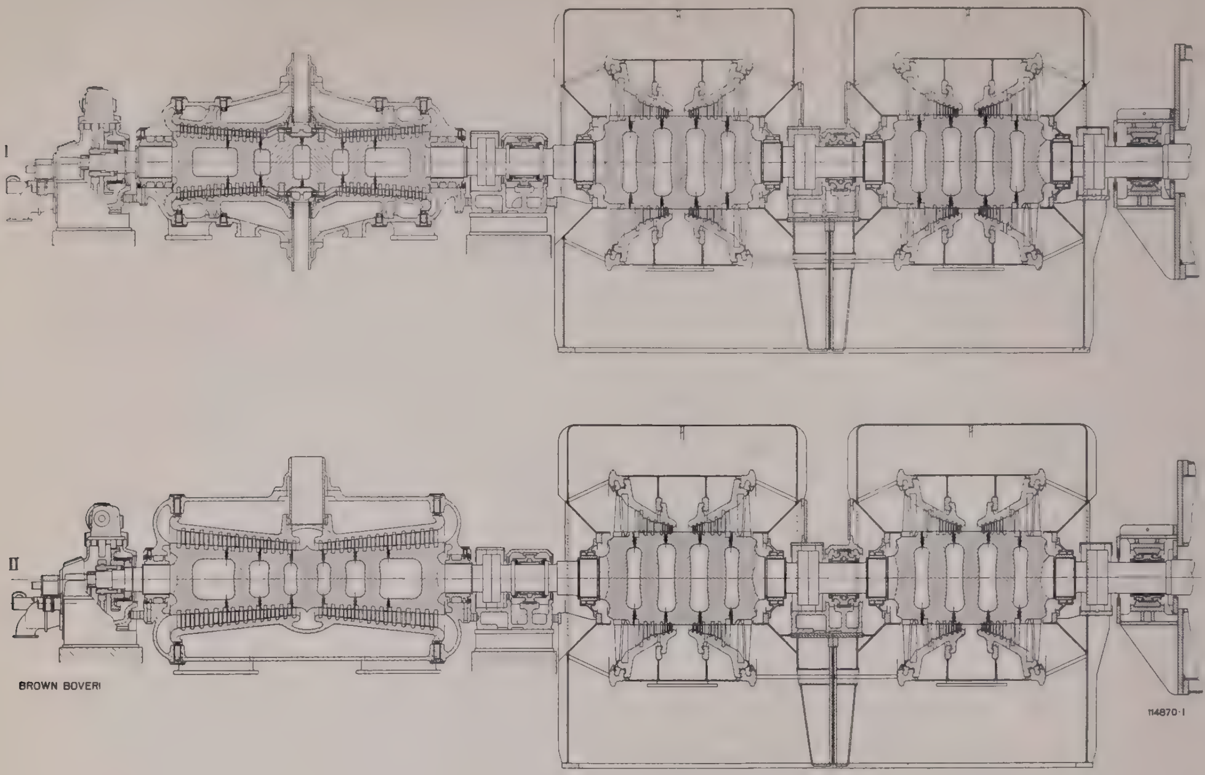

Fig. 9. – Sectional elevations through the two lines of the 500-MW turboset for TVA

I = Line I (h.p.) II = Line II (l.p.) Live steam at 2400 psig, 1050 °F
Both lines run at 3600 rev/min Reheat to 1000 °F, vacuum 1·5 in. Hg

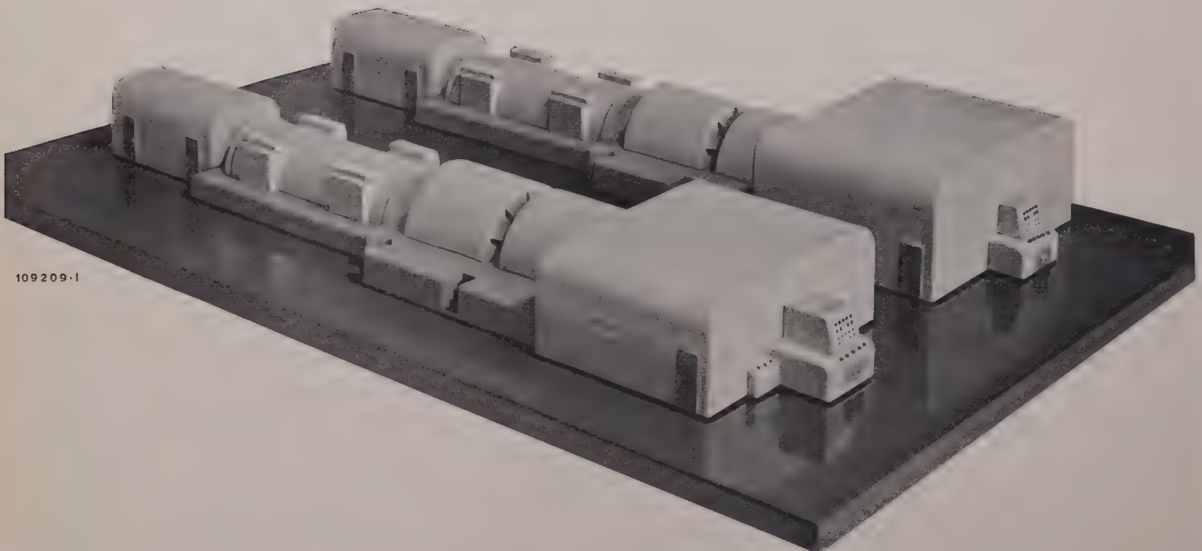

Fig. 10. – Model of the 500-MW cross-compound turboset for TVA, for installation indoors

ent on the back pressure. For starting and synchronizing, it is ideal for each line to have a h.p. or i.p. cylinder. Moreover, with this arrangement both lines are about the same length (Fig. 10).

Owing to the large amount of live steam handled, it was considered advisable to increase the number of valve chests to four. Each chest contains an emergency stop valve and two regulating valves, the four chests operating in parallel. For testing in service the stop valves 1 and 3 can be closed simultaneously, likewise 2 and 4. With this arrangement there is no need for any connecting pipe. Each pair of regulating valves feeds a group of nozzles; in all there are four groups of nozzles which are in a ring split horizontally, the halves being bolted together.

Each side of the double-flow h.p. cylinder has a single set of impulse blading followed by reaction blading. This arrangement completely balances the axial thrusts and obviates the need for a balancing piston. The h.p. cylinder is of double-shell design with a straightforward inner shell in the middle. This is surrounded by steam at bleeding pressure (feed-heater H_8), the last few stationary reaction stages at each end being held in blade carriers. The design of the cylinder is therefore very simple and symmetrical. The internal parts are centred in the outer shell and free to move on expansion in the normal manner. Through four interceptor valves, whose layout and operation correspond exactly to those already described for the 230-MW turbine, the reheated steam is conveyed to the double-flow i.p. cylinder at the head of line II. The steam enters through four symmetrically arranged inlets. The double-shell cylinder is even simpler than the h.p. cylinder and is also completely symmetrical. Hence the thrusts are balanced. The exhaust steam emerging from four outlets is collected in two pipes which lead to the four double-flow l.p. cylinders.

Each of these l.p. cylinders has two identical sets of divergent blading, each pair of cylinders exhausting into a common outlet to the condenser. As regards the number and magnitude of the l.p. flows the same remarks apply as to the 230-MW turbine. The choice of eight exhausts, although of the next larger size to the turbines for Los Angeles, was found to be appropriate. Only in this way did it become possible to adopt the favourable arrangement previously described, since each l.p. cylinder is inherently balanced. With two triple-flow l.p. cylinders this would not have been the case. Owing to the larger diameter, the centrifugal forces are so large that tangential fixture of the last row of moving blades, as employed in the 230-MW turbine, is not sufficient and axial fir-tree roots have to be used. The l.p. casings are so simple that it is worth adopting a welded fabrication. Naturally, from the production aspect, the division into four almost identical units is very favourable.

Each line has a thrust bearing which does not normally experience any load, since all cylinders are inherently balanced. It is merely provided to meet the eventuality of blades becoming fouled on one side, e.g. by incrustation. All bearing pedestals are firmly attached to the foundations. For lubrication, each line possesses its own oil pump driven directly by the shaft, thus ensuring an adequate supply of oil to each line. Each line has its own emergency trip gear and speed governor which actuate the stop or regulating valves of the whole turbine. The speed governor of No. I line actually governs the speed of the whole turbine, that of No. II line merely acts as a speed limiter. Starting up this set presents no problems because regulating interceptor valves are employed which can be made to assume any desired position. Thus the speed of each line can be controlled independently and synchronization is quite a simple matter. Each line has its own barring gear.

As regards the blading, the same remarks apply as to the 230-MW machines; all are of stainless steel. The higher live-steam temperature has no effect on the choice of material for the nozzles and blades, because the 12 % chrome-steel used exhibits excellent properties at 566 °C.

Due to the rotor being welded, the individual forgings are not particularly large, even for this high output, and by no means exceed those so far used for large turbines.

Now that Brown Boveri have an order for such a large unit one is tempted to ask whether this is the ultimate limit for turbines of this design. If the relatively short, rigid and—resulting from the welded construction—lightweight l.p. rotor is considered,

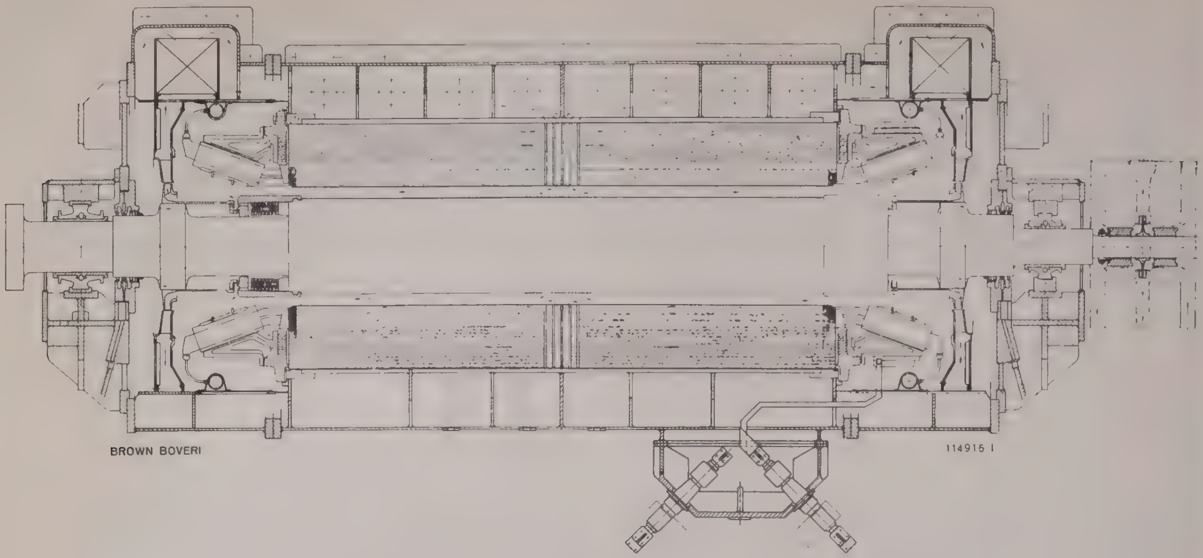

Fig. 11. – Sectional elevation through one of the generators for the Tennessee Valley Authority (TVA)

there is no apparent reason why a further double-flow section should not be added. The overall length would then not exceed that of the 230-MW machine. By increasing the outlet area by 50% it would be possible to attain an output of up to about 800 MW. Bearing in mind that the l.p. cylinder used in this case is not the largest available size but that, for a speed of 3600 rev/min, Brown Boveri have a l.p. cylinder with a 20% larger outlet area, the resultant maximum attainable unit capacity works out to roughly 1000 MW.

Generators

The generators for the cross-compound arrangement are identical and rated 305·555 MVA at a hydrogen pressure of 60 psig, or 277·777 MVA at a pressure of 45 psig, 24 kV, power factor 0·9, 60 c/s. Fig. 11 shows a sectional elevation of one generator. A high-capacity cooling system is provided: two large centrifugal fans force the hydrogen at a high pressure through axial passages in the stator laminations and through the end-plates. Thus not only the iron but also the end spaces are effectively cooled. The pressure created by the fans is added to the natural pressure of the rotor in the rotor cooling circuit, so that here the cooling effect is much more powerful than with self-ventilation. The hot gas emerging from the middle of the rotor passes through the air-gap towards both ends where it is recirculated by the fans. The coolers for the hydrogen are situated immediately following the fans. This system, which is known as induced-draught ventilation, has the advantage that the fan losses are immediately dissipated and the cold gas is not preheated. The coolers are housed in flanged-on end-casings which are removed from the stator for transport and despatched separately. Shipping problems are thus greatly simplified.

As in the generators for Los Angeles, the stator copper is cooled with low-viscosity oil under a cushion of inert gas. The oil system is also designed on the principle previously described.

The design of the rotor is in principle the same as for Los Angeles, i.e. the body is of the normal sectional type, the copper of hollow sections and the end-bells are floating. A new feature is that the gas passes through the hub of the fans; this arrangement is a result of the series connection of the pressures of the fans and that due to self-ventilation.

The alternators are excited by main exciters driven through gearing from the generator shaft. The voltage is controlled by magnetic amplifiers with a booster set as output stage.

P. HUMMEL
R. NOSER

Bibliography

[1] P. Hummel: Operation and Constructional Evolution of Large Steam Turbines. Brown Boveri Rev. 1958, Vol. 45, No. 7/8, p. 310–24.

[2] E. Wiedemann: The Design of Very Large Turbo-Alternators. Brown Boveri Rev. 1958, Vol. 45, No. 1, p. 3–13.

[3] W. Kellenberger: Computing the Strength of Turbo-Alternator End-Bells. Brown Boveri Rev. 1958, Vol. 45, No. 3, p. 113–27.

[4] F. Müllner and E. Wiedemann: Potential Possibilities in the Construction and the Use of Large Turbo-Alternators of the Single-Shaft Type. CIGRE Report No. 106/1958.

FULL-LOAD THROW-OFF TESTS WITH A REHEAT TURBINE

621.165–53

As a supplement to earlier publications, a report is given on full-load throw-off tests with a 120-MW reheat turbine. It is evident from these tests that the acceleration regulator employed by Brown Boveri has led to favourable results.

An EARLIER article dealt in detail with results of load throw-off tests on a 60-MW turbine.[1] It is now possible to augment that article by reporting on a full-load throw-off test with a 120-MW reheat turbine,[2] the control system of which operates in exactly the same way as that of the 60-MW turbine mentioned. In addition this plant has a bypass arrangement to the high pressure (h.p.) and low pressure (l.p.) section of the turbine operating independently of the turbine control system. The h.p. bypass valve is regulated by the live steam pressure, the l.p. bypass valve receives a lift pro-

---

[1] A. Oberle: Control and Safety Gear of Large Steam Turbines. Brown Boveri Rev. 1958, Vol. 45, No. 7/8, p. 325–38; Load throw-off tests see p. 335–8.

[2] A. Angiolini and E. Maraini: Santa Barbara: A New Steam Power Station in Italy. Brown Boveri Rev. 1959, Vol. 46, No. 3, p. 163–81.

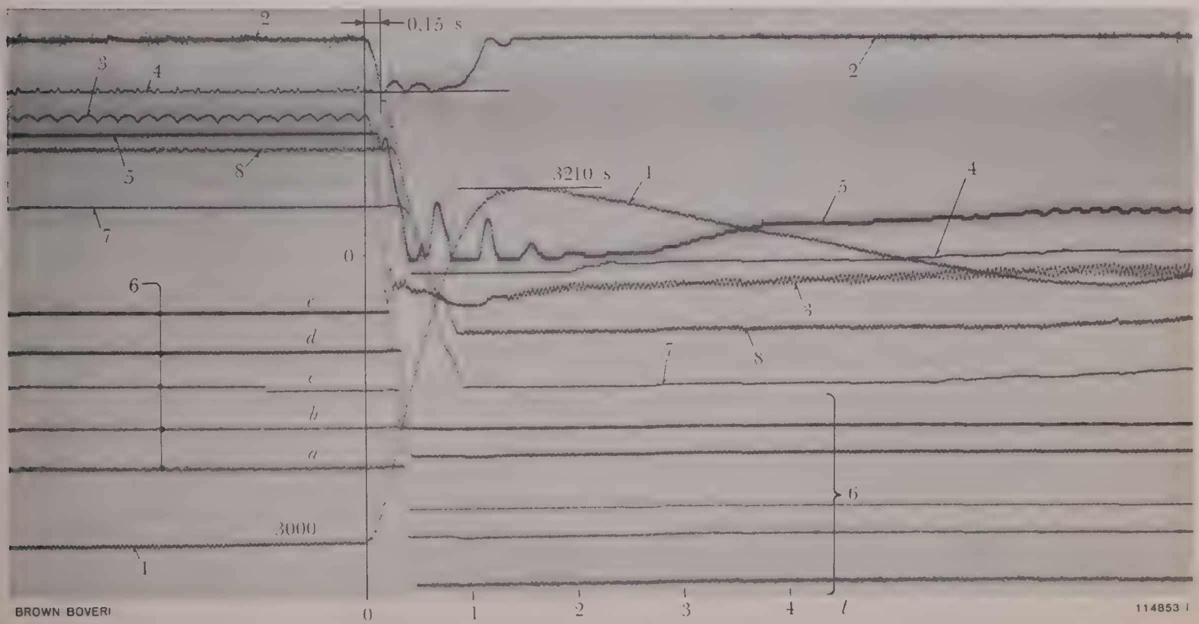

Fig. 1. – Record of the turbine control

0 = Time 0, instant of the load throw-off
1 = Speed curve
2 = Travel of the acceleration regulator
3 = Control pressure of the governor
4 = Control pressure of the h.p. regulating valves
5 = Control pressure of the interceptor valves
6 = Travel of the h.p. regulating valves *a–e*
7 = Travel of the left-hand interceptor valve
8 = Travel of the right-hand interceptor valve

portional to the area of the h.p. valve. Unfortunately registration of the live steam pressure and the travel of the h.p. bypass valve failed. Here we must therefore be content with the reproduction of the record strip of the turbine control (Fig. 1). To simplify the comparison with the results of the previous publication, the same sequence is maintained in discussing the diagram.

The curve 1 shows the speed. The maximum speed is reached after approx. 1·4 s and is 3210 rev/min or 7% above the nominal speed. The second speed maximum evident with the 60-MW set is completely absent with this 120-MW set. The explanation for the different behaviour is simple: on turbines without a bypass the interceptor valves open before the regulating valves with increasing oil control pressure;[3] on turbines with a bypass, however, the interceptor valves open simultaneously with the h.p. valves. Therefore the additional speed rise due to the discharging of the reheater disappears. The reheater discharges itself through the l.p. bypass into the condenser.

The travel of the acceleration regulator is depicted by curve 2. After 0·15 s the maximum designed travel is reached. The governor plunger thus experiences a travel corresponding to a speed change of 150 rev/min[4] in less than 0·05 s. After about 0·8 s—with the flattening of the speed curve—the acceleration regulator begins to return.

The control pressure of the governor (curve 3) also reacts suddenly. The minimum pressure is already reached after 0·2 s.

The control pressures of the h.p. valves (curve 4) and the interceptor valves (curve 5) fall approximately at the same rate, but with a delay of about 0·1 s relative to the control pressure of the governor as the pressure begins to drop and, with a fairly flat curve, with 0·2 s delay at the end. The minimum of these two pressures is reached after 0·4 s. The control pressure to the interceptor valves (curve 5) still oscillates slightly then; three distinct maxima are discernible at approx. 0·45 s intervals. The reason has not been clarified.

Corresponding to the rapid drop in pressure, the closure of the valves is also very fast. On the h.p. side, only the travels of the first five valves to open were registered (curve 6). The first valve to close began its movement after 0·2 s and after 0·45 s all the h.p. valves were closed. The actual closing times of the individual valves occupied about 0·1 s.

The curves 7 and 8 depict the movement of the two interceptor valves left and right. The right-hand valve (curve 8) starts to close after about 0·25 s, that on the left (curve 7) about 0·05 s later. The curves of both movements are very similar, the right-hand valve is closed after 0·85 s and the left after 0·9 s.

The comparison of these closing times with the values of the earlier tests[5] mentioned at the beginning, show that despite approximately the same rapid pressure reductions in the oil control systems, the closing times of the regulating valves are generally slightly longer. This is due partly to the larger, but geometrically similar, servomotors that develop approximately the same velocity of the power piston. With the longer valve travel, this leads to slower closing times. A reduction in the closing time of the interceptor valve servomotors would have been possible, by increasing the area of the pilot piston for example. In view of the favourable test results with a 7% speed rise at full-load throw-off, such measures are unnecessary.

At the conclusion of the previous article, it was forecasted that the speed rise with a Brown Boveri reheat turbine would reach 8% when full-load was thrown off. It has been satisfactorily confirmed that the facts proved slightly more favourable than the prognosis.

(AL) A. OBERLE

---

[3] See article in footnote 1, Fig. 5, p. 327.

[4] Corresponding to the normal proportional band of 5% of the speed range.

[5] See article in footnote 1, Fig. 18, p. 337.

THE CONTROL OF A REHEAT TURBINE WITH A BYPASS

621.165:621.313.322:621-53

The article deals with a newly developed control system for reheat turbines, in particular for plants in which a bypass is provided parallel to the turbine. It explains that, by coupling the bypass control to the turbine control system, the steam distribution through the h.p. and the l.p. turbines can be maintained constant independent of the loading of the bypasses and the live-steam conditions. In conclusion, a description of the starting and load throw-off process is given.

IN 1958 an article was published on the control of reheat turbines [1],[1] in which the control of the interceptor valves after the reheater was explained with the aid of a control diagram. During rapid unloading, these valves are temporarily closed by the pressure-gradient relay to prevent the set from being accelerated to inadmissibly high speeds due to the rapid discharge of the reheater. Brown Boveri applies this elementary principle with success on all reheat turbines not provided with a bypass. However, in recent years such sets have been increasingly provided with bypass arrangements, consisting of a h.p. bypass connected between the superheater outlet and reheater inlet and a l.p. bypass from the reheater outlet to the condenser or back-pressure system. This offers the advantage that the rigid coupling between the boiler and the turbine, as occurs in unit-construction plants, is eliminated. The boiler load can then also be maintained via the bypass, when the turbine cannot take all the steam flow. This development was necessitated, on the one hand, by the increased use of once-through boilers which need an induced circulation through the heating tubes during starting, and on the other hand, by the greater freedom afforded by the bypass during starting, in that it allows the starting time to be short, particularly when the turbine is still hot. During load throw-off the reheater is protected against unduly high metal temperatures [2]. This tendency motivated the development of the combined control of turbine and bypass described here.

The bypass system must be designed in conjunction with the boiler supplier. The capacity of the h.p. bypass depends on the behaviour of the steam generator, for example during starting or load throw-off. It is usually determined by the boiler supplier. The capacity of the l.p. bypass however is determined by the maximum steam flow expected at starting, according to the starting diagrams drawn up during the planning. It is then possible for the capacity of the h.p. bypass to be much greater than that of the l.p. bypass, so that when heavy loads are thrown off, part of the steam is blown out through the safety valves on the reheater. This Company is of the opinion, though, that this relatively rare occurrence does not justify the increased costs of a larger l.p. bypass; besides, the condenser is not unnecessarily overloaded.[2]

Principle of the Control

The control system developed by Brown Boveri is built on the following principle: With parallel operation of turbine and bypass, e.g. during starting or after a load throw-off, the area ratio of the l.p. bypass valve to the h.p. bypass valve is always kept the same as the ratio of the areas of the turbine interceptor valves to the h.p. regulating valves. Hence every partial flow through the reheater, i.e. through the bypass and the turbine, considered by itself, leads to the same intermediate pressure, the result of which is that opening the bypass does not influence the steam distribution through the h.p. and l.p. turbines.

---

[1] The figures in brackets refer to the bibliography on p. 26.

[2] At full load operation about 70% of the live steam is condensed; with a bypass system designed for 100% live steam flow the condensate can amount to 140%, since a total water flow of about 40% of the steam throughput is needed for the cooling in the two bypasses.

The advantages of this solution are summarized here: The effect of the cross-connection between the turbine and the bypass system as necessitated by the reheater has no effect on the steam distribution. During simultaneous turbine and bypass operation it is not possible for the flow through one turbine section relative to another section to be severely or even completely reduced, thereby leading to intense heating through ventilation. If the bypass loading is changed, e.g. during starting or after a load throw-off, the performance remains unchanged provided the position of the turbine governor remains unaltered, i.e. the turbine is solely controlled by this governor. The effect of the live-steam conditions on the steam distribution in the turbine is also automatically eliminated. This is of particular advantage during starting, when the live-steam pressure is often raised relatively quickly from a low initial value. At a load

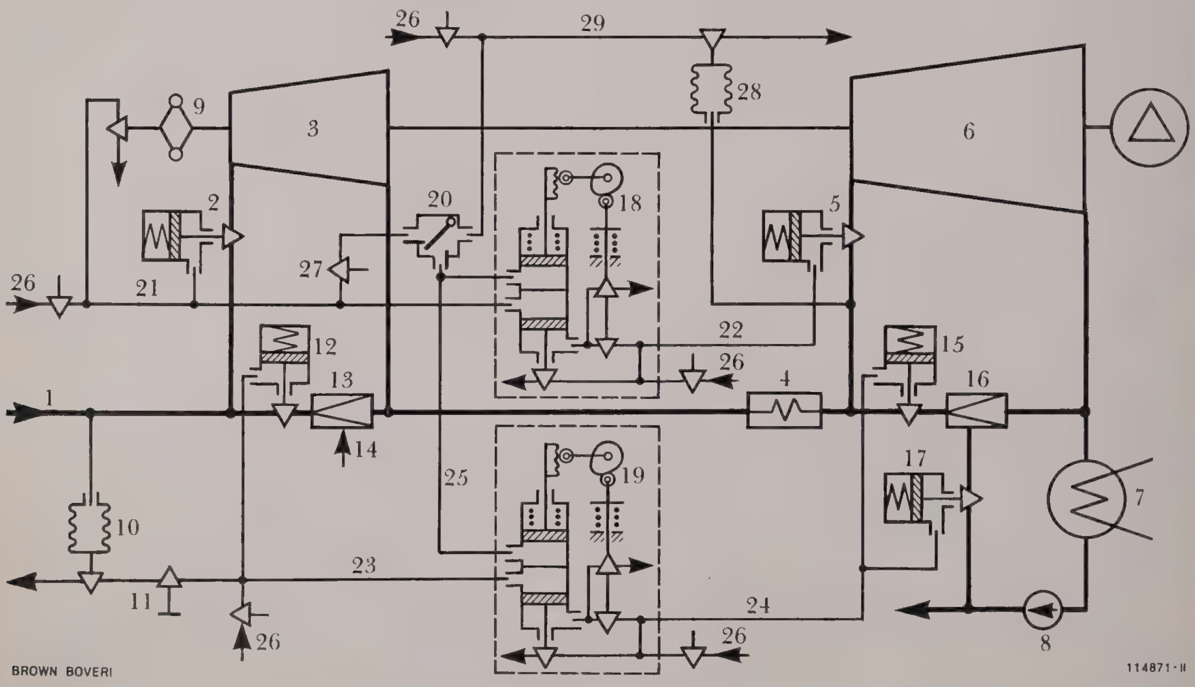

Fig. 1. – Principle employed for controlling a reheat steam turbine with a bypass

1 = Live-steam pipe
2 = Regulating valves with servomotor
3 = High-pressure turbine
4 = Reheater
5 = Interceptor valves with servomotor
6 = Low-pressure turbine
7 = Condenser
8 = Condensate pump
9 = Speed governor
10 = Admission-pressure regulator for 12
11 = Hand-control valve for 12
12 = H.P. bypass valve with servomotor
13 = Cooling device
14 = Water injection
15 = L.P. bypass valve with servomotor
16 = Steam admission device
17 = Water regulating valve for 16 with servomotor
18–19 = Relays with adjustable transmission ratios
20 = Diverting relay
21 = Control system for the admission valves 2
22 = Control system for the interceptor valves 5
23 = Control system for the h.p. bypass valve 12
24 = Control system for the l.p. bypass valve 15
25 = Control system for adjusting the transmission ratios of relays 18 and 19
26 = Main pressure system
27 = Throttle orifice
28 = Pressure limiter after the reheater 4
29 = Control system for the pressure limiter 28

removal the l.p. bypass only opens when the h.p. bypass also opens. Since the thermal shock on the bypass valves is severe when opened suddenly, it is of advantage to minimize the frequency of these openings. The control system is easily understood, since the bypass control and turbine control are similar and the same apparatus is used for both systems; manipulation is simple, which is very desirable with complicated modern plants.

Design of the Control System

The principle of the circuit is illustrated symbolically in Fig. 1. For simplicity, the machine is represented by the h.p. turbine 3 with the regulating valves 2 and the l.p. turbine 6 with the interceptor valves 5 as the admission valves; the h.p. bypass with the reducing valve 12 and the cooling apparatus 13 being also shown. The water injection at 14 is generally governed by the influence of the temperature regulator. The l.p. bypass consists of the reducing valve 15 and the steam admission apparatus 16 with the water valve 17. The lift of the valves 2, 5, 12 and 15 is determined by the fluid pressure in the corresponding control systems 21, 22, 23 and 24: The relation between the valve lift and control pressure is always made such that for a constant steam condition before the valve the steam flow is proportional to the control pressure. For a given live-steam condition, the pressure in system 21 controls the performance of the set, while the pressure in system 23 determines the loading of the bypasses. The pressure in 21 is hereby influenced by the speed governor 9, that in 23 by the admission pressure regulator 10 or the hand control valve 11. For the regulation of the pressures in systems 22 and 24, two similar relays 18 and 19 with adjustable transmission ratios are provided between 22 and 24 and between 21 and 23. The pressure in system 21 acts as the input signal for relay 18, and pressure 22 as the output signal. The ratio between these pressures, the so-called transmission ratio, is determined by the pressure in system 25. The same applies for relay 19, with 23 as the input system and 24 as the output system; the transmission ratio is again determined by the pressure in 25.

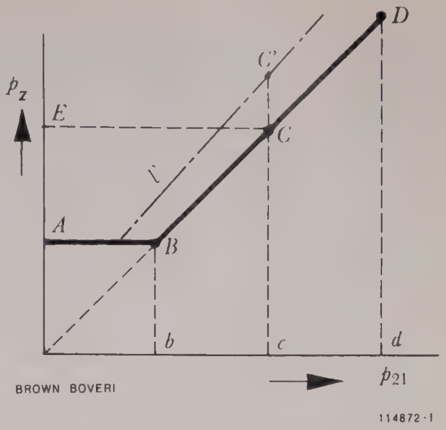

Fig. 2. – Pressure variation after the reheater

The diagram applies for constant values of live-steam pressure, live-steam temperature and reheat temperature.

p_{21} = Pressure in control system 21 of the admission valve 2
p_z = Steam pressure after the reheater 4
A–B–D = Pressure curve at steady conditions
at *A* = Admission and interceptor valves closed
at *B* = Interceptor valves fully open
at *D* = Admission valves fully open
C = Arbitrary operation point
C–E = Pressure curve, directly after a load throw-off
C' = Arbitrary operating point with accumulated reheater pressure
l' = Pressure curve with accumulated reheater pressure

Principle of Operation

To explain the principle, it is first assumed that the bypass is completely closed, i.e. that the systems 23 and 24 are not under pressure. The total steam flow generated by the boiler passes through valve 2 into the h.p. turbine 3 and through the reheater 4 and interceptor valve 5 into the l.p. cylinder. In steady-state operation or approximately steady conditions, when the pressure in system 21 remains constant or only changes slowly, the pressures in the control systems 21 and 22 are related to each other in such a way that the steam pressure p_z after the reheater as a function of the pressure in system 21 results (as shown in Fig. 2 by the continuous line *A–B–D*). Along *A–B* the pressure p_z is prevented from dropping below the minimum value required for the boiler by throttling by the interceptor valves. At *B* the interceptor valves are completely open. Along *B–D* the pressure is given by the intake capacity of the l.p. turbine. At point *D* the regulating valves are fully opened. The l.p. flow is thereby equal to the

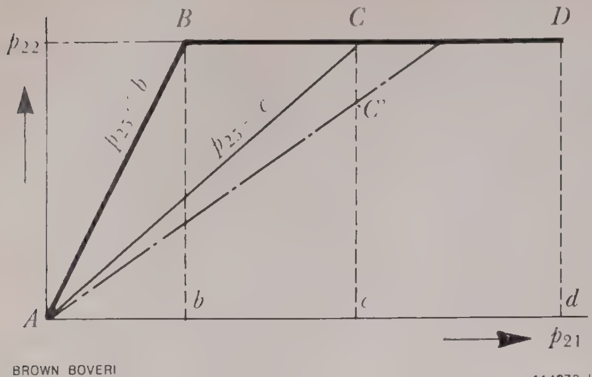

Fig. 3. – Characteristic of the relay with adjustable transmission ratio for regulating the interceptor valves

p_{21} = Pressure in control system 21 of the admission valves 2
p_{22} = Pressure in control system 22 of the interceptor valves 5
p_{25} = Pressure in the control system 25 for adjusting the transmission ratio of the relay
A–B–D = Setting at steady conditions
at *A* = Admission and interceptor valves closed
at *B* = Interceptor valves fully open
at *D* = Regulating valves fully open
A–B = Characteristic of the pressure in system 25 $\leqslant b$
C = Arbitrary operation point
A–C = Characteristic for pressure in system 25 constant equal to *c*, e.g. directly after a load throw-off
C' = Arbitrary operating point with accumulated reheater pressure
A–C' = Characteristic for operation with accumulated reheater pressure with the pressure in system 25 equal to *c*.

h.p. flow, and this is again proportional to the pressure in system 21. Since the pressure and temperature before the interceptor valves are constant between *A* and *B*, the l.p. flow along *A–B* is simultaneously proportional to the pressure in system 22. Therefore along *A–B* the pressure 22 must increase linearly with that in 21.

Fig. 3 shows the relationship between these two pressures and how it is attained by setting the relay 18. Thereby the points *A* to *D* represent the same operating conditions as the corresponding points in Fig. 2. Along *A–B* the ratio between the pressures 22 and 21 remain constant. At *B* the interceptor valves are fully opened. For a further pressure increase in 21, the pressure in 22 now remains constant, i.e. the interceptor valves just remain fully open during steady-state operation. The ratio of the pressures in the systems 22 and 21 is thus continually altered. At the operating point *C* for example, the ratio is represented by the slope of the line *A–C*. The transmission ratio of the relay 18 can be altered as a function of the pressure in the control system 25, which acts on a spring-loaded piston built into this relay. The movement of this piston caused by the change in pressure in 25 is transmitted to a double orifice system by a cam disc, whose setting determines the transmission ratio by alterating the feedback (Fig. 1). During normal operation the system 25 is in direct connection with system 21 through a diverting relay, which is described later, and a throttle orifice 27. During steady conditions the pressures in 21 and 25 are the same; at the operating point *C*, Fig. 3, for instance, the pressure in 25 will be equal to *c*.

If now, starting at point *C*, the pressure in 21 were allowed to sink, but the pressure in 25 kept constant at *c*, then the pressure in 22 would decrease along *A–C*. Thus the pressure after the reheater would remain constant, as described before for the line *A–B*, this process being illustrated by line *C–E* in Fig. 2. At *C* the interceptor valves are fully open and the unthrottled intermediate pressure in the reheater corresponds to this load. Thus a relationship is obtained between the intermediate pressure and the pressure in system 25. When the pressure in system 21 sinks, the characteristic of the interceptor valves rotates retarded in an anticlockwise direction, e.g. from *C–A* to *B–A*. The steepest obtainable characteristic *A–B* and thereby the lowest pressure in the reheater, is set by a mechanical limit stop. Since this relationship between intermediate pressure and pressure in system 25 is obtained by coupling the valve lifts, this is obviously only valid for certain live-steam conditions. However it will be shown later that these conditions have no influence on the steam distribution.

Until now it has been assumed that only the turbine is charged with steam. The opposite case is now considered: the turbine valves are closed, and the entire steam flow generated by the boiler passes through the bypass valves and the reheater into the condenser. The amounts of steam flowing through valves 12 and 15 (Fig. 1) are equal or proportional to one another when considering the cooling water injected at 14.

The relay 19 is inserted between the control systems 23 and 24 of the h.p. and l.p. valves, as was the case with 18 between 21 and 22. The transmission ratio of 19, which is the ratio of the pressures in 24 and 23, is again governed by the pressure in system 25 (Fig. 4). Since the conditions are the same as for the case of the turbine, there also exists a definite relationship between the intermediate pressure p_z and the pressure in 25 in this operating condition. The relay 19 also has a mechanical limit stop that prevents the characteristic from turning further in an anti-clockwise direction when the pressure in system 25 falls below the value *b* (Fig. 3 and 4).

If for the two cases dealt with, i.e. operation with either turbine or bypass alone, the same relation between the intermediate pressure p_z and the pressure in 25 is now chosen, then the turbine and the bypass would each always produce the same pressure after the reheater. This means that during parallel operation with turbine and bypass, the ratio of the steam flow through the h.p. and l.p. turbines is not affected by the loading of the bypass. This requirement is easily fulfilled by giving the cam discs of relays 18 and 19 the appropriate form.

As long as the interceptor valves are not fully open, the method of governing the pressure in 25 does not influence the steam distribution. During normal turbine operation, however, these valves are fully open, i.e. the control pressure in system 21 is greater than *b* (Fig. 2 and 3). Since the intermediate pressure then depends only on the flow through the l.p. turbine and its intake capacity, the pressure in 25 must be governed by a value corresponding to the steam flow through the turbine. In the example given, the pressure in control system 21 is chosen as this value. As already mentioned, the systems 21 and 25 are normally linked directly with one another via the throttle orifice 27 and the diverting relay 30. This relay is designed so that its output pressure, i.e. the pressure in 25, is always equal to the higher of the two input pressures at a given instant, i.e. after the orifice 27 or in system 29. As long as the limiter 28 is not engaged, the system 29 remains pressureless, the pressures in 21 and 25 are the same at steady conditions and the intermediate pressure p_z will adjust itself according to the line *A–B–D* (Fig. 2). For unsteady conditions, refer to the example given later regarding load throw-off.

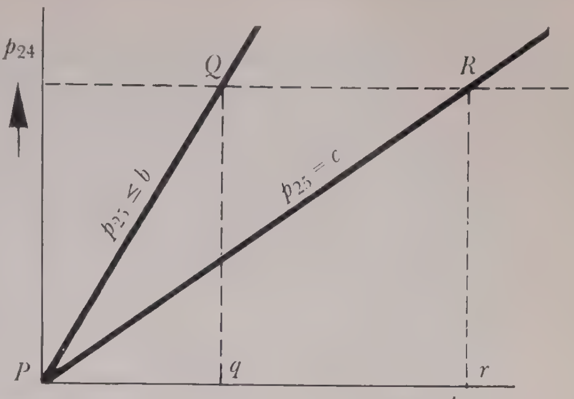

BROWN BOVERI 114874-I

Fig. 4. – Characteristic of the relay with adjustable transmission ratio for regulating the l.p. bypass valve

p_{23} = Pressure in the control system 23 of the h.p. bypass valve 12

p_{24} = Pressure in the control system of the l.p. bypass valve 15

p_{25} = Pressure in the control system 25 for adjusting the transmission ratio of the relay

at *P* = H.P. and l.p. bypass valves closed

P–Q = Characteristic for pressure in system 25 $\leq b$

P–R = Characteristic for pressure in system 25 $= c$

Along *Q–R*: L.P. bypass valve fully opened.

For values *b* and *c* compare with Fig. 3.

In certain cases it may be necessary to limit p_z to a minimum value which is greater than corresponds to the line *A–B* (Fig. 2). Let us assume that the desired minimum value lies on the line *E–C*; the setting of the limiter 28 is then adjusted to this value. This increases the pressure in 29 (Fig. 1) until the relay 20 switches over and the pressure in 29 and 25 becomes equal to *c*.

Effect of the Live-Steam Conditions

In the above considerations the live-steam conditions were assumed to remain steady, in which case a definite relationship exists between the intermediate pressure and the pressure in 25. It is easily understood that for a given ratio of h.p. valve area to l.p. valve area, the pressure in the reheater varies proportionally with the live-steam pressure. In this way the percentage steam distribution between the individual paths is not impaired. If another bleeding point is provided for a feed-heater in or at the outlet of the h.p. cylinder, then the flow through the h.p. and l.p. turbines is not the same, but approximately proportional. This influence, however, can be included in the design by relating the valve areas accordingly. Recapitulating, this means that when the relationship between the valve areas has been calculated for one specific live-steam condition, it is also correct for all other live-steam conditions. Two further examples are now given to illustrate the principle.

Starting with the Bypass

When steam generation has commenced after firing the boiler, the bypass is opened with the hand valve 11 (Fig. 1) according to requirements. Since no steam has entered the turbine yet, the system 21 is not under pressure to begin with. The setting of the relays 18 and 19 therefore corresponds to the lines *A–B* and *P–Q* in Fig. 3 and 4. As long as the limiter 28 is not actuated, the intermediate steam pressure p_z is proportional to the live-steam pressure. At very low live-steam pressures, p_z can fall below the minimum permitted for the boiler, e.g. to allow for draining of the reheater. In this case the desired minimum pressure can be maintained with the aid of limiter 28, which then takes over the governing of the pressure in system 25 from system 21. The characteristics *A–B* and *P–Q* are then turned in a clockwise direction, which results in increased throttling by the l.p. bypass valve.

The boiler is now gradually raised up to pressure and temperature. When the temperatures have attained values that lie within the desired relationship to the metal temperatures of the turbine cylinders, the turbine is started, the generator switched on the line and eventually loaded. The pressure in system 21 is thus gradually increased. At the same time the interceptor valves open. The bypass closes due to the gradual lowering of the pressure in system 23. The pressure in control system 25 is thus either governed by limiter 28, in which case the intermediate pressure p_z remains constant equal to the set point of the limiter, or it follows the pressure in system 21 exactly, in which case p_z depends on this pressure and the live-steam pressure in such a way that, for a given value of the pressure in 25, it is proportional to the live-steam pressure. In certain cases, e.g. during starting with a very low live-steam pressure in plants with a relatively large h.p. bypass, it can happen that the l.p. bypass valve is fully open before the h.p. bypass valve has finished its travel. In this case, for example, the pressure in 25 dictates the characteristic *P–Q* for the relay 19; the pressure in 23 is however greater than *q* (Fig. 4). The correct steam distribution for parallel turbine-bypass operation is thus slightly disturbed. However, this is not important, but should maintainance of the correct distribution be desired, this can be attained by raising the setting of the limiter 28.

Operational Load Throw-Off or Heavy Load Shedding

The operating condition before load shedding is represented by the point *C* (Fig. 2 and 3). The bypass is then closed. At a sudden speed increase the governor 9 will reduce the pressure in 21 corresponding to its proportional band. The closure of the regulating valve causes a pressure rise in the live-steam line, which engages the admission-pressure regulator 10, which results in a pressure rise in system 23, causing the bypass to open. The accumulating action of the spring-loaded piston of the relays 18 and 19 and the throttle orifice 27 causes the pressure in 25 to fall slowly down to the new value of the pressure in system 21. In the first instant the interceptor valves close along *A–C* (Fig. 3), the bypass valves open along *P–R* (Fig. 4). The intermediate steam pressure p_z remains momentarily constant. With the gradual sinking of the pressure in 25, the characteristics of the relays 18 and 19 are turned in an anti-clockwise direction. The interceptor valves and the l.p. bypass valve thus open slowly, until the new steady condition is attained. During this period the reheater gradually discharges through these valves without a high inadmissible speed being reached.

Solo Operation by a Reheat Turbine

If, by way of exception, a reheat turbine should be allowed to run solo with rapid load surges, a fairly large transient frequency decrease is generally

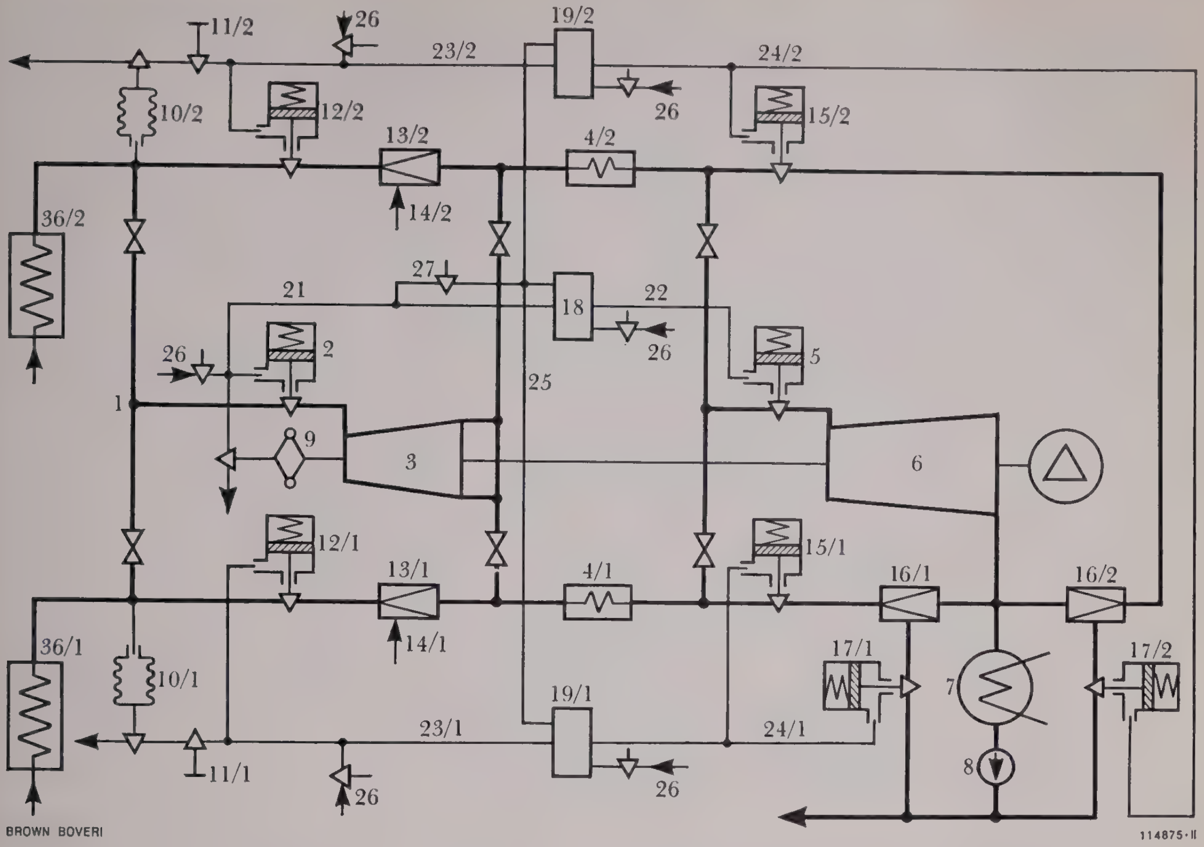

Fig. 5. – Principle employed for controlling a reheat turbine in a double-boiler unit-construction plant

1 = Live-steam pipe
2 = Regulating valves
3 = High-pressure turbine
4 = Reheater
5 = Interceptor valves
6 = Low-pressure turbine
7 = Condenser
8 = Condensate pump
9 = Speed governor
10 = Admission pressure regulator
11 = Hand-control valve
12 = H.P. bypass valves
13 = Cooling devices
14 = Water injection
15 = L.P. bypass valves
16 = Steam admission devices
17 = Water regulating valves
18–19 = Relays with adjustable transmission ratio
21 = Control system for the admission valves 2
22 = Control system for the interceptor valves 5
23 = Control systems for the h.p. bypass valves 12
24 = Control systems for the l.p. bypass valves 15
25 = Control system for adjusting the relays 18–19
26 = Main pressure system
27 = Throttle orifice
36 = Superheaters of the steam generator

unavoidable as the load increases. Since the steam flow through the l.p. turbine with fully opened interceptor valves is proportional to the intermediate pressure, the reheater must be momentarily raised to the higher pressure corresponding to the larger steam flow, before the l.p. turbine shares fully in the load increase. Solutions are known in which this charging is accelerated with the aid of accumulators; in other cases reheater steam is led temporarily to a lower stage of the l.p. turbine. All these solutions are complicated and reduce the life of the turbine, due to the rapid temperature changes. The control system described, on the other hand, permits operation under steady conditions in a simple way and without marked additional costs, with slightly accumulated intermediate pressure by throttling with the interceptor valves. At a sudden load increase, the l.p. flow can be rapidly increased by momentarily opening these valves to the same extent as the h.p. flow is increased by opening the admission valves. It is sufficient for this purpose to slightly shift the relationship of the transmission ratio of the relay 18 to the pressure in the system 25 and 21, i.e. to turn the characteristic of the interceptor valves according to the indicated broken-line characteristic *A–C′* (Fig. 3) with a pressure equal to *c* in system 25. Thus the interceptor valves no longer open fully in steady operation and the reheater pressure is built up to the value *C* (Fig. 2).

Double-Boiler Plant

A case in which the control principle described is particularly suited is the plant with two boilers each with a 50% capacity as indicated schematically in Fig. 5. Both are provided with a bypass system for their maximum output. By coupling the two bypasses with the turbine control via the system 25, and assuming the same live-steam pressure after both superheaters, each bypass alone will always maintain the same pressure after the reheater like the turbine control before the interceptor valves. Hence it follows that the second boiler can be connected or disconnected at any time without disturbing the operation of the turbine. The only prerequisite is that at the moment of the changeover both boilers are equally loaded, since the steam flow through both reheaters also adjusts itself equally due to the equal pressure difference in parallel operation.

Universal Application of the Brown Boveri Control System

In many cases the boiler manufacturer will supply the h.p. bypass and Brown Boveri the l.p. bypass. For the coupling of the control systems, an impulse from the h.p. bypass must then be given to the l.p. bypass which corresponds to the steam flow through the h.p. bypass for given steam conditions. Either the control pressure of this valve can be used, or the valve lift can be conveyed electrically.

With Benson boilers a starting circuit is usually provided for starting, in addition to the h.p. bypass; the issuing steam can be led through the reheater and the l.p. bypass into the condenser. Thus in this case the h.p. bypass must be capable of independent closure. Before the turbine is started, the live steam is again taken over by the h.p. bypass, the coupling of the h.p. and l.p. bypass thus being set in operation again. The correct steam distribution through the turbine is thereby not impaired. The system described is thus universally applicable for all reheat sets with a bypass.

(AL) F. WEEHUIZEN

Bibliography

[1] A. OBERLE: Control and Safety Gear of Large Steam Turbines. Brown Boveri Rev. 1958, Vol. 45, No. 7/8, p. 325–38.

[2] P. HUMMEL: Operation and Constructional Evolution of Large Steam Turbines. Brown Boveri Rev. 1958, Vol. 45, No. 7/8, p. 310–24.

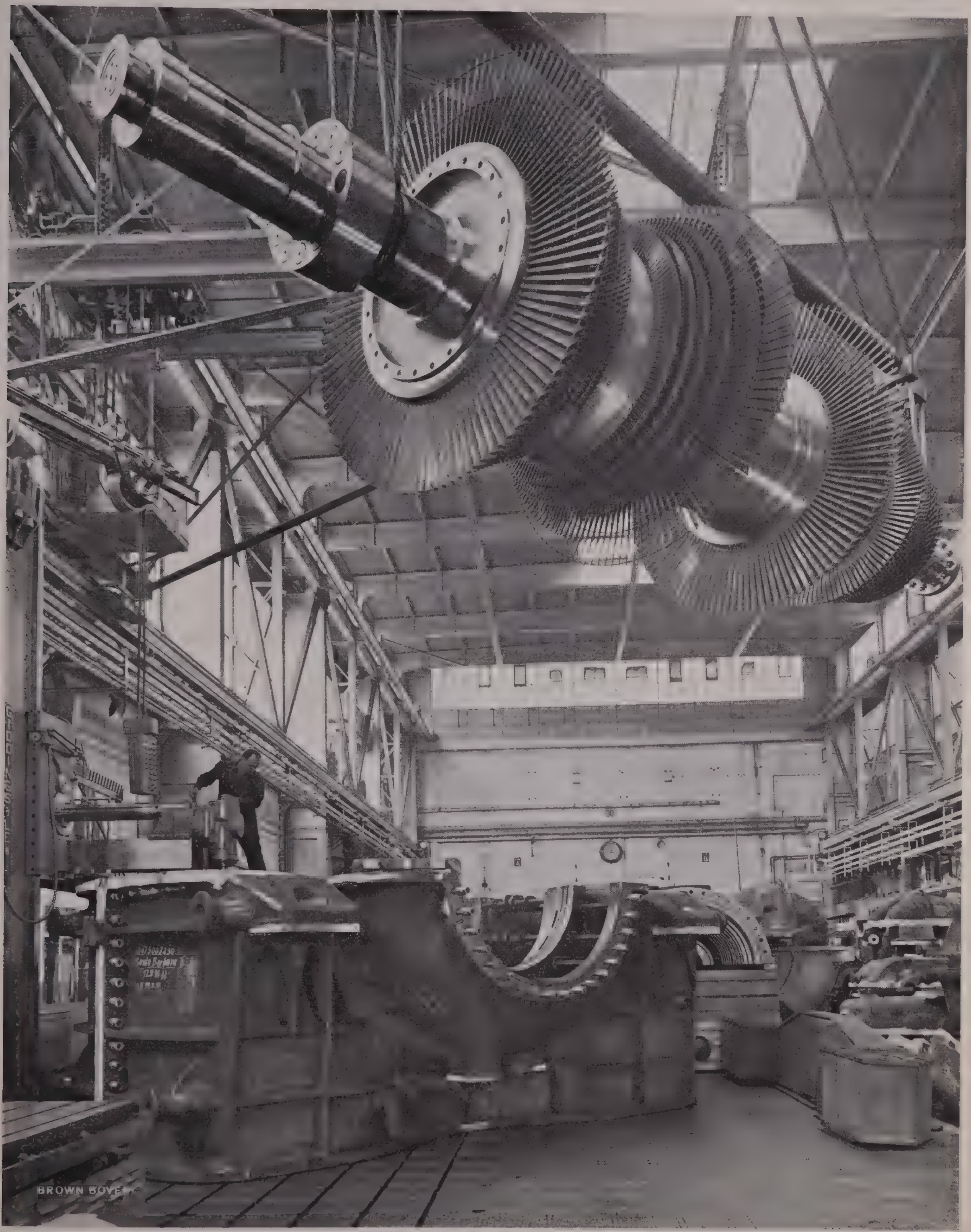

The intermediate/low-pressure rotor of a 150-MW reheat turbine for Frimmersdorf power station in Germany, hanging from the crane in the Baden workshops

On the extreme right of the shaft is the i.p. blading, followed by three sets of l.p. blades.
Speed of the set 3000 rev/min.

THE COOLING-WATER SUPPLY FOR THE DARAGAÇ POWER STATION IN TURKEY

621.175.3

Daragaç power station is the main source of electricity for the city of Smyrna (Izmir). The cooling water required for the existing condensing turbosets is conveyed to the pump-shaft in an open channel from the sea. When the station was extended in 1955, a new cooling-water plant was built, in which the water is pumped from a point out in the sea, employing the siphon principle.

General Remarks on the Cooling-Water Supply

THE INITIAL cost of the water supply plant for a steam power station, comprising the water intake, pump-shaft, pumphouse with machinery, water-cleaning equipment, channels, pipework, electrical equipment, etc., represents quite a large proportion of the total cost of the station. In order to obtain the most economical arrangement of the power station it is necessary to allow for the cooling-water plant in the overall planning.

The layout of the water supply installation is, of course, governed by the location of the station. The space available, the nature of the soil—clay, loam, sand or rock—the position and variation of the water level at the intake and discharge, the degree of contamination of the water, and so on, are all factors which influence the layout.

In most plants the water runs under gravity in open or closed channels or pipes from the intake to the pump-shaft. If the pump is above the highest water level, the intake pipe of the pump must be evacuated or filled with water (foot valve) before starting up.

It is relatively rare for large quantities of water, such as are required for steam power plants, to be conveyed on the siphon principle. In view of this fact the water plant designed by Brown Boveri for the Daragaç power station, Smyrna, is described below. This plant has been in satisfactory operation for some years (Fig. 1 and 2).

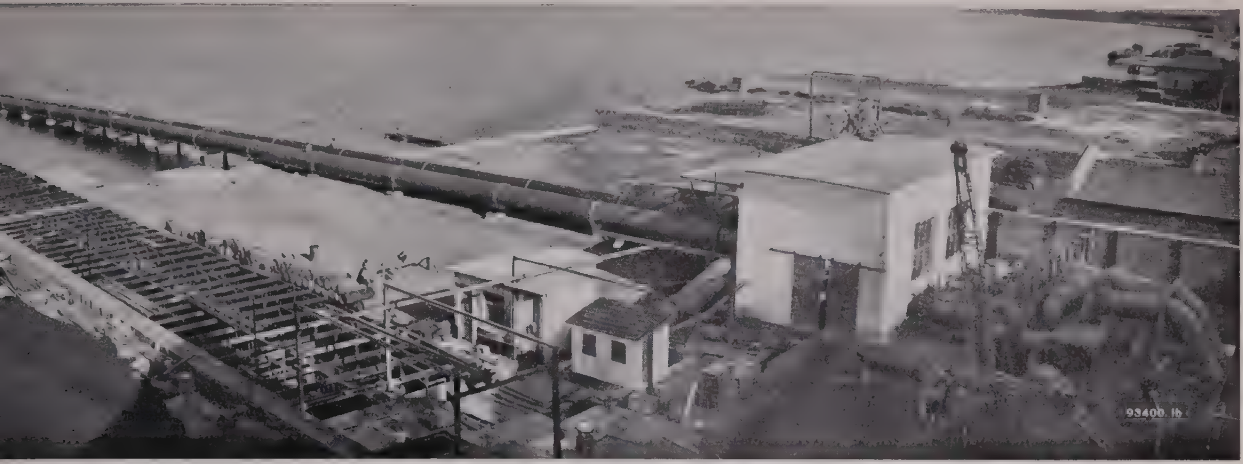

Fig. 1. – Panoramic view of the water supply plant and coal store of Daragaç power station on the Gulf of Smyrna, Turkey
On the right is the pumphouse with the two siphon pipes; in the centre the old intake channel and on the left the coal store.

Daragaç Power Station, Smyrna

This power station is on the shores of the Gulf of Smyrna, as seen in the location plan. The first stage of the power station was equipped with two steam turbosets, each with an output of 2500 kW. It was later extended to include three turbines, each of 5000 kW output. In 1955 the power station undertaking decided on a second extension of the plant (Fig. 3). A new boiler-house was built, with one boiler having an output of 100 tons of steam, also a machine-room for a 20 000-kW condensing turboset of Brown Boveri manufacture (Fig. 4) with feed-heating and evaporating plant, together with buildings for the electrical equipment. The cooling-water plant shown in Fig. 5 supplies the water required by the condenser of the turboset.

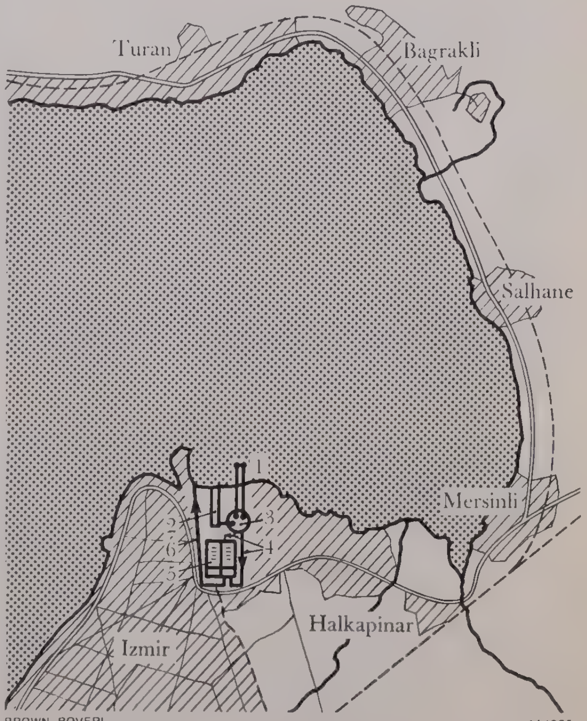

Fig. 2. – Location plan showing the position of Daragaç power station on the Gulf of Smyrna

1 = Siphon pipes
2 = Old water intake channel
3 = Pumphouse with pump-shaft
4 = Pressure pipes
5 = Power station
6 = Water outlet channel

The Water Supply Plant for Daragaç Power Station

Fig. 6 shows the arrangement of this plant and the internal layout of the pumphouse and the pump-shaft. If the intake had been immediately adjacent to the shore, an extensive and costly water-cleaning

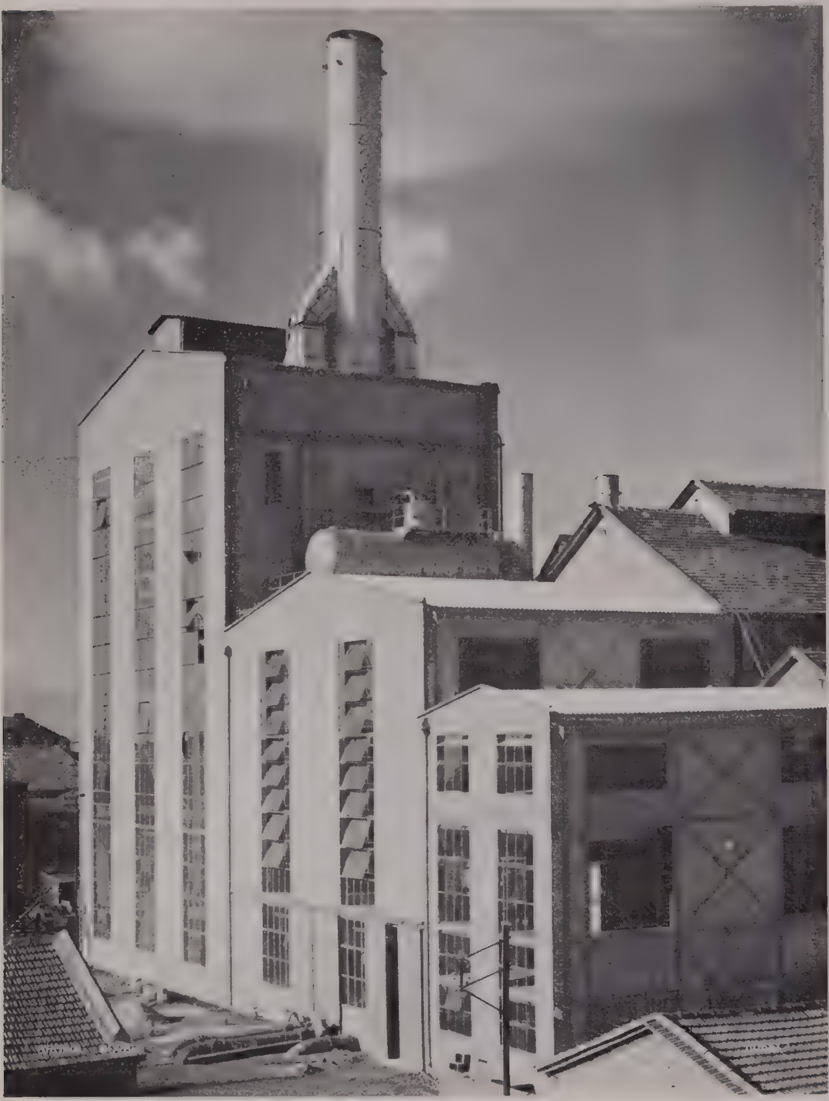

Fig. 3. – View of the steam power station, extended in 1955

Left, boiler house; centre, machine room; right, transformer and switchgear bay.

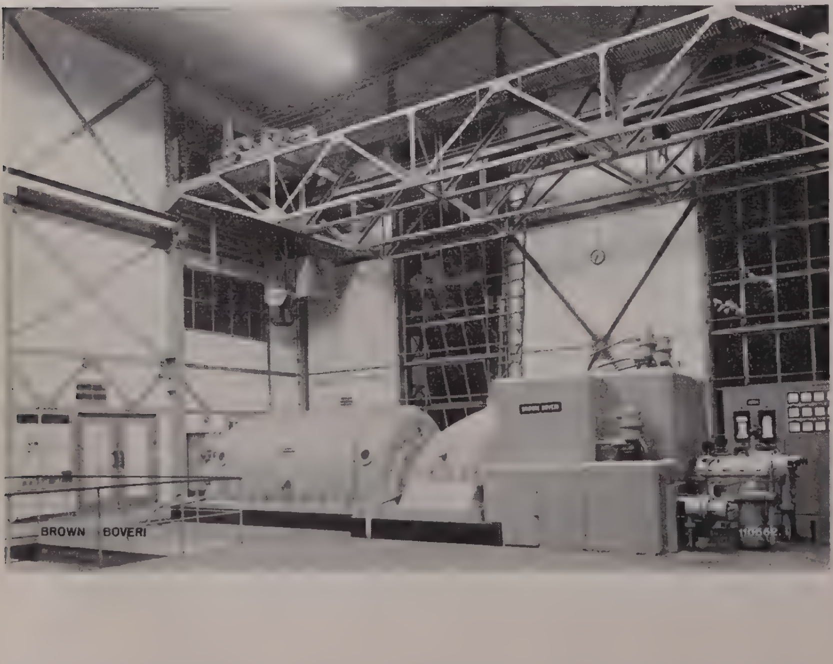

Fig. 4. – 20-MW condensing turbo-set supplied by Brown Boveri

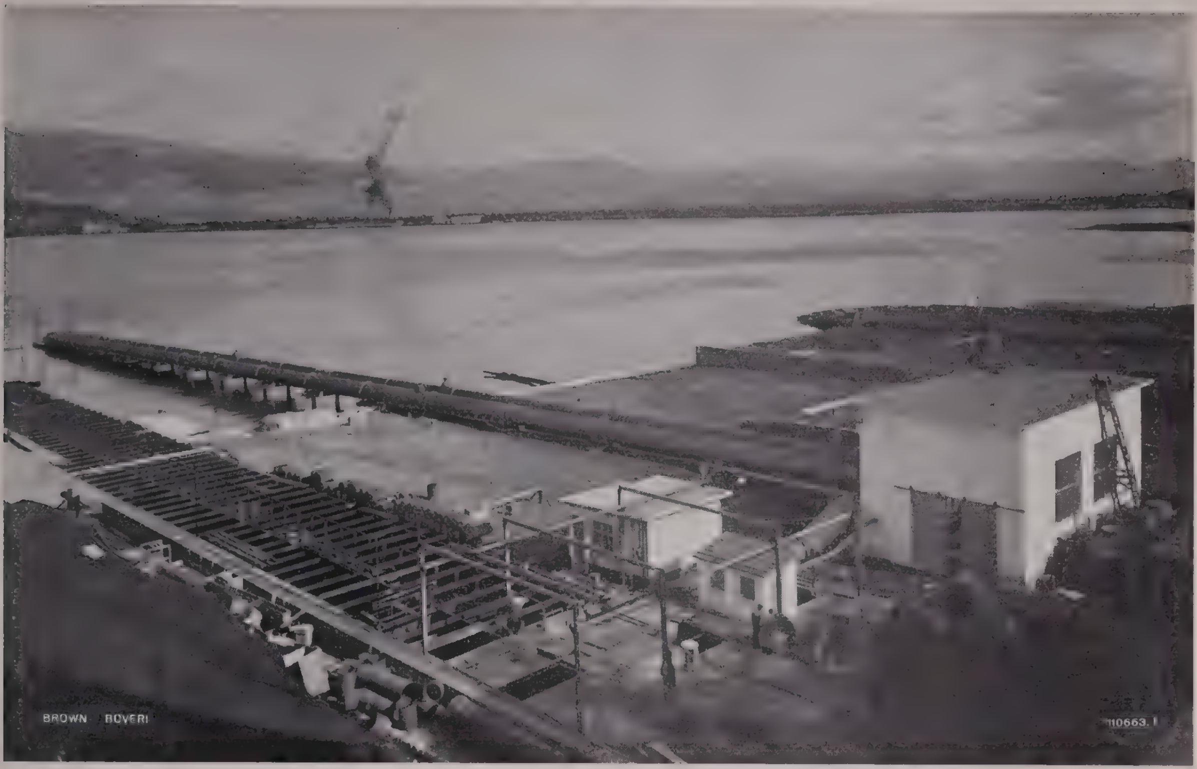

Fig. 5. – Pumping station for the cooling water, with two siphon pipes leading from the intake in the sea

Total length of the siphon pipes from intake to outlet	151 m
Diameter of pipes	140 cm
Max. rate of flow through one pipe	5500 m³/h
Water speed	1 m/s
Slope of the siphon pipes	1·5 %

installation would have been necessary, due to the unusually severe contamination near the shore. Detailed studies showed furthermore that such an installation could not be built near the shore, even on a continuous slab foundation, due to the unsuitability of the soil for building purposes—flooded loam, permeated by strong streams of water and reaching to considerable depth. The following solution appeared most economical. The intake would be at a distance of about 90 m from the shore and the water transferred by siphon pipes to a pump-shaft between the shore and the power-station building. The very moderate contamination at the intake at a depth of about 3 m simplifies the water-cleaning plant and thereby makes the power station more economical.

For present requirements, only one siphon pipe and two circulating pumps are necessary. However, with a view to later extension of the power station, the water supply plant was equipped for double capacity, i.e. two siphon pipes were installed.

The Siphon Pipes

The two siphon pipes are made of steel plate and were delivered from Switzerland in 10 m lengths to the site, where they were welded together. The finished pipes rest on small concrete platforms spaced at 10 m intervals between the pumphouse and the intake. These platforms rest on the seabed and are generously underpiled on account of earthquake danger, the force of the waves, and wind pressure

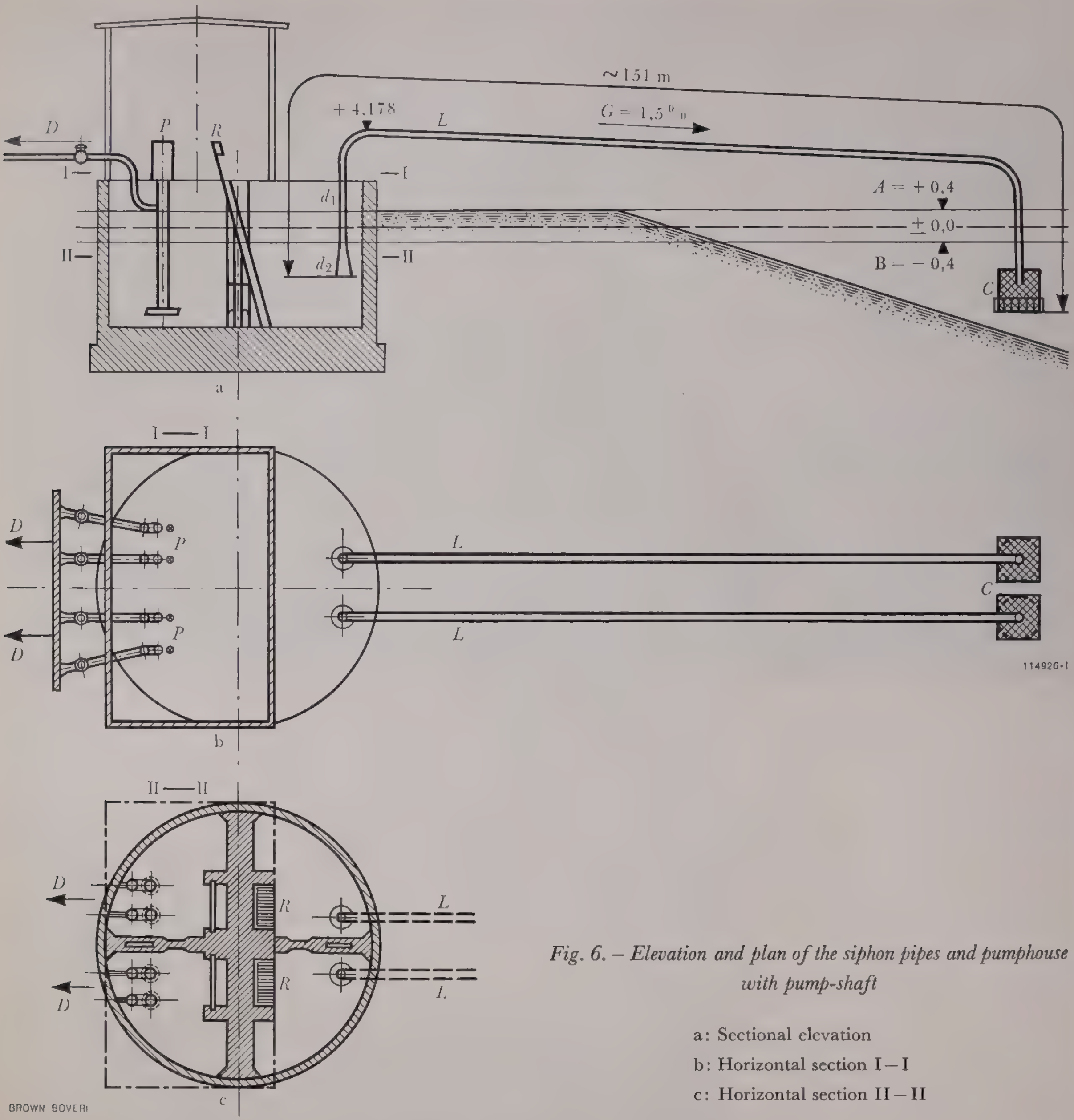

Fig. 6. – Elevation and plan of the siphon pipes and pumphouse with pump-shaft

a: Sectional elevation
b: Horizontal section I – I
c: Horizontal section II – II

$A - B$ = Difference in water level due to wave action and tides
C = Intake screen on the siphon pipes, with mechanical cleaner
D = Pressure pipes to the condensers
G = Slope
L = Siphon pipes
P = Cooling-water pump-set
R = Screen with mechanical cleaner
d_1 = 140 cm diameter of siphon pipes
d_2 = 180 cm diameter of the outlet bell of the siphon pipes in the pump-shaft

on the pipes. The pipes are on rollers and are anchored near the pumphouse, so that they expand towards the sea under the influence of temperature changes. The upper side of the pipes is painted a light colour and the underside dark to reduce the effect of temperature difference. The inner surfaces are treated with anti-corrosive paint. An elbow is fitted at the intake, equipped with a cylindrical, coarse screen, constructed of bars. The screen can readily be cleaned from the service platform at the

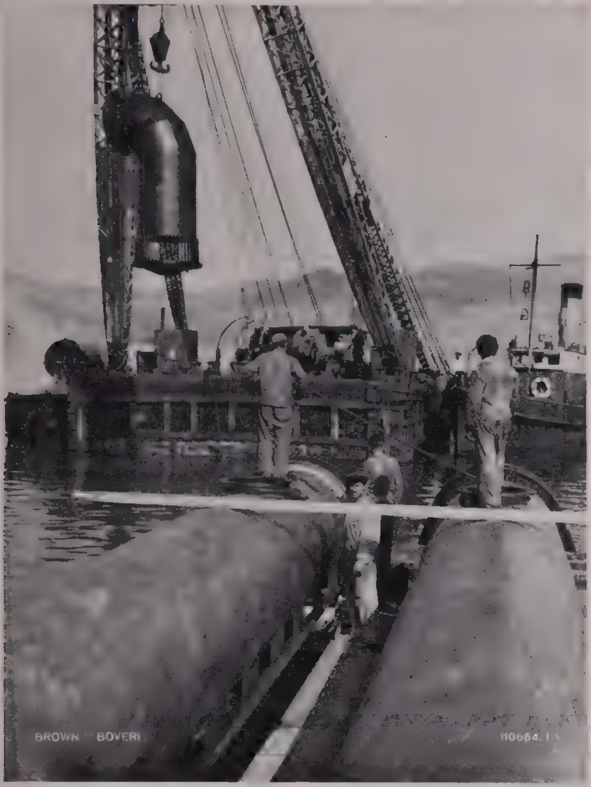

Fig. 7. – Placing the intake and coarse screen at the end of a siphon pipe by means of a floating crane

At the end of the two pipes can be seen the platform from which the mechanical cleaners of the screens are operated.

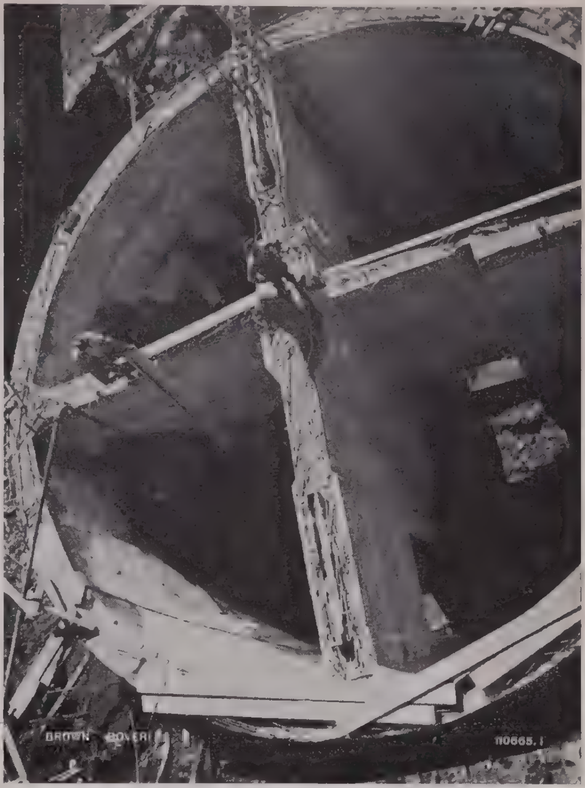

Fig. 8. – The concrete pump-shaft partly lowered during construction

Diameter of the shaft: 12 m

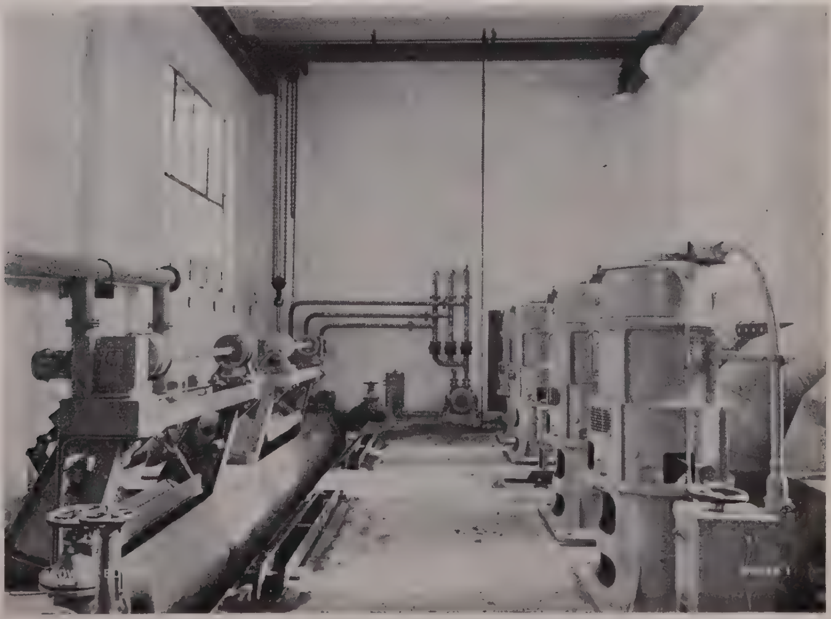

Fig. 9. – View inside the pumphouse

Right, the motors driving the four cooling-water pumps; left, the drives of the two automatic screen cleaners; in the background are the vacuum pumps serving the two siphon pipes.

surface. The outlet from the siphon pipes in the pumpshaft is bell-shaped, the diameter increasing from 1400 to 1800 mm.

The Pumping Station

Two vacuum pumps of different size are installed in the pumphouse for rapid evacuation of the siphon pipes. One pump handles 8200 litres of air per minute at 60–65% vacuum, with a power consumption of 20 h.p. The other, smaller pump handles about 1700 l/min, also at 60–65% vacuum, with a power consumption of 4·5 h.p. With both pumps in operation a siphon pipe can be evacuated in about 25 minutes. To prevent air from accumulating in the siphon pipes, only the small vacuum pump runs when the station is in operation.

The pump-shaft is divided into four compartments which can be isolated from one another. Fig. 8 shows the shaft during construction. In it there are two automatic screen cleaners and four vertical screw pumps. In order to attain the most favourable flow conditions and to minimize turbulence and wave motion, special attention was paid to the design of the structure inside the shaft. The kinetic energy of the water in the siphon pipe would cause the level in the shaft to fluctuate if the circulating pumps were to breakdown suddenly. Therefore the cover of the shaft was placed at such a height that it is not reached even when the maximum amplitude of about 800 mm is experienced. The soft soil permitted the concrete shaft to be constructed on the surface and gradually sunk as the excavation of the shaft progressed.

The pump-house is built on top of the shaft. In Fig. 9 the motors driving the four screw pumps can be seen on the right, with the drives of the two automatic screen cleaners on the left. Against the rear wall of the pumphouse are the two vacuum pumps and other pumps for emptying the shaft. The cooling water is piped under pressure from the pumphouse to the condensers in the power station. From there it flows back to the sea in an open channel.

(CI) E. KOHLMANN

BROWN BOVERI GAS TURBINES FOR AN INLET TEMPERATURE OF 750 °C

621.438

Following some introductory remarks on the quality of the fuel, the choice of constructional materials, cooling and the principle of the blading for gas turbines with a high inlet temperature, this article describes the Brown Boveri gas-turbine installations with an inlet temperature of 750 °C which are now in service and discusses the operational experience gained with them.

THE MAXIMUM admissible gas inlet temperature of a gas turbine is governed by a number of factors, of which the following are the most important:

1. The quality of the fuel.
2. The material used for the blading, rotor, turbine casing and the gas admission pipes.
3. The cooling of the parts directly in contact with the hot gases.
4. The system adopted for the blading, i.e. impulse or reaction.

Quality of the Fuel

Brown Boveri still hold the view that fuels with a high ash content are unsuitable for high-temperature gas turbines. When such fuels are used there is no really dependable means of keeping corrosion and incrustation of the blading in economically tolerable limits when the temperature before the turbine is more than about 620 °C. The well-known additives for the prevention of corrosion and incrustation are all either too expensive or inadequately effective. Many proposals have indeed been made in this respect, but they are still a long way from being economical in industrial applications [1].[1]

These considerations, however, must not be centered on the gas turbine alone, but must always risk the comparison with other prime movers, in order that the purchaser may be correctly advised. If other generating plants can utilize cheaper fuels, this must be taken into account accordingly. The use of the gas turbine is then governed by the suitability of the fuel. Hence we now take the view that, according to the present state of engineering progress, for an inlet temperature of 750 °C the only suitable fuels are either liquid fuels with an ash content of less than 20–30 ppm or gaseous fuels with a dust content between 1 mg/Nm^3, if the ash or dust contains aggressive ingredients. The latter include compounds of sodium, vanadium, zinc and lead. The figures mentioned above are only indicative of the approximate magnitude since, in practice, the dust or ash content is not the sole factor but, as already suggested, the proportions of the aggressive substances contained therein. This group of problems is a subject of its own and its detailed discussion would by far exceed the scope of this article. However, it is an established fact that the quality of the fuel largely determines the admissible temperature before the turbine.

Choice of Material

The designer can nowadays choose from quite a wide selection of materials. The heat-resistant steels which have lately come on the market are continually being tested by the major manufacturers in their laboratories to establish their creep limits, embrittlement, and so on. Also the degree of scatter in the fatigue-limit values obtained for the various materials have for the most part been investigated, as well as their resistance to corrosion and erosion. The designer will select the material which is best suited to the operating temperature of the material, and according to the fuel employed. With the special steels available today it is possible to build reliable gas turbines for a gas inlet temperature of 750 °C.

---

[1] The figures in brackets refer to the bibliography on p. 64.

Cooling

The designer is able to provide cooling for those parts which experience the highest gas temperatures. Provided the gas inlet temperatures are not too high, there is sufficient relatively cool air not required for combustion available for this purpose. With it rotors, blading, casings and piping can be kept at a safe temperature in spite of the high gas temperature. By expedient guidance of the stream of air at gas temperatures of 750 °C or more, it is possible to keep the temperature of the turbine rotor down to little more than 500 °C, so that it can be still made from ferritic steel.

For very high gas temperatures, particularly when the amount of excess air after combustion is small, and consequently insufficient air is available for cooling, it would be possible to employ water cooling; in other words, the turbine becomes a boiler. But this is then encroaching on the dual-cycle turbine which will not be discussed at this stage.

Principle of the Turbine Blading

Here it is possible to choose between three blading systems, the classical impulse system, reaction blading and the centripetal turbine. For large pressure ratios and input volumes the latter is unsuitable, but the other two types are both manufactured. At high input capacities the reaction turbine has a better efficiency than the impulse turbine. But since it is not the efficiency alone, but the permissible temperature before the turbine which decides whether a machine with high output and low fuel consumption can be built, the following factor must not be overlooked. The impulse turbine utilizes almost the whole of its pressure drop in the fixed row of blades. Since these are not subjected to centrifugal force they can be designed for lower stresses than the subsequent row of moving blades. Thus for the same temperature of the moving blades it is possible to raise the inlet temperature. On the other hand, since it is easier to cool an impulse turbine, one might be led to believe that it would be preferable for the gas turbine to be built as an impulse turbine. But this is only interesting and only benefits from the above advantages when the pressure drop can be utilized in a small number of stages. To attain a reasonable efficiency this is only possible with very high peripheral speed. But the latter leads, on the one hand, to high gas speeds and appreciable losses and, on the other, to increased centrifugal stresses in the blades and the rotor, and so to lower safety factors. Hence the gain from higher gas temperature is mostly offset by poorer utilization of the pressure drop. In the limiting zone of the moving blades the gas is retarded and the corresponding energy converted into heat. At high gas velocities, as are experienced with impulse blading, the temperature rise in the boundary layer is considerable. This increases the temperature of the material well above the mean gas temperature in the blade chamber, thereby reducing the advantage of impulse blading still further. Summarizing, it may be said that, although the impulse turbine permits a higher gas temperature than the reaction turbine, the latter attains practically the same performance as regards limiting output and fuel consumption for equal material conditions and at a much lower inlet temperature. Moreover, the machine with the lower inlet temperature is more reliable.

For these reasons Brown Boveri decided to adhere to the reaction turbine, after carrying out numerous experimental investigations into both systems. With lower stresses and gas inlet temperatures, but admittedly with slightly more material, it allows an economical machine with low maintenance costs to be built.

Having examined all these factors, the Company decided that, for certain applications, gas turbines would be built as reaction turbines for an inlet temperature of 750 °C, but for installations burning heavy oil, the temperature of 620 °C would be adhered to, as before. Thus, in contrast to other manufacturers, Brown Boveri produce two different types of gas turbine, one for 750 °C, the other only suitable for 620 °C, and are thereby in a position to offer reliable machines for all purposes.

Following these introductory remarks, a detailed description will be given of the gas turbines for 750 °C which have been installed so far, and their operational performance.

St. Dizier Gas-Turbine Station of Electricité de France

Terminal Output 6000 kW

The EdF had shown interest for some time in the gas turbine as a means of meeting peak-load demand. It appeared to be an ideal machine for their peak and emergency generating stations. The proposed plan was to erect such stations in areas of concentrated load in order to reduce the cost of power transmission. When the turbine was not running, the generator would be employed as synchronous capacitor and thus improve the power factor of the system.

In 1954 the EdF decided to order a gas turbine. Since machines with an inlet temperature of 620 °C had already proved their aptitude, there was no need to try out such machines for suitability. The desire of EdF was to obtain a machine for the highest possible temperature and efficiency, with the simplest design. On this account Brown Boveri decided to build a turbine for 750 °C at the inlet, of as simple and robust a design as possible. As a pilot plant it had not to be unduly large, therefore it was agreed that it should have a terminal output of about 6000 kW.

Before design work on the turbine could begin, though, a number of fundamental problems had to be settled. On the one hand the pressure ratio of the compressor should be made over 5, which of course could lead to the well-known trouble due to "stalling" during starting. On the other we wanted to keep to the tried reaction blading, for which the rotor would consist of discs and shaft extensions welded together, as had previously been the case. Since ductile, weldable, and easily forgeable ferritic material had to be used for the rotor, experiments had to be carried out to determine whether the

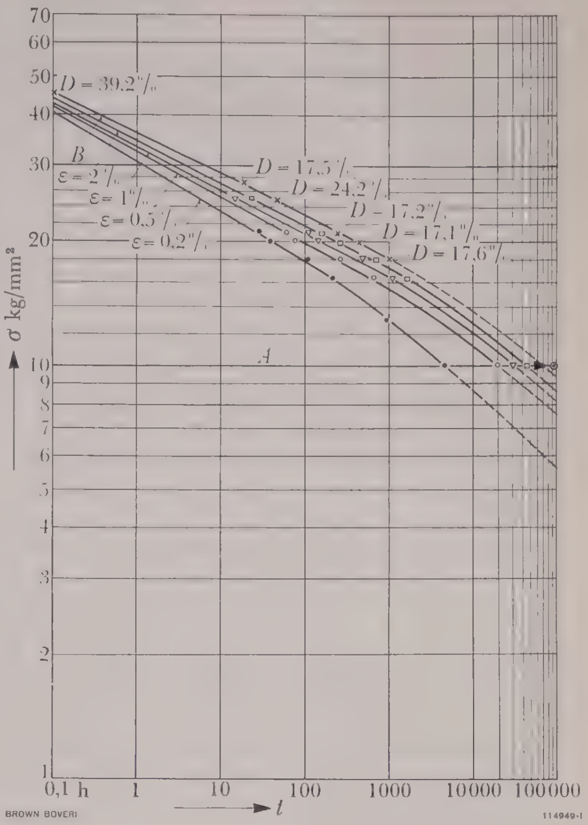

Fig. 1. – Creep-test curves for specimens of a material used for the blading of gas turbines for a thermodynamic inlet temperature of 720 °C

Test temperature: 700 °C
Abscissae: t = Time in h
Ordinates: σ = Load in kg/mm²

A = Specimen bar still unbroken after 95 600 h
B = Fracture curve
D = Elongation on fracture
ε = Creep elongation

In this diagram the points are plotted for ε = 0·2, 0·5, 1 and 2%, and for fracture. The dotted parts are extrapolations. The elongation of this material admittedly decreases with time but embrittlement is relatively slight, since the specimens still have a fracture elongation of 17% after 1000 h.

Specimen bars are still unbroken after being under test for 95 600 h at a load of 10 kg/mm². After this time the creep elongation amounts to 2·86%. From this diagram it can be seen that the extrapolation after 50 000 h was rather too cautious.

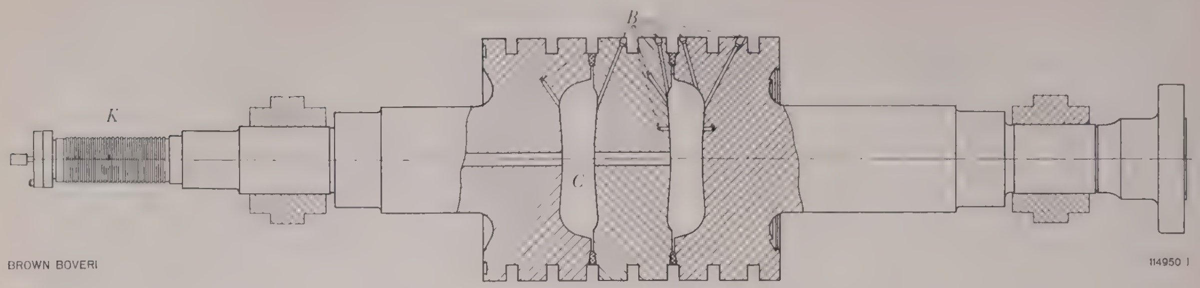

Fig. 2. – Section through the experimental rotor for the St. Dizier gas turbine of Electricité de France

Inside this rotor, holes *B* were bored to accommodate thermo-couples enabling the temperature to be measured at various points during run-up, on application of load, at steady load, while shedding load, and during the cooling period. The leads from the thermo-couples were run through a central hole *C* to the collector system *K* on the shaft extension, where brushes with compensated leads convey the readings to a temperature recorder. Thus the ambient temperature at the slip rings had no influence on the readings. A twelve-point high-speed temperature recorder with an error tolerance of ±2 °C was employed.

The drilled rotor was replaced by one without holes on completion of the experiments. Since such gas turbines have to be started up frequently and quickly, experimental rotors with holes are unsuitable for industrial service. They would run the risk of stresses being produced at the edges of the holes after several starts, the magnitude of which can amount to twice the normal figure and thus lead to cracking.

temperature of the rotor could be kept down to 500 ° C, when the gas entered at 750 °C. First the temperature in the rotor was calculated from first principles. To check the calculation an analogue test was undertaken in the electrolytic tank. These preliminary investigations confirmed that it was possible to construct a gas turbine for 750 °C with a ferritic rotor. A ductile, easily cast ferritic steel of the same quality as used for the 620 °C turbine was chosen for the cylinder of the turbine. Ferritic materials for the shaft and cylinder possess the great advantage of better thermal conductivity and smaller coefficient of expansion than austenitic steel, thus reducing the steady and transient thermal stresses. Consequently, by design measures and a good system of air cooling for the shaft and cylinder, we succeeded in employing the same materials, in spite of the gas inlet temperature being over 100 °C higher. Only the turbine blading had to be made of a more highly alloyed steel containing cobalt, which had been thoroughly tested in the creep-rupture laboratory, in anticipation. Up to the present this material has been tested for over 95 000 hours at 700 °C without fracturing (Fig. 1).

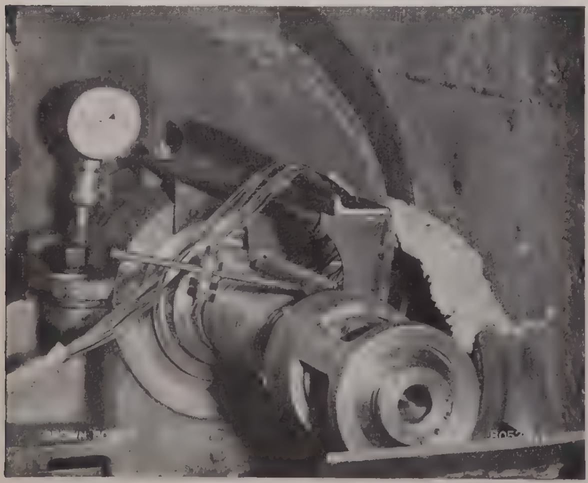

Fig. 3. – Collector system with brushes and compensated leads for picking up the thermal voltage

When the rotor is running at 4750 rev/min the peripheral speed at the brushes is about 22 m/s.

Since the St. Dizier turbine was, in effect, a prototype for a new series of gas turbines, it underwent comprehensive tests at full-load on the test-bed. In order to check the theoretical temperature distribution in the rotor obtained in the electrolytic tank, a special rotor was built, with holes bored from inside into which thermo-couples were inserted. By this means it was possible to measure the temperatures in the rotor during starting, during load-up, then at full load and finally on shut-down. The readings

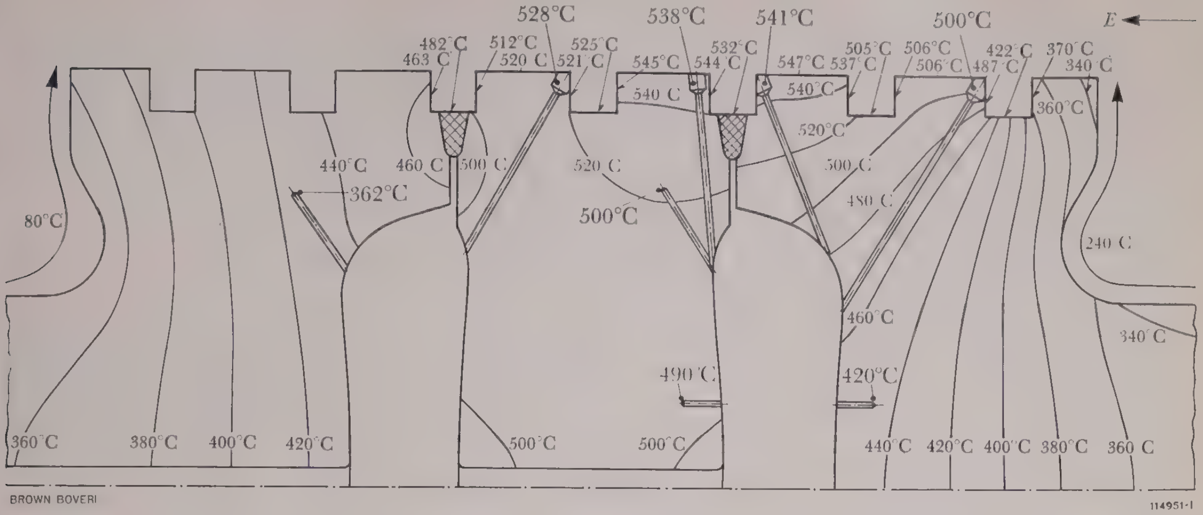

Fig. 4. – Steady-state temperature distribution in a gas turbine at full load

Gas inlet temperature before turbine: 750 °C
Cooling-air temperature on gas inlet side of rotor *E*: 240 °C

The plotted curves were obtained from calculation and by analogy in the electrolytic tank. The measurements recorded at steady full load are plotted as points. In the critical zone the calculated values agree very well with the measurements. For calculation allowance was made for the variation of the thermal conductivity with temperature, as well as the dissipation of heat in the hollow interior of the rotor by natural convection of the air enclosed therein.

from the thermo-couples were conducted to a slipring collecting system attached to the shaft extension of the rotor, and from there via copper brushes to a temperature recorder. In order to minimize the error, the compensation method was adopted (with zero current).

Fig. 2 shows a sectional elevation of the rotor and the collector system, Fig. 3 a close-up of the collector alone. The results obtained were very conclusive; not only did they agree closely with the calculated heat transfer from the hot gas to the surface of the rotor, and the conductivity between the body of the rotor and the blading when the machine was running at steady load; they also provided valuable information regarding the temperature gradient during starting and application of load, as well as during load removal and shut-down. Fig. 4 reproduces the steady-state temperature distribution in the gas-turbine rotor at full load. Fig. 5 shows the rise in temperature at various points during starting and loading. With the aid of these temperature curves it was possible to exactly determine the steady and transient thermal stresses.

The turboset could easily be run up to full speed in about ten minutes from cold. The amount of fuel consumed during starting, 150 kg, is equal to the amount consumed in three minutes at full load. Such a low consumption during starting is a pronounced advantage in a peak-load station where the machines are only in service for a few hours a day. The various curves plotted during a start of this kind are shown in Fig. 6.

The acceptance tests proved that the guarantees which had been given to the customer were on the safe side. The guaranteed and informatory values can be compared with measured values in Table I.

In order to test the control of the set, the change in speed was recorded during sudden load application and throw-off. From Fig. 7 it will be seen that, for a sustained deviation of 5·3 % the maximum momentary difference amounted to 6·8 %. The set also took up a sudden load of over 5000 kW. In this case the sustained speed was 4·2 %, with a maximum transient drop of 5·75 %.

Exhaustive measurements were also carried out to establish the behaviour of the compressor at

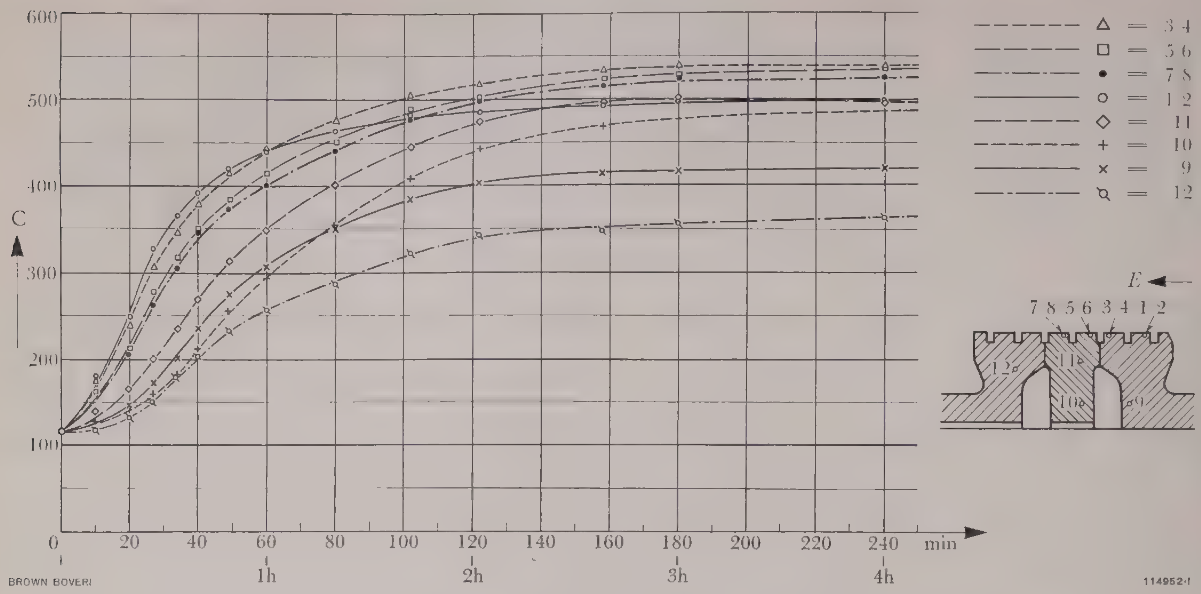

Fig. 5. – Transient temperature distribution in the rotor illustrated in Fig. 2 during starting and loading

Zero time was taken as the instant the combustion chamber was ignited. From these measurements it is possible to determine the thermal stresses. In the first and middle disc the maximum temperature gradients occur after about 40 minutes. At this point the stresses are a maximum, and afterwards they tail off.

E = Gas inlet side

different speeds; especially during starting it is very useful to know how the compressor and turbine behave at low speeds.

On completion of the acceptance tests in the presence of the customer, the set was run for ten days under operational conditions in the factory. During this period it supplied electricity to the works system running from 7 a.m. till 5 p.m. each day.

Since, as stated earlier, this set was intended for peak-load and emergency operation and, when the turbine was not running, the generator would be used as a synchronous capacitor, a clutch was fitted

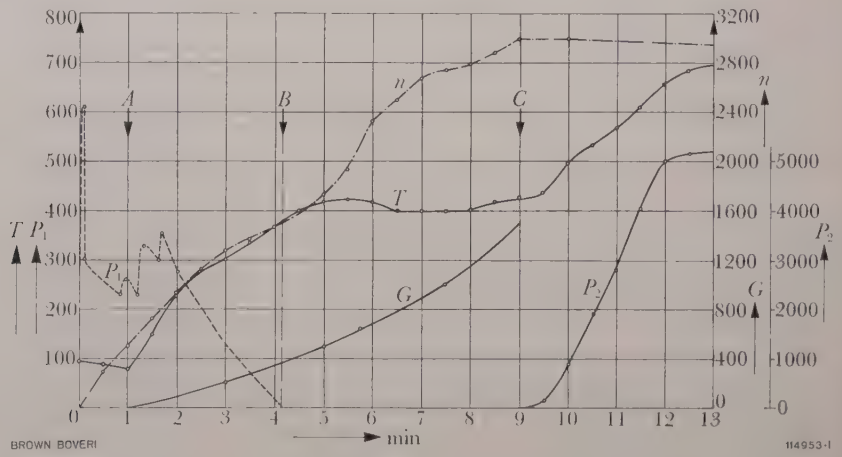

Fig. 6. – Starting diagram of the St. Dizier gas turbine

The total fuel consumption until the set reaches synchronous speed is about 150 kg, which roughly corresponds to the consumption in 3 min at full load or 5% of the full-load fuel consumption per hour.

Abscissae: Time in min

Ordinates:

T = Temperature before the turbine in °C

P_1 = Terminal rating of starting motor in kW

P_2 = Load on generator in kW

n = Speed of generator in rev/min

$G/10$ = Fuel consumption to reach full speed

A = Ignition

B = Starting motor switched off by inverse-power relay

C = Generator loaded

TABLE I

Guaranteed and informatory values supplied for the St. Dizier gas-turbine set compared with the figures measured during acceptance tests

	Units	Guaranteed and informatory values	Values measured during acceptance tests
Power at the generator coupling	kW	6080	6708
Thermal efficiency at the coupling	—	0·203	0·218
Air inlet temperature	°C	20	20
Air inlet pressure	kg/m² abs	10 300	10 300
Speed of the set	rev/min	4750/3000	4755/3004
Pressure ratio of the compressor	—	5·53	5·28
Temperature at compressor outlet	°C	241	222
Temperature at turbine inlet	°C	750	706
Quantity of air	kg/s	56·0	57·2
Thermodynamic efficiency of the gas turbine	%	—	87·3
Thermodynamic efficiency of the compressor	%	—	88·0

between the turbine and the generator (Fig. 8 and 9) enabling them to be coupled and uncoupled in service. It is thus possible for the generator to be permanently connected to the system. If the set is required to generate electricity, the gas turbine is run up by the starting motor and, on reaching full speed is coupled to the generator and loaded. Conversely, when the load has been completely removed, the turbine can be uncoupled and stopped, while the generator continues to run as synchronous capacitor.

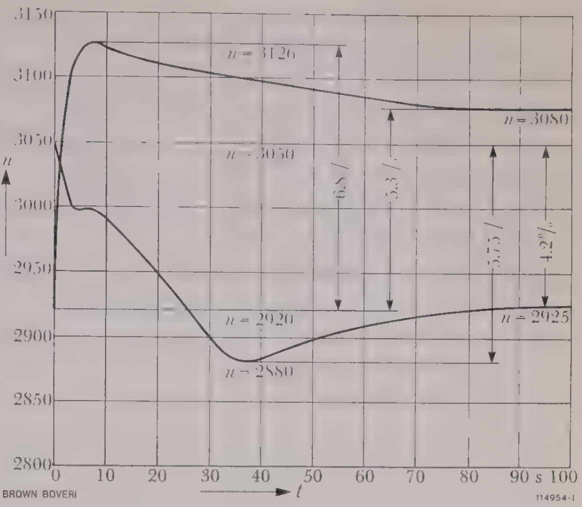

Fig. 7. – Speed change caused by sudden application or removal of load on the St. Dizier gas turbine

The generator load was simulated by a water resistance.

Abscissae: t = Time in s
Ordinates: n = Speed in rev/min

Upper curve: Sudden reduction from 5250 kW to no-load. The speed at full load was 2920 rev/min, temporarily increasing by 6·8% and remaining with a sustained deviation of 5·3%.

Lower curve: Sudden increase from no-load to 5250 kW. The no-load speed was 3050 rev/min which decreased temporarily by 5·75% and sustained 4·2%.

During the tests in Baden the turbine ran on a distillate fuel with the properties shown in Table II. At St. Dizier (Fig. 10) it ran at first on domestic fuel oil and, more recently, changed over to heavy oil with a high viscosity and high sulphur content but low ash content (see Table II). Firing with these fuels did not result in any appreciable blade corrosion. Since this is an experimental machine as far as EdF is concerned, preparations are at present being made to enable it to burn still heavier fuels with a higher ash content in the future. These fuels will require suitable treatment before use.

The total number of running hours of the St. Dizier gas turbine is low because it is normally used only in the winter for about four hours a day. By the end of 1959 the total was only 2000 h, but in this period it had started no fewer than 580 times.

The success of this gas turbine, both as regards its mechanical performance and the output and fuel consumption achieved, which may be attributed to

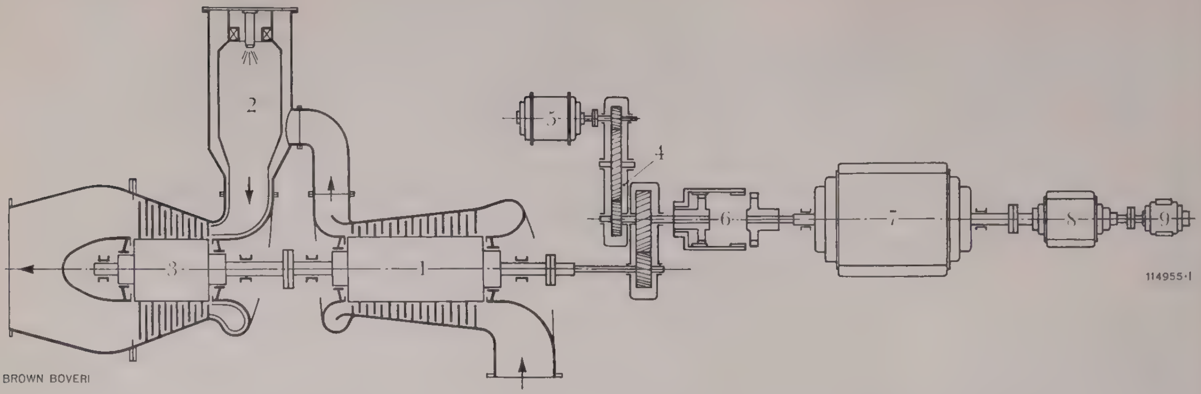

Fig. 8. – Schematic layout of the St. Dizier gas-turbine set with a clutch between the turbine and the generator

The starting motor of the turbine is not coupled to the shaft extension of the generator, but to the gearing between the generator and the compressor, in order that it may start the turbine when the generator is running.

1 = Compressor	4 = Gear train	7 = Generator
2 = Combustion chamber	5 = Starting motor	8 = Generator starting motor
3 = Gas turbine	6 = Clutch	9 = Exciter

the thorough investigation of all new problems encountered, encouraged us to release a further number of sets of the same design for sale.

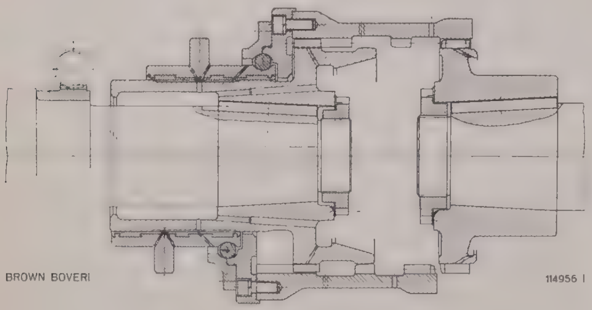

Fig. 9. – Clutch of the St. Dizier gas-turbine set

It permits the generator to be permanently connected to the power system. If a power output is required, the gas turbine is started up by means of its starting motor and, when it has reached its synchronous speed, is coupled with the generator by a synchronizing device. The clutch is always engaged or released at no-load. The synchronizing device is not visible in the sketch.

Upper half: Clutch engaged
Lower half: Clutch disengaged

Gas Turbine of Niederrheinische Hütte AG. Duisburg, Germany

Power at Coupling, 6000 kW

This installation (Fig. 11 and the coloured plate inside the front cover) is practically the same size as that at St. Dizier. Thus the same components could be used for the high-temperature part of the turbine. For Duisburg, where the set has to run at low loads and burns blast-furnace gas, it was stipu-

TABLE II

Properties of the fuels used in the St. Dizier gas turbine

	Units	Fuel used for accep-tance test	Domestic fuel oil used in St. Dizier	Heavy fuel oil used in St. Dizier
Specific weight at 20 °C	g/cm^3	0·832	0·84	1·011
Viscosity at 20 °C	cSt	4·11	5·6	9478
Lower calorific value	kcal/kg	10 140	—	—
Sulphur content	%	0·8	1·16	1·5
Ash content	ppm	traces	12	17
Composition of ash:				
V_2O_5	%	—	21·4	2·3
Na_2O K_2O	%	—	14·2	3·2
CaO	%	—	—	1·6
MgO	%	—	—	< 1·0
SO_3	%	—	—	23·0

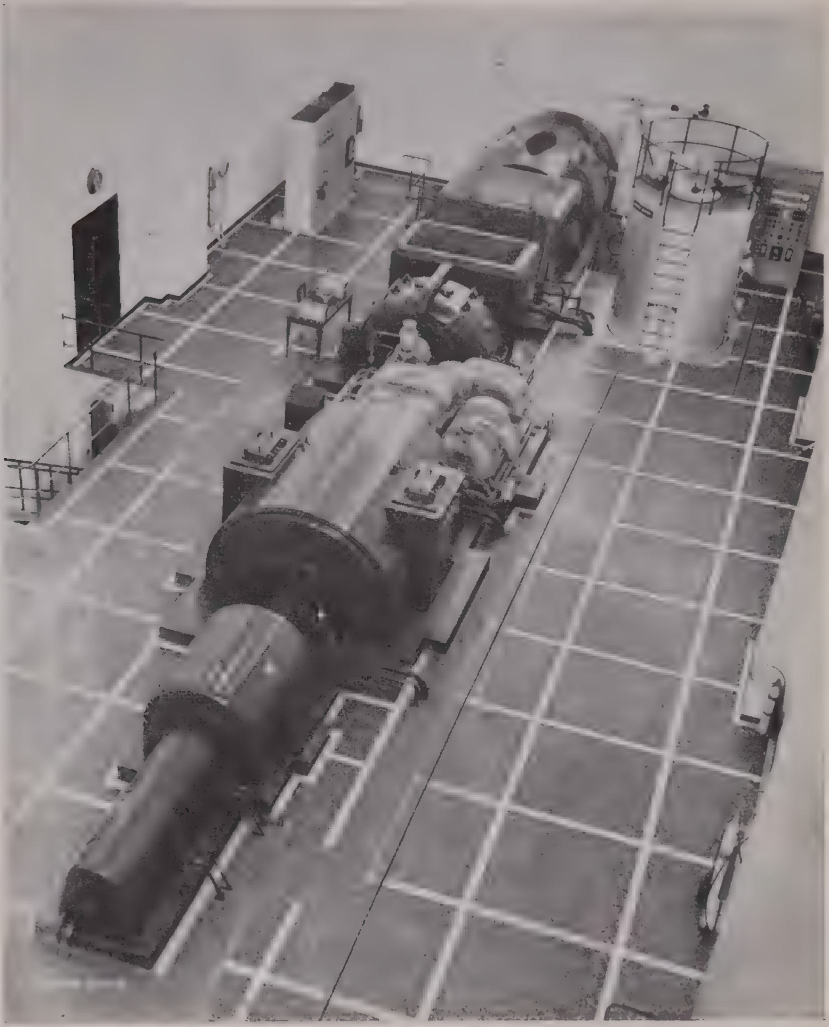

Fig. 10. – View of the gas-turbine set at St. Dizier, France

By the end of 1959 the set had completed 2000 hours in service with 580 starts. In the background is the gas turbine with its axial outlet pipes, beside it the combustion chamber and the control board with the thermal instruments. Successively towards the front are the compressor, the gear train with the clutch system and the turbine starting motor, and the generator with its starting motor and exciter.

lated that the machine should have a low fuel consumption at partial loads. Now it is well-known that gas turbines whose compressors run at constant speed have a high fuel consumption at partial load [2]. Therefore for this installation a two-shaft machine had to be provided (Fig. 12). Since, with this arrangement, the h.p. turbine does not give up any useful power outside the set and must therefore always be in equilibrium with its compressor, but the power balance can be disturbed by external influences, such as variation in the intake temperature and the degree of contamination of the blading, it is necessary for a means to be provided to compel the maintenance of this equilibrium. In this plant the first row of stationary blades in the l.p. turbine can be moved. When they are opened, the pressure between the h.p. and l.p. turbines is reduced, so that the enthalpy drop is increased in the h.p. turbine and a power deficit on the part of the h.p. line is corrected. Conversely a surplus of power due to low intake temperature can be reduced by closing the blades. Each blade in this row is pivoted in a bearing and connected through a linkage to a ring which actuates all the blades. The ring itself is hydraulically controlled by an oil servomotor (see Fig. 13).

This machine commenced regular industrial service in the early part of 1957 and by the end of 1959 had completed 14 500 hours service with about 100 starts.

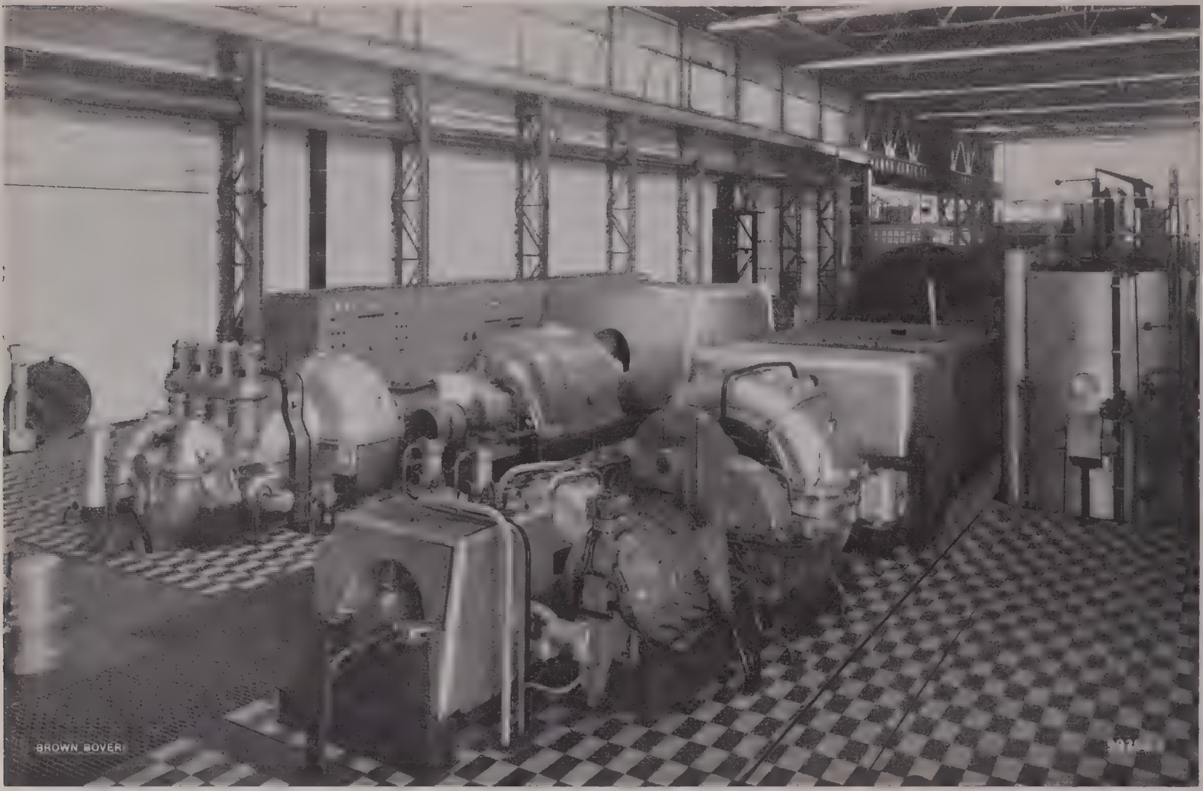

Fig. 11. – Gas-turbine set at Niederrheinische Hütte, Duisburg, Germany

In the foreground from left to right: Blast-furnace gas blower, starting motor, gear, combustion air compressor, h.p. gas turbine; to the right of the latter is the combustion chamber. In the rear line, also from left to right: furnace blower, exciter, gear, generator, l.p. gas turbine.

Table III lists the running hours of the set over a period of several months. From May 1st, 1955 till October 25th, 1959 it was in operation for a total of 4080 hours out of the possible 4272, i.e. an availability factor of 96 %. The acceptance tests were carried out on July 17th and 18th, 1959 by the Technischer Überwachungsverein, Essen, and confirmed the guarantees given. The results of a subsequent check after 13 000 hours at the beginning of November 1959 are also rather interesting as comparison (Table IV). For the latter measurements the gas preheater was cut out, for reasons which will be given later.

As regards the operational experience gained with this set, the following may be said: two notable difficulties were experienced. A resonant torsional oscillation in the compressor caused the gearing between the h.p. line and the gas compressor to break down in October 1958. Whereas such oscillations are well-known in piston engines, and the crankshafts of new designs are examined to check their oscillation range, it is not usually considered necessary to check turbines because they produce a constant torque. Since the gear teeth were loaded on both flanks, it must be assumed that, by chance, an oscillation coincided with the service speed. By changing the masses in the gear-train and uncoupling the starting motor after run-up, it was possible to eliminate this resonance phenomenon.

A second phenomenon, previously unknown, occurred in the gas preheater. The air and gas preheaters are of identical pattern, a cross-current of air or fresh gas flowing between the heater tubes which carry the exhaust gas (Fig. 14). The tubes are held in the tube-plate by rolled joints (Fig. 14a). Although the air and gas preheaters are identical,

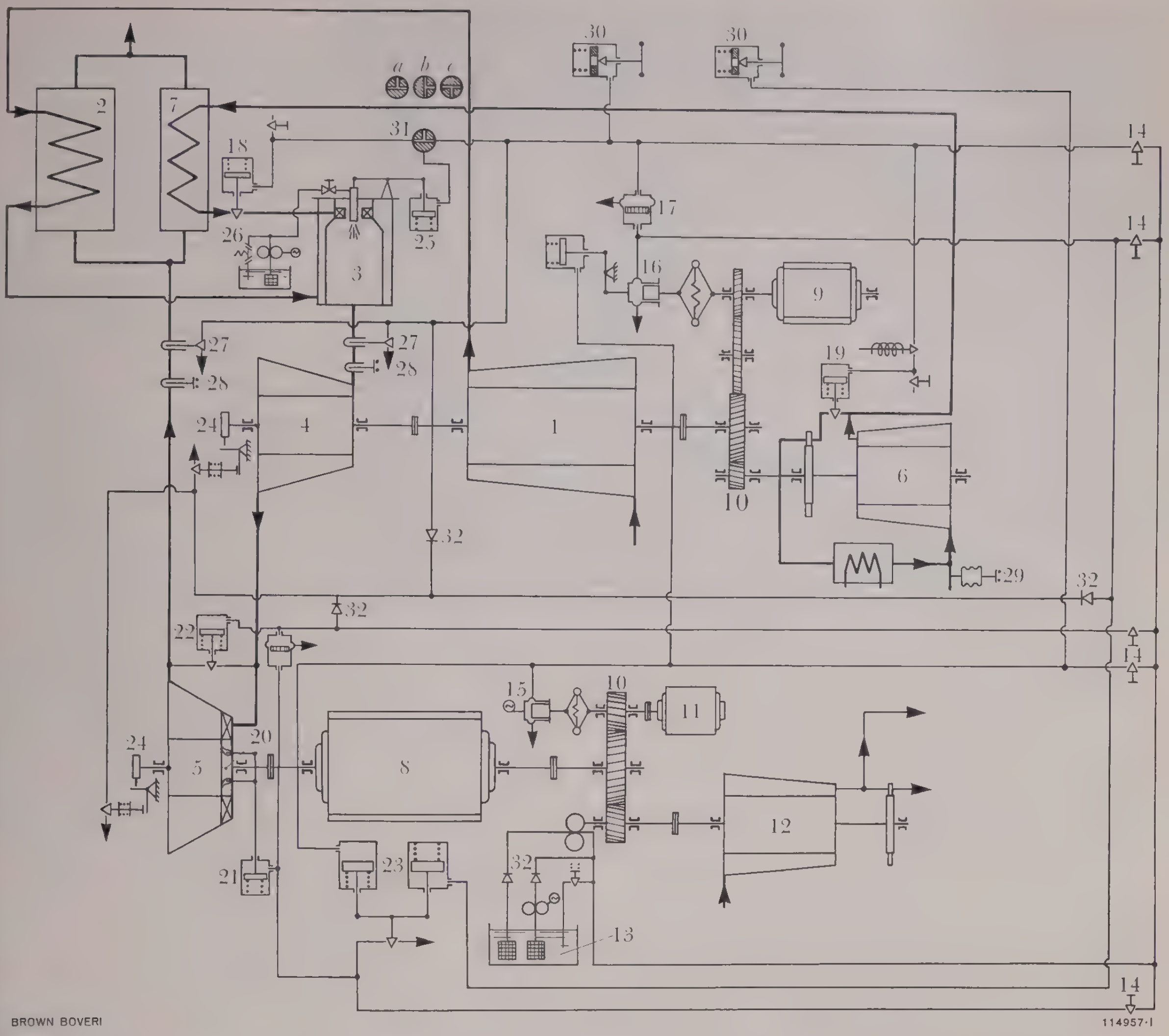

Fig. 12. – Simplified thermal and control circuit of the gas-turbine set of Niederrheinische Hütte, Duisburg, Germany

1 = Air compressor
2 = Air pre-heater
3 = Combustion chamber
4 = H.P. gas turbine
5 = L.P. gas turbine
6 = Gas compressor with recuperation turbine
7 = Gas pre-heater
8 = Generator
9 = Starting motor
10 = Gear
11 = Exciter
12 = Furnace blower with recuperation turbine
13 = Oil tank for lubrication and control, with direct-driven main pump and motor-driven auxiliary pump for starting
14 = Adjustable orifices
15 = Centrifugal governor of the l.p. line
16 = Centrifugal governor of the h.p. line
17 = Pressure transducer
18 = Gas regulating valve
19 = Regulating valve of the recuperation turbine for the gas compressor
20 = Adjustable stationary blades of l.p. turbine
21 = Power piston for adjusting 20
22 = Bypass valve
23 = Servo-motors for regulating the oil pressure of piston 21
24 = Safety governor
25 = System regulating the flow to the firing nozzle when burning fuel oil
26 = Feed pump for fuel oil
27 = Regulating thermostats
28 = Safety thermostats
29 = Pressurestats for the back pressure in the gas line
30 = Manually operated starting valves
31 = Changeover valve from gas to oil firing
  a = Gas alone
  b = Oil alone
  c = Gas and oil together
32 = Non-return flaps

TABLE III

Showing the numbers of hours per month during which the gas turbine of the Niederrheinische Hütte was running, up to September 1959, producing electricity and blast air

Year		1958			1959								
Month		Oct.	Nov.	Dec.	Jan.	Feb.	Mar.	Apr.	May	June	July	Aug.	Sept.
Availability factor for power generation	%	83	96	76	100	98·5	Idle during modifications	Idle during modifications	85	91	81	77·5	94
Load factor of generator	%	75	79	74	77	87			77	70	64	64	67·5
Availability factor for blast generation	%	87	96	76	97	98			85	91	79	76	94
Load factor of the blast blower	%	82	50	60	83	86			74	73	79	76	78

TABLE IV

Gas turbine of the Niederrheinische Hütte, Duisburg

Guaranteed and informatory values are compared with figures measured during a check by the Technischer Überwachungs-verein (TUV), Essen on November 7/8th, 1959, when the machine had completed 13 000 hours running.

The figure quoted is the one at which optimum thermal efficiency is obtained. The actual readings during the check measurements were: Air inlet temperature 7 °C, speed of blower 4290 rev/min, gas inlet temperature 755 °C and power at generator coupling 6650 kW.

	Units	Guaranteed and informatory values	Check measurements by TUV after 13 000 h in service Optimum
Power at the generator coupling	kW	5820	6110
Thermal efficiency at the coupling	—	0·27	0·286
Air inlet temperature	°C	15	5
Gas inlet temperature	°C	750	750
Exhaust-gas temperature in chimney	°C	—	326
Pressure ratio of compressor	—	5·13	5·0
Speed of blower set	rev/min	maximum 4750	4054
Speed of generator set	rev/min	3000	3000

the latter failed after a few thousand hours. The rolled joints in the lower tube-plate were leaking. On inspection, some of the tubes were found to have their bottom ends squeezed together and even broken off. Since no such phenomenon has ever been observed with any of the air preheaters, it was assumed to be due to the blast-furnace gas. A detailed investigation gave the following explanation. The gas contains mainly carbon monoxide and hydrogen as combustible ingredients. Now CO is only completely stable above about 600 °C. Below 300 °C its decomposition is so slight that it may be considered stable. In the presence of fine iron dust, as in blast-furnace gas, or when in contact with oxidized surfaces, the following chemical action takes place at temperatures between 300 and 600 °C

$$2\ \mathrm{CO} + \text{catalyst} = \mathrm{CO_2} + \mathrm{C}$$

which releases carbon. Since the lower tube-plate of the gas heater is at a temperature of about 400 °C, this action can take place there, the oxidized surface of the heater tube acting as the catalyst. In the gap between the tube and the tube-plate—a microscopically narrow gap is always present—carbon is deposited from the gas, which occupies a much larger volume and eventually squeezes the tube. The tube behaves exactly as if it had been subjected to external pressure. At the upper tube-plate no such phenomenon was observed, thus proving that it does not take place at the temperature

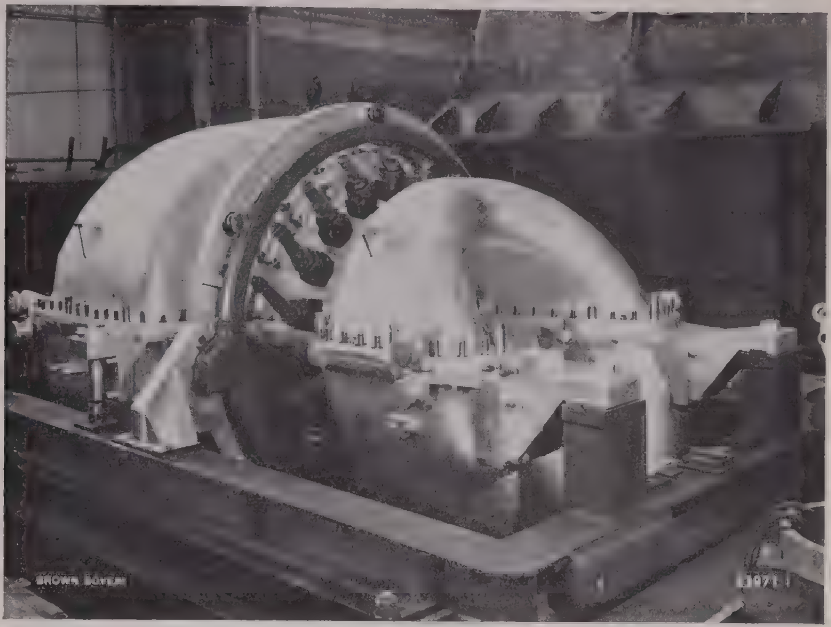

Fig. 13. – Low-pressure gas turbine at Niederrheinische Hütte, Duisburg, showing the mechanism for rotating the first row of stationary blades (see also Fig. 12)

of 200 °C, as prevails there. Gas preheaters with over 50 000 hours service have confirmed this. Consequently it was decided that all gas preheaters would be changed over to air.

Except for these two difficulties the machine has rendered excellent service. Nevertheless an appreciable amount of corrosion has been experienced at the blading, due to the composition of the dust which is drawn in with the air and the blast-furnace gas, in spite of good cleaning by electrostatic precipitators. Efforts are being made to overcome this problem too. On more than half a dozen gas turbines

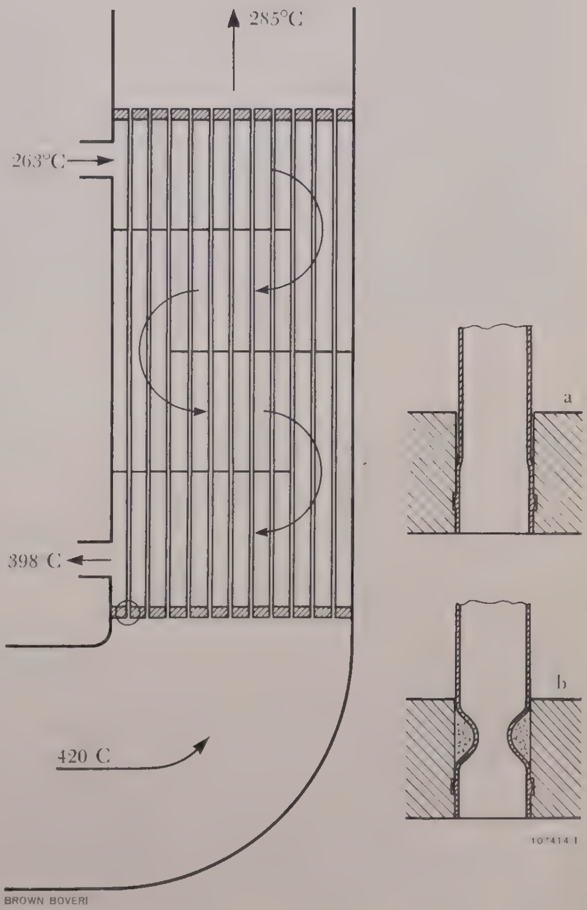

Fig. 14. – Principle of the gas pre-heater

The turbine exhaust gases flow upwards through the heater tubes. The gas or air to be heated flows from the top downwards between the tubes in cross-flow.

a: Shows a close-up of the rolled joint at the tube-plate. The tubes are rolled exactly flush at the hot bottom end and the cold top end.

b: The end of the tube has been squeezed by the deposit of carbon between the tube and tube-plate, produced by the catalytic action on the carbon monoxide of the iron oxide on the surface of the tubes. The carbon's increase in volume continued until the pressure squeezed the end of the tube inwards. In some cases it completely squashed the end of the tube.

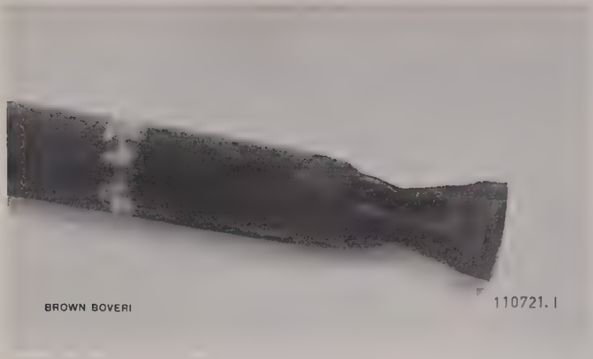

Fig. 15. – The end of the heater tube squeezed as in Fig. 14.

It looks as if the tube had been subjected to a high external pressure. The typical squeezing folds can be recognized. This phenomenon takes place between 300 and 600 °C. In this range the carbon monoxide is unstable in the presence of iron oxide as catalyst and decomposes, forming CO_2 and C.

in steelworks it has been established that the rate of incrustation in the compressors and turbines, and the corrosion rate of the turbine blading, not only depends on the quantity of dust in the gas and air, but primarily on the composition of the dust. It is impossible to lay down any hard and fast rule; the conditions vary from one steelworks to another. To judge from our own experience in a large number of works we estimate that the incrustation rate and corrosion rate, given the same degree of filtration of the air and gas, may vary in the ratio 1:10. Installations have been inspected which, after 10 000 hours service, exhibited neither severe corrosion nor marked incrustation. When a compressor in one steelworks was examined for the first time after 11 000 hours, it was still as good as new and did not require cleaning, even after this length of time.

As a result of the experience gained, we are now in a position to give customers very exact advice. The information provided by one or two machines in a particular steelworks is not enough to allow a generally valid statement to be made. It is essential to collect information from several places over a reasonably long period before correct advice can be offered. With this object systematic investigations were carried out with pilot plants in several countries, enabling us to judge the effect of a given quantity and composition of dust on the corrosion and incrustation rates. As an example, Fig. 16 shows the corrosion rate of the same steel in four different steelworks, three in Germany, one in France. The gas was taken from the gas line following the cleansing plant, and the quantity and composition of the dust measured. The dust content corresponded to that in gas engines which are also employed in one of these works.

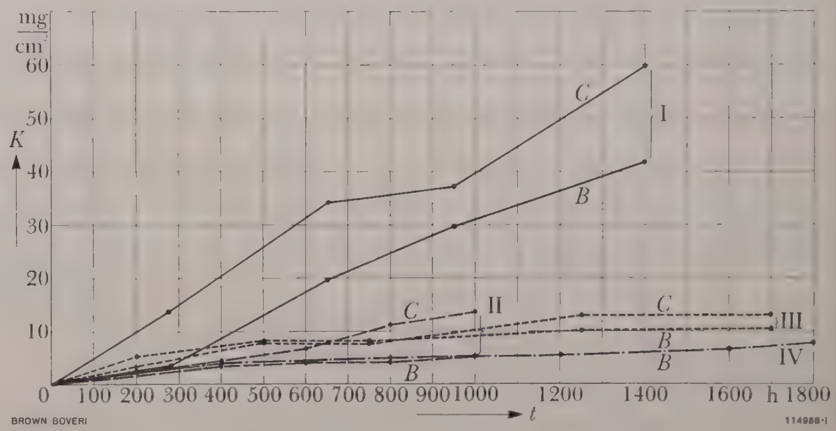

Fig. 16. – Corrosion tests with pilot plants in steelworks

t = Duration of the test in hours
K = Loss due to corrosion in mg/cm²

The curves show the different corrosion losses of the austenitic steels B and C used for gas-turbine blades.

I = Corrosion tests in steelworks I
II = „ „ „ „ II
III = „ „ „ „ III
IV = „ „ „ „ IV

It will be observed that the corrosion rate varies with the material used, and differs appreciably from one steelworks to another. The difference between I and IV is remarkable. The composition of the dust in the blast-furnace gas differed noticeably from one works to the next. In every case the dust content was measured after the gas-cleaning plant. The gas thus had a dust content equivalent to the gas used for piston engines.

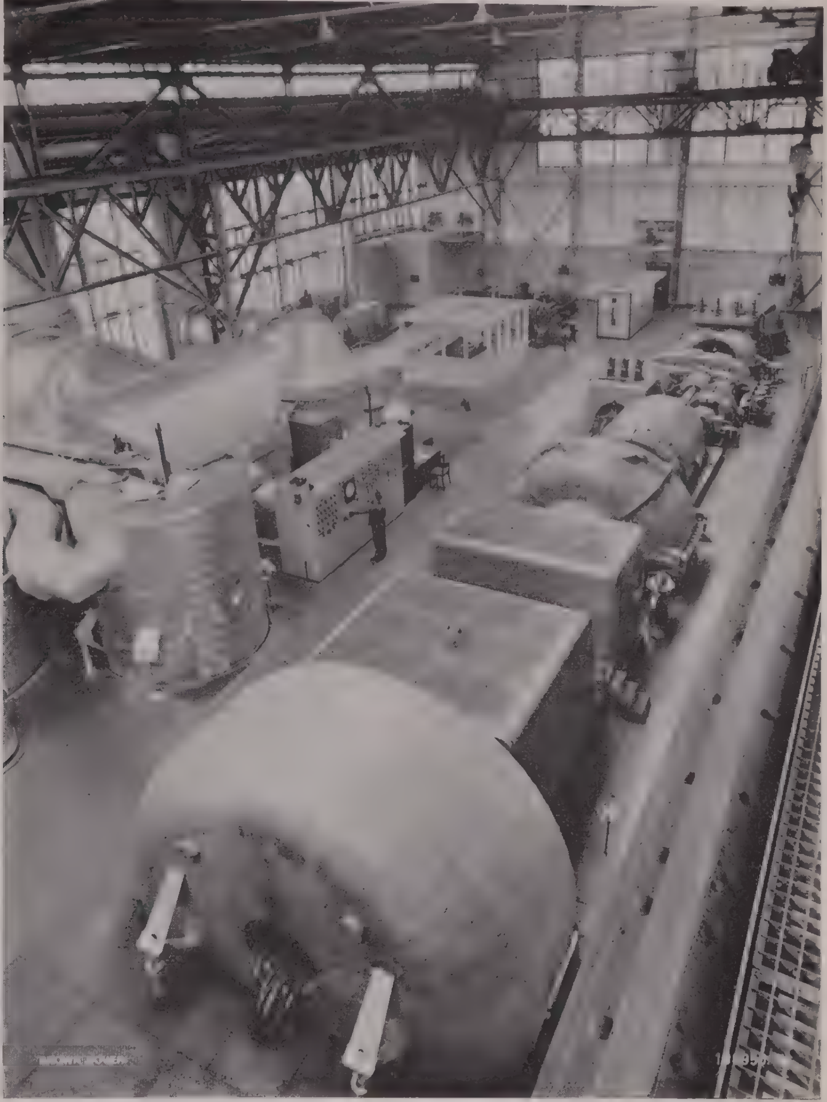

Fig. 17. – Gas-turbine set at the Klöckner steelworks, Hagen-Haspe, Germany. Terminal output without blast blower 15 000 kW

At the front is the gas turbine with combustion air compressor, starting motor and gas compressor, gear and blast blower. On the left is the combustion chamber and switchboard, with the air and gas pre-heaters in the background.

To what degree cleansing of the gas, and possibly the air too, should be taken can only be settled by collaboration with the customer. This requires knowledge of the dust content of the air and the gas, as well as the composition of the dust.

Gas Turbine at the Klöckner Steelworks Hagen-Haspe, Germany

Power at the Coupling 15 000 kW

This company ordered a gas turbine in 1955, to act as a base-load machine (see Fig. 17). Since operation at partial load was ruled out, it was decided that a single-shaft machine would be supplied since, although the fuel consumption is quite high at partial loads or when idling, the layout and control of the set is much simpler than that of a two-shaft machine (Fig. 18).

In July 1958 comprehensive measurements were taken to provide exact details of this machine's performance. Table V contains the measured and guaranteed or informatory figures for this installation. Up to December 1st, 1959 this machine had completed 9330 hours running with 161 starts. The majority of these starts occurred during the commissioning period and while the staff were under

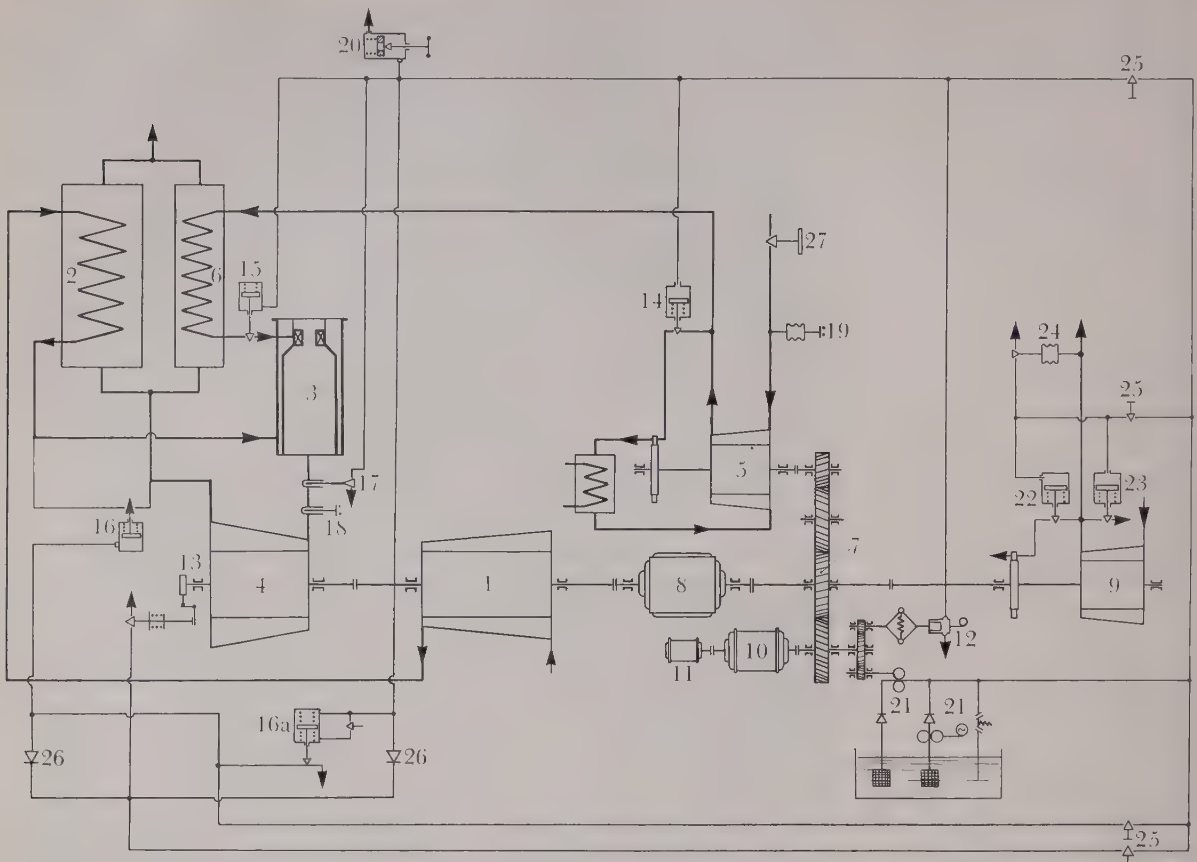

BROWN BOVERI

114959-I

Fig. 18. – Thermal and control circuit of the gas-turbine set at the Klöckner steelworks, Haspe

1 = Air compressor
2 = Air pre-heater
3 = Combustion chamber
4 = Gas turbine
5 = Gas blower with recuperation turbine
6 = Gas pre-heater
7 = Gear
8 = Generator
9 = Blast blower with recuperation turbine
10 = Starting motor
11 = Exciter
12 = Centrifugal governor
13 = Safety governor
14 = Valves for recuperation turbine 5
15 = Gas regulating valve
16 = Blow-off valve
16a = Oil-pressure control for valve 16
17 = Temperature regulator
18 = Thermostat before the turbine
19 = Pressurestat in the gas pipe
20 = Starting valve for the gas turbine
21 = Pumps for lubricating and control oil
22 = Regulating valve for recuperation turbine of the blast blower
23 = Blow-off valve of the blast pipe
24 = Pressure regulator for the blast
25 = Throttle valves
26 = Non-return valves
27 = Manually operated stop valve

tuition, and accounted for 110. Also counted in the starts were the brief interruptions caused by excessive voltage drop in the steelworks. Such interruptions due to external circumstances were sometimes experienced several times in a single day. At other times the set ran for several months without interruption, and thus almost all the time at full load. The average gas inlet temperature was 740 °C. Before compression, the blast-furnace gas is passed through an additional electrostatic precipitator and the combustion air through a rotary oil filter. The machine was shut down at the beginning of

TABLE V

Gas-turbine set at Haspe

Guaranteed and informatory values compared with readings measured on July 25th, 1958

	Units	Readings obtained July 25th, 1958	Readings converted to guarantee conditions	Guaranteed and calculated figures
Terminal output	kW	15 170	—	—
Power at the coupling	kW	15 625	16 570	14 000
Thermal efficiency at terminals	—	0·251	—	—
Thermal efficiency at coupling	—	0·2585	0·269	0·272 ±5%
Air inlet temperature	°C	21·1	15	15
Air inlet pressure	kg/m² abs	10 190	10 000	10 000
Gas inlet temperature	°C	55	—	50
Gas inlet pressure	kg/m² abs	10 185	—	10 100
Speed	rev/min	3060	3000	3000
Temperature after air combustion chamber	°C	228·7	—	214
Pressure after air combustion chamber	kg/m² abs	53 160	—	51 000
Temperature after gas compressor	°C	282·7	—	263
Pressure after gas compressor	kg/m² abs	55 010	—	53 500
Temperature before turbine	°C	746	—	750
Utilization factor of air preheater	—	0·74	—	0·78
Exhaust-gas temperature in chimney	°C	293	—	260
η_{pol} of air compressor	—	0·87	—	—
η_{pol} of gas compressor	—	0·85	—	—
η_{pol} of turbine	—	0·86	—	—
Quantity of air	kg/s	134	—	135
Lower calorific value of wet gas	kcal/kg	723	—	782

December 1959 and thoroughly inspected. After 9330 hours running it was in excellent condition and only a very slight amount of corrosion was detected. Fig. 19 shows the state of the turbine blading when the machine was opened up. As can be seen, the amount of incrustation is very small.

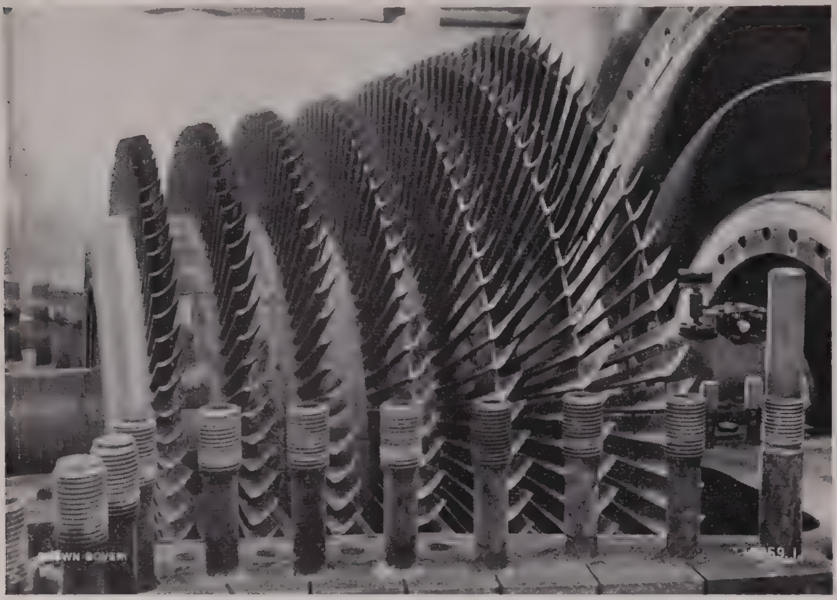

Fig. 19. – Rotor blading of the Haspe gas turbine after 9330 hours service with blast-furnace gas at an inlet temperature of 750 °C

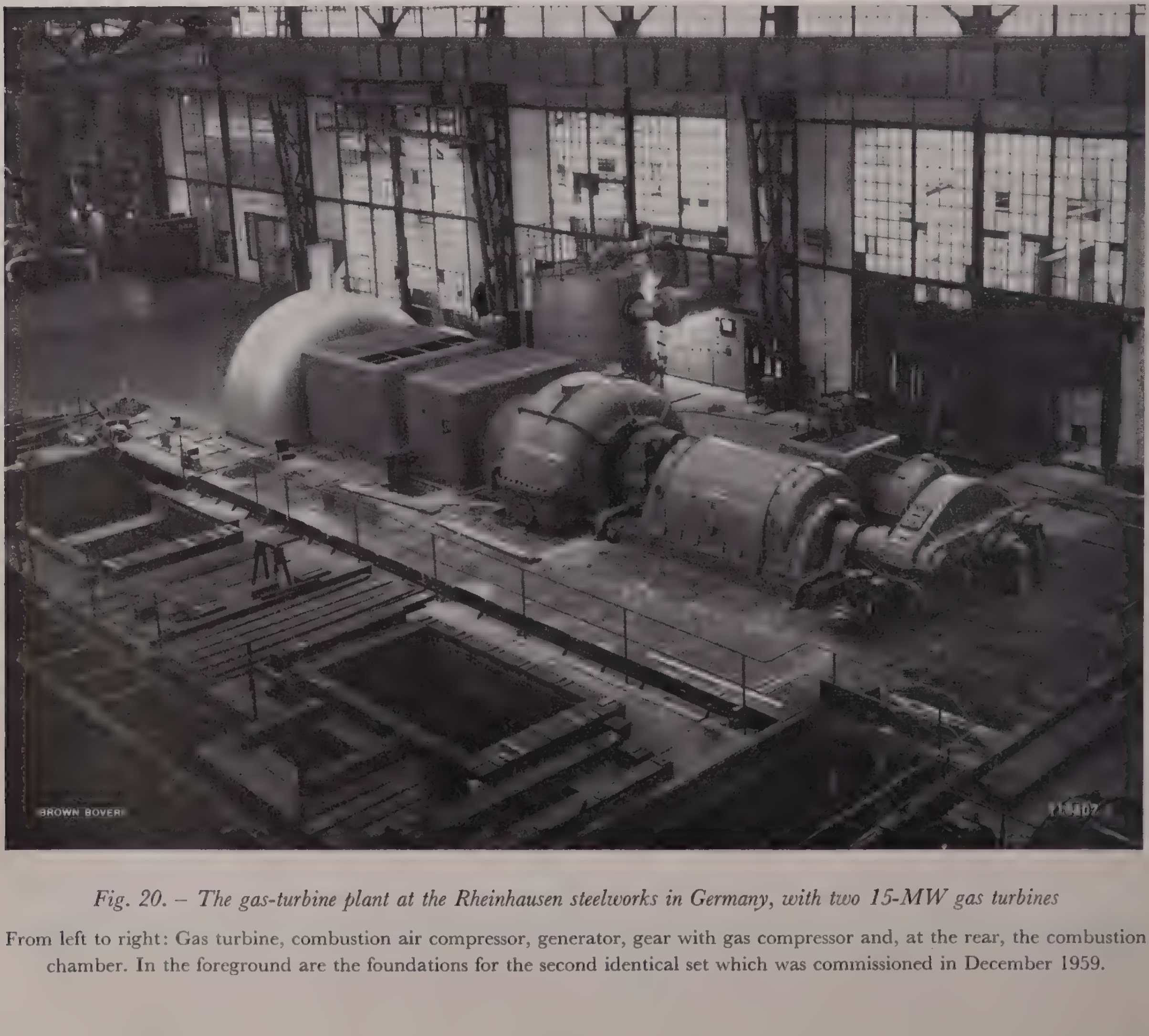

Fig. 20. – The gas-turbine plant at the Rheinhausen steelworks in Germany, with two 15-MW gas turbines

From left to right: Gas turbine, combustion air compressor, generator, gear with gas compressor and, at the rear, the combustion chamber. In the foreground are the foundations for the second identical set which was commissioned in December 1959.

Gas Turbine at Rheinhausen Steelworks, Germany

Power at the Coupling 15 000 kW

This steelworks ordered two 15-MW gas-turbine sets, the first of which came into service in the autumn of 1958, and the second towards the end of 1959. Since these sets are only used for the generation of electricity and do not have to run in parallel with either the RWE power system, or the steelworks' own distribution system, single-shaft machines were chosen, as for Haspe. The machine is of the same type as supplied to Haspe, the only difference being in the starting arrangement. Due to lack of space the starting motor was omitted, the generator being provided with a special starting winding. By reducing the length of the machine in this way it was possible to accommodate two gas-turbine sets in the existing space. The layout is shown schematically in Fig. 21.

By the end of December 1959 the first machine had completed 6200 hours in service, at which time it was examined. It had then performed 65 starts, of which the majority were again during the initial commissioning period. Normally it is not shut down on Sundays and is therefore continuously in operation. During the above period the temperature before the turbine averaged 745 °C.

In this plant neither the blast-furnace gas nor air is filtered. The gas used, with a dust content of 3 to

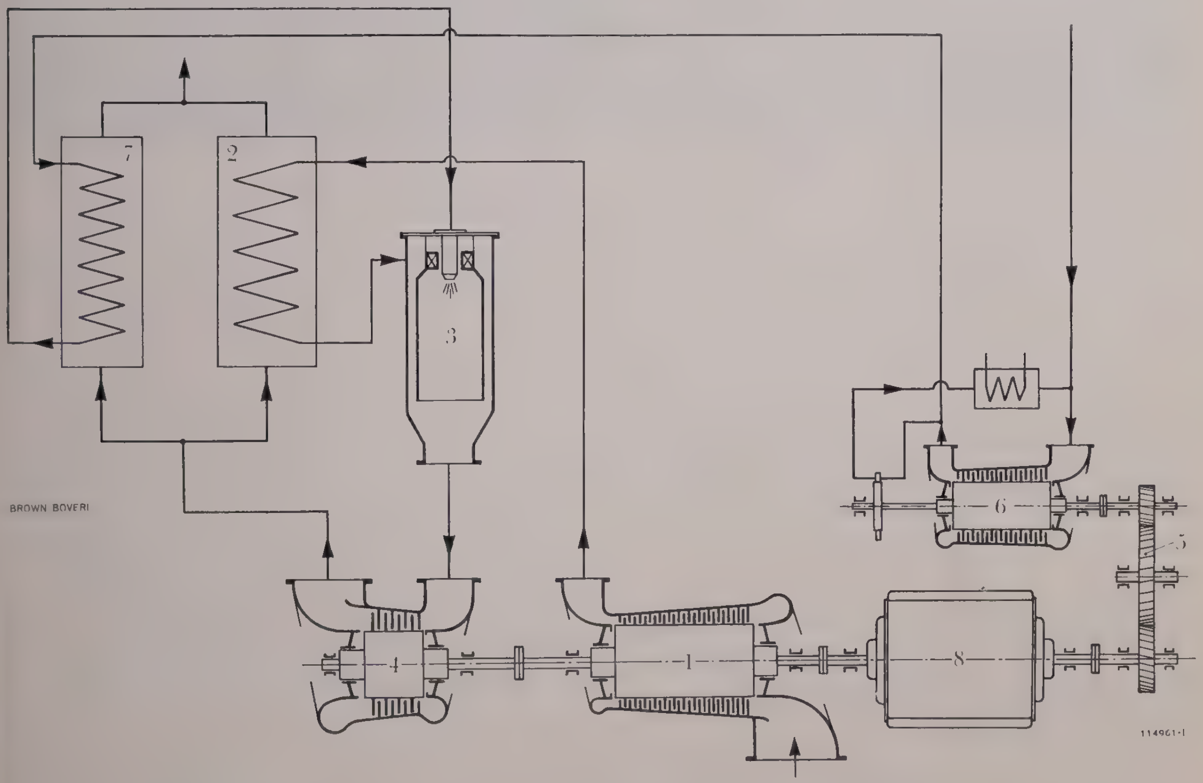

Fig. 21. – Schematic diagram of the Rheinhausen gas turbine — Terminal output 15 000 kW

1 = Air compressor
2 = Air pre-heater
3 = Combustion chamber
4 = Gas turbine
5 = Gear
6 = Gas compressor with recuperation turbine
7 = Gas pre-heater
8 = Generator

This machine has no starting motor, it is started by the generator acting as a motor. With this compact layout it was possible to accommodate two sets in the available space. The control system is similar to Haspe.

TABLE VI

Comparison of guaranteed and measured values for the gas turbine Rheinhausen I

	Units	Calculated or guaranteed	Measurements					
Test number	—	—	1	2	3	4	5	6
Date	—	—	11/5/59		12/5/59			
Analysis of dry blast-furnace gas	by volume							
CO_2	%	—	9·8	10	10	9·8	9·8	9·8
CO	%	—	31·2	30·8	31·0	31·8	30·8	30·8
H_2	%	—	1·9	1·9	1·5	1·9	1·9	1·9
N_2	%	—	57·1	57·3	57·5	57·5	57·5	57·5
Gas constant of the dry gas	m/°K	—	29·15	29·12	29·02	29·15	29·15	29·15
Barometric pressure	mmHg	—	759·1	759·5	762·3	763·0	764·3	765·0
Absolute air pressure	kg/m^2 abs	—	10 250	10 251	10 299	10 304	10 320	10 325
Absolute gas pressure	kg/m^2 abs	—	10 590	10 583	10 662	10 672	10 702	10 698
Absolute humidity of the gas	$\frac{g\ H_2O}{kg\ dry\ gas}$	—	37·5	23·5	28·0	36·5	36·4	35·5
Gas constant of the wet gas	m/°K	—	29·82	29·56	29·57	29·81	29·8	29·785
Lower calorific value of the wet gas	$kcal/Nm^3$	—	933·5	942·8	933·1	924·2	924·6	926·1
Quantity of wet gas	Nm^3/h	—	52 932	49 832	58 003	56 982	47 918	41 770
Heat input of gas	kW	—	57 500	54 600	62 900	61 150	51 600	45 000
Terminal output of generator	kW	—	14 300	11 900	16 475	15 544	10 510	6 669
Thermal efficiency at terminals	—	—	0·2489	0·2178	0·2618	0·2538	0·204	0·1483
Air inlet temperature	°C	10	27	28	15·2	20·9	25·2	24·6
Back-pressure before compressor	kg/m^2	50	51	51	51	51	51	51
Air inlet pressure before compressor	kg/m^2 abs	10 200	10 199	10 200	10 248	10 253	10 651	10 647
Terminal output corrected to guarantee conditions	kW	15 000	17 380	14 640	17 450	17 530	12 480	7 860
Thermal efficiency corrected to guarantee conditions	—	0·278	0·2772	0·2442	0·2705	0·2716	0·2245	0·1625
Gas temperature before turbine	°C	750	742·5	699	746	744·8	665	590

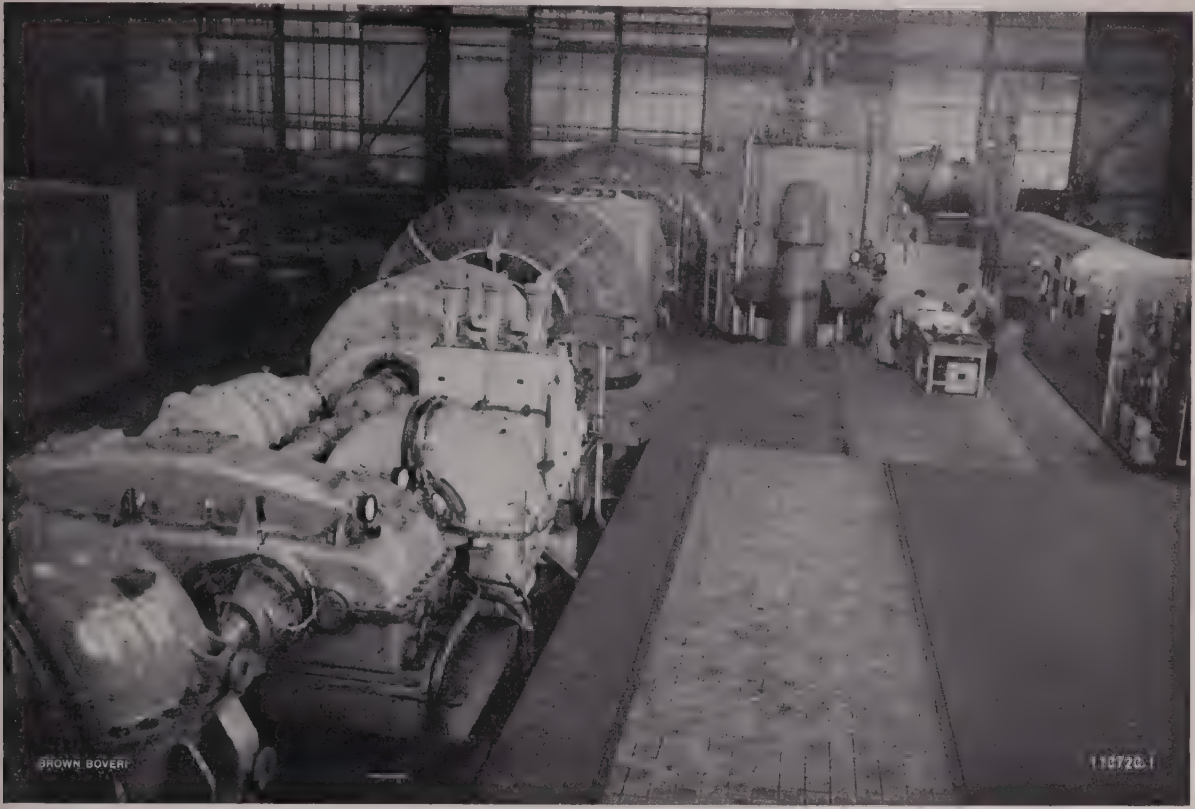

Fig. 22. – Gas-turbine set of the Österreichische Alpine Montangesellschaft at Donawitz steelworks, Austria. Power at the coupling 15 000 kW

From front to rear: Blast blower, gear, gas compressor and starting motor, generator, combustion air compressor and gas turbine; at the rear the combustion chamber and on the right the switchboard.

6 mg/Nm^3, is taken directly from the Theissen cleaners. Consequently incrustation in the turbine is somewhat more extensive than at Haspe. During the 6200 hours this set had been in service its output had dropped by about 8 % as a result of incrustation in the compressor and turbine, an interesting point being that this decrease all took place within the first 1000 h, and remained constant from then on. The percentage increase in the specific heat consumption during the period in service was much less than the drop in output, because some of the lost heat is returned to the cycle in the heat exchangers.

During the inspection after 6200 hours, signs of rather more severe corrosion were observed in the first rows of blades in the gas turbine. These were more severe than at Haspe but less than at Duisburg, which again proves that the main factor is not the amount of dust, but its composition. Table VI compares the measured values with the guaranteed data of the machine.

Gas Turbine at Donawitz (Austria) in the Steelworks of the Österreichische Alpine Montangesellschaft

Power at the Coupling 15 000 kW

This machine (see Fig. 22) is of the same type as at Rheinhausen and Haspe; also the layout is the same as in the latter steelworks. In such plants a gas turbine usually has to be accommodated in an existing building, so that the dimensions are fixed from the start. Frequently the building previously housed

TABLE VII

Acceptance measurements on the Donawitz gas turbine compared with the guaranteed and calculated values

	Units	Guaranteed and calculated values	Measured figures
Barometric pressure	kg/m² abs	10 000	9 735
Air inlet temperature	°C	15	15·2
Speed	rev/min	3 000	3 000
Gas inlet temperature	°C	750	726
Terminal output	kW	—	10 510
Correction for inlet temperature	kW	—	0
Correction for inlet pressure	kW	—	286
Generator losses	kW	—	252
Power at blower coupling	kW	5 680	5 920
Power at turbine coupling	kW	14 000	16 968
Quantity of blast-furnace gas	Nm³/h	—	75 100
Lower calorific value (average for 1 h)			
Measured by calorimeter H_1	kcal/Nm³	—	674
Orsat gas analysis H_2	kcal/Nm³	—	713
Calculated value	kcal/Nm³	756	—
Heat input			
with H_1	kW	—	58 800
with H_2	kW	—	62 300
from calculation	kW	51 800	—
Thermal efficiency at coupling			
with H_1	—		0·288
with H_2	—		0·272
from calculation	—	0·27	—
Temperature after air compressor	°C	220	210
Temperature after gas compressor	°C	280	254
Pressure after air compressor	kg/m² abs	54 600	56 735
Pressure after gas compressor	kg/m² abs	57 000	58 535
Utilization factor of air preheater	—	0·75	0·748
Exhaust-gas temperature	°C	263	280

piston engines, which are being replaced because they have become obsolescent. For this reason it is not always easy to decide on a layout which satisfies all requirements. For instance, at Donawitz the air and gas preheaters had to be erected outdoors owing to lack of space in the machine room, and this resulted in long interconnecting pipes.

Up to November 8th, 1959 the set had run 4760 hours, with 76 starts, the last month continuously at almost full load. In November 1959 the machine was inspected while certain minor modifications were carried out; it was in very good condition. The air is cleaned in Delbag filters while the gas passes through additional electrostatic precipitators. Incrustation in the compressor was very slight; the blast-furnace blower came into service about a year before the gas turbine, during which time it was driven by the generator acting as a motor. This blower, which had run for 11 780 hours at the time the inspection took place in November 1959, was in such a good condition that it did not need cleaning. The deposit in the turbine, the gas compressor and in the first rows of turbine blading was also small. No corrosion was detected on the latter; the combustion chamber likewise proved to be in very good condition.

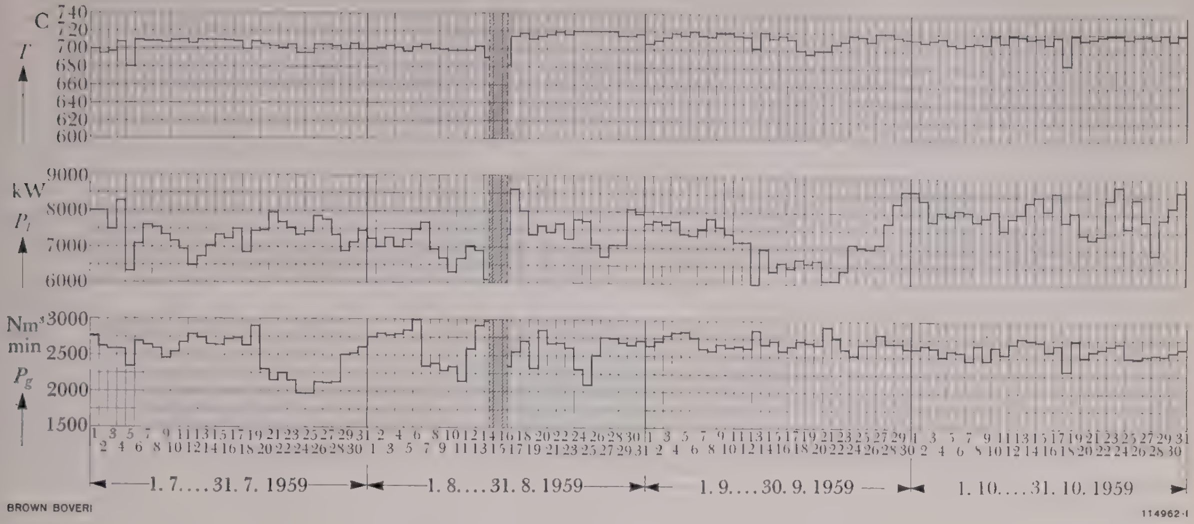

Fig. 23. – Load diagram of the Donawitz gas turbine

Abscissae: Calendar days and months

Ordinates: T = Gas temperature before turbine
P_E = Terminal output of generator
P_g = Delivery rate of the blast blower

Shaded portion: idle due to repairs to furnace

The generator output and the blast blower delivery combined add up to the full gas-turbine output of 15 000 kW. From the diagram it will be seen that the gas turbine has been almost continuously in service since July 1959.

The acceptance tests were carried out in May 1959 after 930 hours running. From then until inspection in November the set had been in service for 3830 out of a possible 4070 hours. Thus during this period the availability factor was 94%. From Table VII it is possible to compare the measured values with the guaranteed and informatory figures. Table VIII lists the machines of this type which have been delivered so far, from which it will be seen that, of the six units, five are already in service.

Gas Turbine of S.A. Minière et Métallurgique de Rodange, Luxembourg

Power at the Coupling 7500 kW

As regards output, this machine is between the types supplied to Duisburg and Haspe. Its schematic layout is shown in Fig. 24. Up to the end of December 1959 it had been in service roughly 6000 hours.

The acceptance tests were carried out by Bureau Vinçotte, Brussels, on April 15/16th, 1959. Tables IX, X and XI permit the guaranteed or calculated values to be compared with readings actually obtained. These measurements were taken with the utmost care, as one would expect of Bureau Vinçotte. As mentioned earlier, the layout of the gas-turbine set in a steelworks is not always ideal, owing to the space restrictions if the building formerly housed piston engines. At Rodange the measuring orifice could not be installed in accordance with the standards, so that it had to be calibrated. For this purpose an additional pipe with a measuring orifice conforming to VDI standards was incorporated in the piping system of the gas compressor. With the aid of this orifice it was possible to calibrate the actual orifice with air. The comparative measurements proved that our fixed orifice indicated 2·39 % less gas than it actually handled. The specific weight of the gas was also exactly determined by the gas analysis and by the Schilling apparatus. The results of the two methods differed by about 0·4–0·9 %. To determine the quantity of gas the average of the two methods was adopted. The humidity was likewise measured and found to be slightly above the

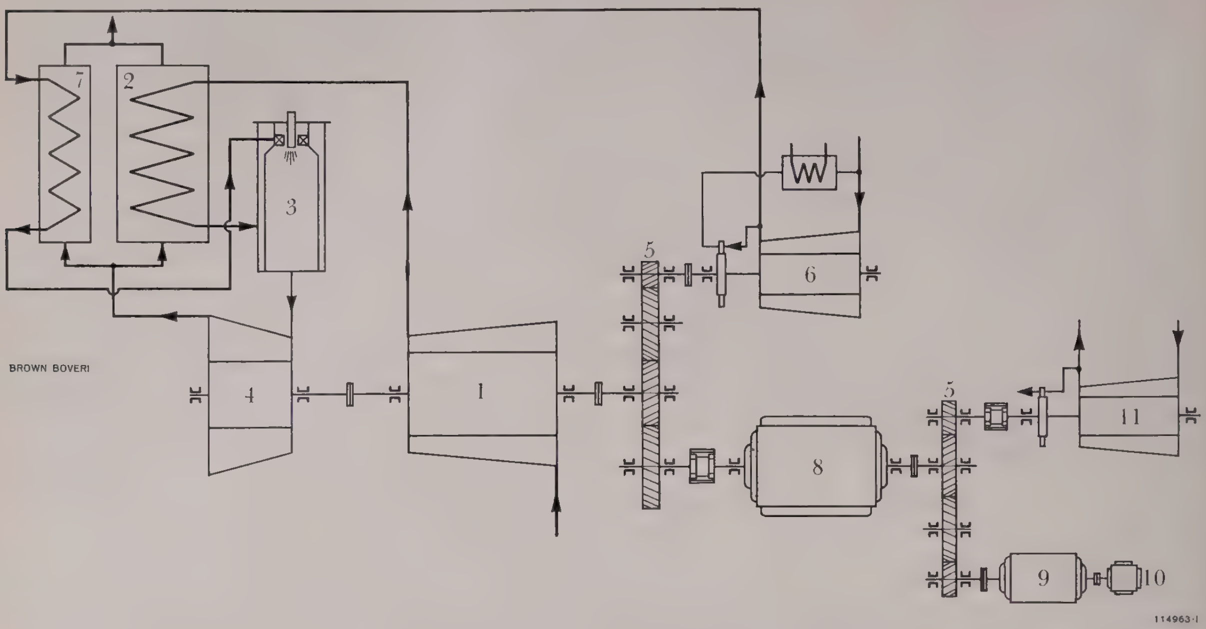

Fig. 24. – Layout of the gas turbines at Rodange, La Chiers and Hagondange, each of which has a terminal output of 7500 kW

1 = Air compressor
2 = Air pre-heater
3 = Combustion chamber
4 = Gas turbine
5 = Gear
6 = Gas compressor
7 = Gas pre-heater
8 = Generator
9 = Starting motor
10 = Exciter
11 = Blast blower with recuperation turbine

saturation point. A precision calorimeter was utilized to determine the calorific value of the gas.

The first series of tests, each of which lasted four hours, was performed with the blast blower uncoupled, in order to measure the output accurately. For a second series of tests the blower was coupled up to the set, while a third series was concerned with measurement of the guarantees of the blower

TABLE VIII

Gas turbines of the Haspe type for a gas inlet temperature of 750 °C which have been supplied by Brown Boveri to steelworks

Steelworks	Order received	Commissioned	Machines driven
Klöckner Hüttenwerk Haspe, Hagen-Haspe, Germany	1955	July 1958	Generator and blast blower
Hüttenwerk Rheinhausen, Rheinhausen, Germany			
Machine I	1955	October 1958	Generators only
Machine II	1957	December 1959	
Österreichische Alpine Montangesellschaft, Donawitz, Austria	1955	February 1959	Generator and blast blower
Union Sidérurgique du Nord de la France, Denain, France	1956	November 1959	Generator and blast blower
Société Métallurgique de Knutange, Knutange, France	1955	January 1960	Generator and blast blower
Aciéries de Rombas, Rombas, France	1957	1960	Generator and blast blower

TABLE IX

Results obtained during acceptance tests on the Rodange gas turbine carried out by Bureau Vinçotte, compared with guaranteed and informatory values. Blast-furnace blower uncoupled, only the generator coupled

	Units	Guaranteed or calculated	Reading on 15/4/59	
Measurement	—	—	1	2
Duration of test	h	—	4	4
Air inlet temperature	°C	15	20	16·8
Barometric pressure	mm Hg	—	732·4	733·6
Inlet pressure before air compressor	kg/m² abs	10 200	9 890	9 907
Gas temperature before gas compressor	°C	—	43·2	43·2
Static head in gas pipe	kg/m²	—	265	259
Analysis of gas	by volume			
CO_2	%	—	11·6	11·9
C_2H_4	%	—	0	0
O_2	%	—	0·1	0·1
CO	%	—	28·9	28·5
CH_4	%	—	0	0
H_2	%	—	3·6	4·0
N_2	%	—	55·8	55·5
Gas humidity	g/m³	—	28·4	28·2
at t	°C	—	27·8	29·0
barometer	mm Hg	—	732·4	733·6
head	kg/m²	—	265	259
Lower calorific value of dry gas referred to 0 °C and 760 mm Hg, measured with Junkers calorimeter	kcal/Nm³	980	956	952
Gas consumption of machine referred to dry gas at 0 °C and 760 mm Hg	Nm³/h	24 000	29 580	27 224
Terminal output of gas turbine (Two-wattmeter method)	kW	minimum 7 200	8 742	7 182
Terminal output of gas turbine (kWh-meter method)	kW		8 705	7 153
Specific gas consumption referred to 0 °C and 760 mm Hg	Nm³/kWh	3·34	3·384	3·790
Heat consumption of turbine under test conditions	kcal/kWh kW/kW	3 280 3·8	3 235 3·76	3 608 4·2
Thermal efficiency at terminals	—	0·2635	0·2658	0·2384
Guaranteed thermal efficiency converted to test conditions	—	0·2622	—	—
Speed of set	rev/min	4 250	4 153	4 150
Temperature before gas turbine	°C	up to 750	716	664
Air temperature before air pre-heater	°C	—	234	227
Air temperature after air pre-heater	°C	—	407	375
Gas temperature before gas pre-heater	°C	—	256	251
Gas temperature after gas pre-heater	°C	—	371	356
Gas pressure after gas compressor	kg/m² abs	—	50 250	49 160
Gas temperature in chimney	°C	—	270	256
Utilization factor of air pre-heater	—	0·78	0·79	0·81
Analysis of exhaust gas, measured in chimney	by volume			
CO_2	%	—	5·1	4·8
O_2	%	—	16·7	17·2
CO	%		0	0

TABLE X

Calibration of the measuring orifice

Since the fixed measuring orifice could not be fitted in accordance with the standards owing to lack of space, and there were no alternative facilities for fitting it to the gas pipe, the gas pipe was replaced by an air line conforming to the standards and the measuring orifice calibrated with air, the gas compressor being driven with air for the purpose.

Measurement	Units	1	2	3
1. Quantity measured with check orifice	m³/h	34 170	24 909	34 169
2. Quantity measured with fixed orifice converted to the conditions of the check orifice	m³/h	33 450	24 294	33 339
Difference between reading 1 and 2	m³/h	+720	+615	+830
Percentage difference	%	+2·15	+2·53	+2·49
Mean percentage difference	%		2·39	

TABLE XI

Acceptance test on the Rodange gas turbine, performed by Bureau Vinçotte, Brussels, with generator and blower coupled

	Units	Reading on 16/4/59		
Duration of test	h	1 h 45 min	1	1
1. *Readings on blast blower*				
Ambient air temperature	°C	15·7	17·6	18·2
Air humidity	%	72·4	63·6	55·5
Air inlet temperature before compressor	°C	17·6	17·6	18·2
Back pressure before compressor	kg/m²	80	80	80·2
Air temperature at compressor outlet	°C	162	162	162
Air pressure at compressor outlet	kg/m²	25 000	24 900	25 100
Delivery rate	Nm³/h	42 219	42 039	41 496
2. *Readings on generator*				
Output (with two wattmeters)	kW	4 650	4 329	5 930
(with kWh-meter)	kW	—	—	5 974
Speed of turbine	rev/min	4 154	4 160	4 190
Inlet gas temperature	°C	631	633	700
Barometric pressure	mm Hg	725	724·5	723
Inlet pressure of combustion air before compressor	kg/m² abs	9 790	9 780	9 760
Inlet pressure of blast blower	kg/m² abs	9 780	9 770	9 750
Blast output, referred to generator terminals	kW	2 250	2 250	2 200
Total terminal output (generator + blast)	kW	6 900	6 579	8 130
Quantity of dry gas consumed	Nm³/h	26 360	25 753	28 471
Lower calorific value of dry gas	kcal/Nm³	971	971	959
Measured thermal efficiency at terminals	—	0·233	0·227	0·256

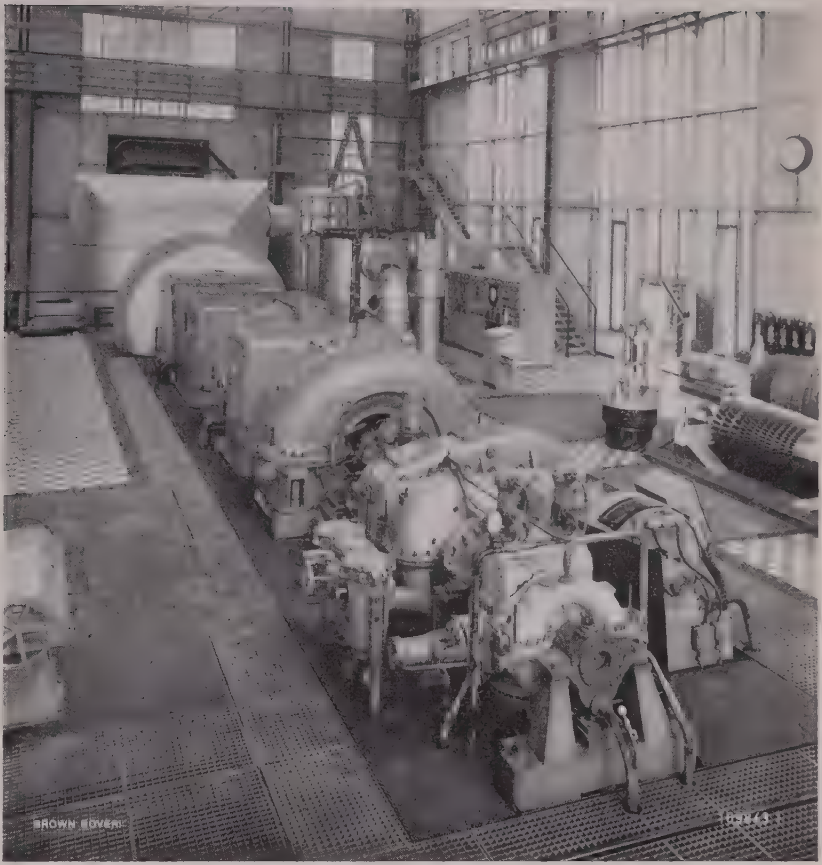

Fig. 25. – Hörde gas-turbine station of the Dortmund-Hörde steelworks, Germany

Successively towards the front: Air and gas pre-heaters, combustion chamber, gas turbine, air compressor, blast blower, gear with starting motor, and gas compressor with recuperation turbine. On the right are parts ready for the second set.

TABLE XII

Measurements of vibration on the Rodange gas turbine at full load

Measurement at		Instrument deflection double amplitude in μ
Turbine bearing, pressure side	vertical horizontal	3 5
Air compressor bearing, suction side	vertical horizontal	10 12
Air compressor bearing, pressure side	vertical horizontal	4 8
Gear I	vertical horizontal	13 15
Blast blower, suction side	vertical horizontal	6 5
Blast blower, pressure side	vertical horizontal	3 3
Gear II	vertical horizontal	5 7

alone, for which the coupling between the gas turbine and the blower was released and the blower driven by the generator acting as a motor.

During these tests the vibration of the set was also measured (Table XII). It is very small at all points, demonstrating how smoothly the machine runs in spite of its high speed.

A second, identical machine has been supplied to the Hauts Fourneaux de la Chiers-Longwy; it has completed roughly the same number of hours service as the one in Rodange. A third for Hagondange is at present under construction.

Gas Turbines for the Dortmund-Hörder Hüttenunion, Germany

This company now has two gas turbines in their Hörder steelworks (Fig. 25) and one in Dortmund. The main difference between these machines and

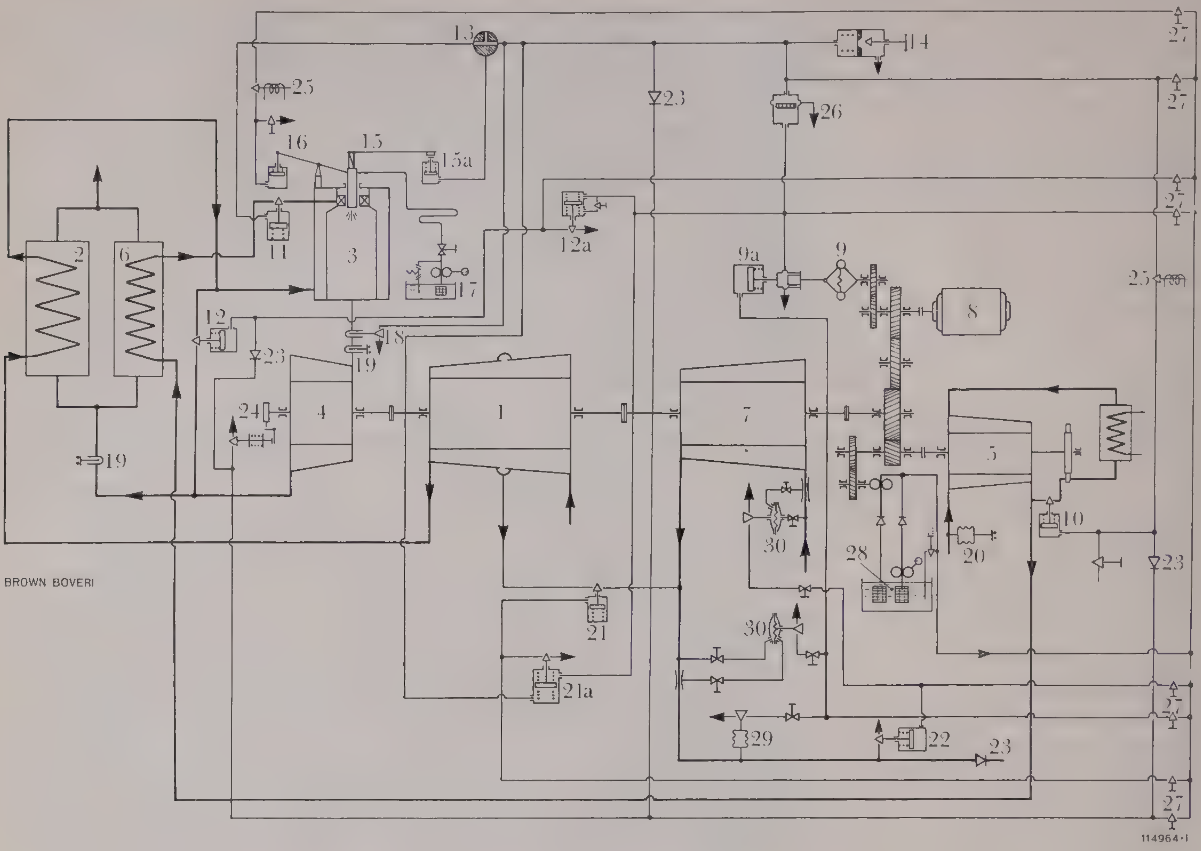

Fig. 26. – Thermal and control circuit diagram of the gas-turbine sets at Hörde and Dortmund

1 = Air compressor
2 = Air pre-heater
3 = Combustion chamber
4 = Gas turbine
5 = Gas compressor with recuperation turbine
6 = Gas pre-heater
7 = Blast blower
8 = Starting motor
9 = Centrifugal governor
9a = Servo-motor for adjusting 9
10 = Recuperation valve for the gas compressor
11 = Gas regulating valve
12 = Blow-off valve
12a = Pressure-gradient relay for 12
13 = Changeover valve from gas to oil
14 = Starting and regulating valve
15 = Fuel nozzle
15a = Servo-motor for fuel nozzle 15
16 = Drawout mechanism for the fuel nozzle
17 = Fuel pump
18 = Temperature regulator
19 = Protective thermostats
20 = Pressurestat in the gas pipe
21 = Regulating valve in the pipe connecting the air compressor and blast blower
21a = Servo-motor for adjusting 21
22 = Blow-off valve in the blast pipe
23 = Non-return flap
24 = Safety governor
25 = Solenoid valves
26 = Pressure transducer
27 = Variable orifice
28 = Oil tank for lubrication and control, with main pump and motor-driven auxiliary pump
29 = Pressure regulator for quantity of blast
30 = Volume regulator for blast

The speed of the set is variable, hence no recuperation turbine is required for the blast blower.

those previously described is the absence of the generator, as may be seen in the schematic diagram. The turbines are only used to drive blast-furnace blowers. Their speed has to be variable in order that the delivery rate of the blast blower may be adapted to the requirements of the furnace. By means of a pipe connecting the combustion-air compressor and the blast-air blower outlet, it is possible to add or subtract power from the gas turbine if the balance of power is in any way disturbed.

TABLE XIII

Calculated and guaranteed values for the gas turbines Hörde I and II

	Units	1	2	3
Furnace blast delivery rate	Nm^3/h	120 000	150 000	160 000
Pressure in blast pipe	kg/m^2 abs	25 000	26 000	28 000
Heat consumption	kW	18 350	23 100	27 350
Isentropic thermal efficiency	—	0·203	0·211	0·207
Air inlet temperature	°C	15	15	15
Air inlet pressure	kg/m^2 abs		10 000	
Gas inlet temperature	°C		35	
Gas inlet pressure	kg/m^2 abs		10 100	
Pressure after air compressor	kg/m^2 abs		48 250	
Pressure at compressor	kg/m^2 abs		31 000	
Pressure after gas compressor	kg/m^2 abs		51 000	
Speed of set	rev/min		3 850	
Utilization factor of air pre-heater	—		0·79	
Consumption of cooling water	m^3/h		70	

TABLE XIV

Calculated and guaranteed values for the Dortmund gas turbine

	Units	1	2	3
Furnace blast delivery rate	Nm^3/h	120 000	150 000	180 000
Pressure in blast pipe	kg/m^2 abs	23 000	23 000	23 000
Heat consumption	kW	16 750	19 550	26 300
Isentropic thermal efficiency	—	0·20	0·215	0·191
Air inlet temperature	°C	15	15	15
Air inlet pressure	kg/m^2 abs		10 000	
Gas inlet temperature	°C		35	
Gas inlet pressure	kg/m^2 abs		10 100	
Pressure after air compressor	kg/m^2 abs		43 300	
Pressure at compressor	kg/m^2 abs		30 500	
Pressure after gas compressor	kg/m^2 abs		45 300	
Speed of set	rev/min		3 580	
Utilization factor of air pre-heater	—		0·79	
Consumption of cooling water	m^3/h		36	

The machines at Dortmund and Hörde I are already in service but they have not been running long enough to permit any definite conclusions. The data of the machines are listed in Tables XIII and XIV. Fig. 27 shows the characteristic of a gas-turbine set of this kind.

Conclusion

The present article would become unwieldy if it were to go into every detail of each plant. Its real object is to pick out some of the problems encountered with this new range of gas turbines and to

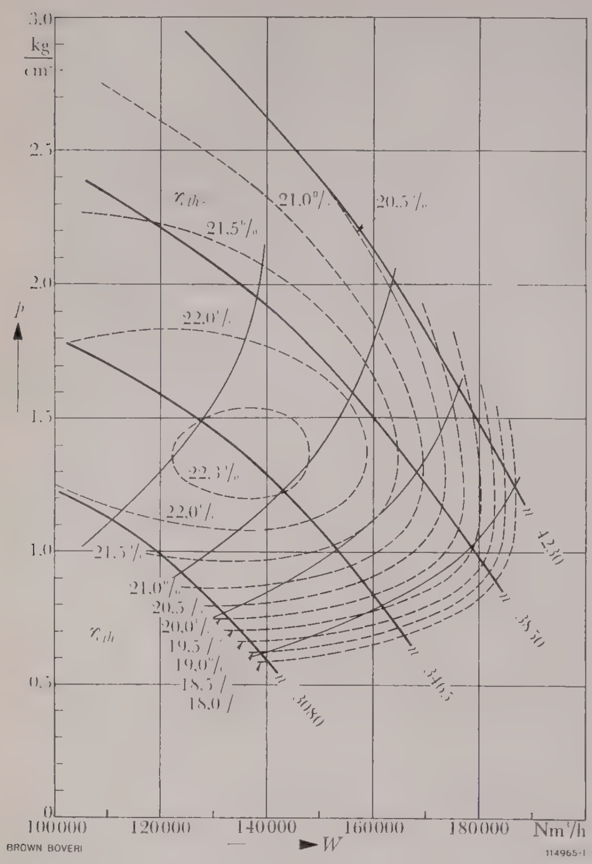

Fig. 27. – Characteristic of the Hörde gas-turbine set at an air inlet temperature of 15 °C and a gas inlet temperature of 710 °C

Abscissae: Amount of blast in Nm³/h
Ordinates: Blast pressure in kg/cm²g

The full lines denote the speed of the set, the dotted lines the isentropic efficiency of the set, given by $\eta_{th} = P_i/Q_f$, where

P_i = Isentropic blast output
Q_f = Heat input from fuel

give a summary of the machines so far built for an inlet temperature of 750 °C.

This new development has shown that success can be achieved with careful design, correct solution of all new constructional and operational problems, and radical research into the basic principles. A noteworthy feature is that the stresses in the materials exposed to the highest temperature are such that their life from the creep limit aspect is over 100 000 hours. The machines have given excellent results and, since a replacement must be found for piston machines in steelworks in the next few years in any case, the gas turbine should prove increasingly popular in such plants.

(KME) H. PFENNINGER

Bibliography

[1] H. PFENNINGER: Swiss experience with fuel additives in gas turbines. 1959 Fifth World Petroleum Congress, Section VI, Paper 4, Supplement.

[2] H. PFENNINGER: Entwicklung und Gestaltung von Gichtgasturbinen-Anlagen auf Grund der thermodynamischen Theorie und der technischen Leistungsgrenzen. Stahl und Eisen 1959, Vol. 79, No. 22, p. 1555–67.

MANAMA GAS-TURBINE POWER STATION, BAHRAIN

621.311.23:621.438 (536.5)

This article briefly describes the construction and commissioning of the Manama gas-turbine generating station, Bahrain. It also brings out the important point that here, for the first time, a public power system depends solely on this new prime mover without any assistance from other means of generation.

IN THE COURSE of the past year sixteen Brown Boveri gas turbines with a combined output of 305 800 kW have been taken into regular commercial service. One of these units was a 6100-kW set installed in the new power station supplying the town of Manama on Bahrain Island. This station commissioned its first gas turbine, of the same size, in the autumn of 1958. When these two were put on line for the first time together a number of diesel generating sets, which had previously supplied the island with power, were shut down. Thus for the first time a public power system became solely dependent on gas turbines as prime movers, an event which may be considered a milestone in the history of the gas turbine, and as such deserves mention in this journal.

Bahrain is an independent Arabian state situated in the Persian Gulf. It comprises a group of several flat islands, the six most important of which cover an area of about 600 km². The main island is about 50 km long, its width varying between 13 and 16 km. The whole group has a population of some 140 000, the town of Manama accounting for roughly 55 000. The northern part of the island, which is most densely populated, is joined to the island of Muharraq by a causeway, both being supplied with electricity from Manama by a high-voltage distribution system. Drives for irrigation water pumps and private householders account for the greater part of the load, industrial consumers being negligible.

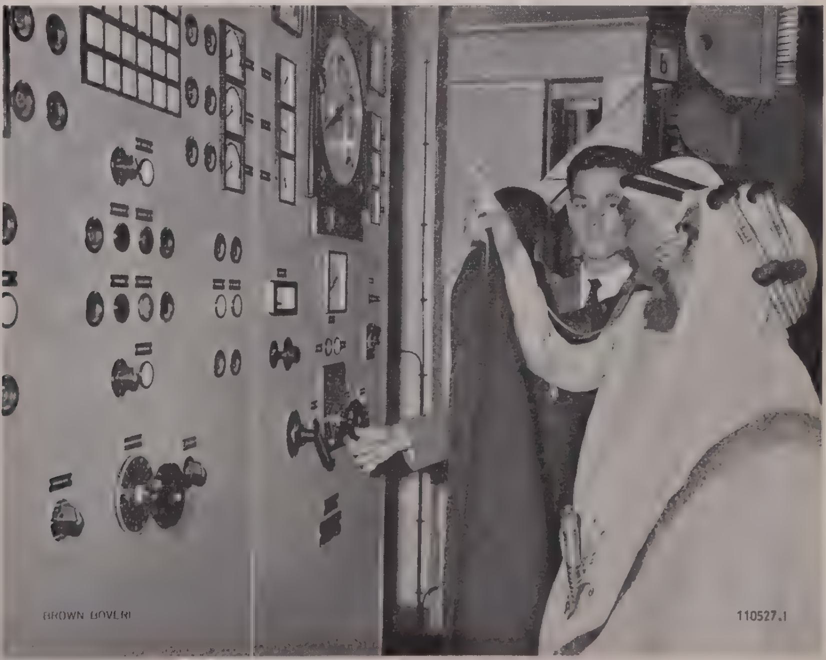

Fig. 1. – His Highness Sheikh Sulman bin Hamed Al-Khalifa, ruler of Bahrain (right)

follows the official commissioning of the second gas-turbine set during the solemn inauguration of Manama power station.

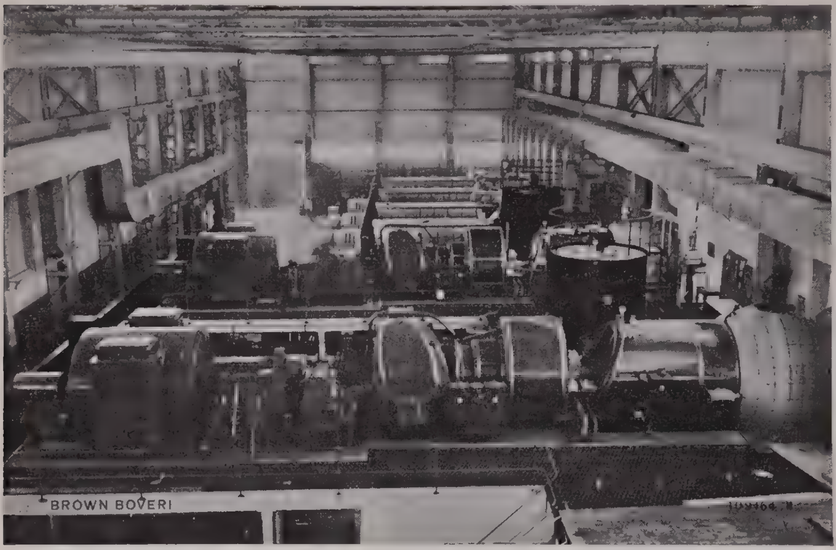

Fig. 2. – View inside Manama power station, Bahrain

In the background are the four 1000-kW diesel generating units which were shut down when the gas turbines commenced operation, and are now used only for standby purposes. In the foreground are the first two of the four gas-turbine sets which are being supplied. From left to right: exciter, generator, reduction gearing, in front of the latter the starting motor, followed by the compressor and the turbine. Behind the turbine is the vertical combustion chamber.

Note the comparative sizes of the 6100-kW gas-turbine sets and the 1000-kW diesel sets.

On April 30th, 1959, the second gas-turbine set was officially commissioned and Manama power station solemnly inaugurated by the island's ruler, His Highness Sheikh Sulman bin Hamed Al-Khalifa (Fig. 1). The presence of prominent islanders, British Middle East authorities and a large number of specialist engineers working in various Gulf countries (who had chosen the inauguration of the station to coincide with their annual meeting) added to the importance of the event.

The installed gas turbines are of the proved single-shaft design (Fig. 2), which is particularly suited to the local climate and operating conditions. Turbine and compressor run at 3600 rev/min, the alternator rated 8750 kVA, 11 kV, being driven at 3000 rev/min through reduction gearing. Power is also taken off the gearbox to drive the main oil pump and the speed governor of the turbine. The starting motor of the gas turbine is located to one side of the main gearbox and drives the turbine through an auxiliary set of gears. The guaranteed terminal output of each machine is 6100 kW at an ambient air temperature of 35 °C. The actual effective output, however, proved to be about 12 % higher. The turbines will normally operate on natural gas obtained from the oil-field about 15 km away. However, they are also equipped to burn diesel oil in an emergency. In contrast to the waterless cooling systems of the other gas turbines operating in the Gulf area, those in Bahrain employ a closed-circuit water cooling system for the lubrication oil and generator, supplemented by cooling towers because this kind of system was previously used for the diesel engines. The resultant water consumption is very small.

The gas turbines have operated very well and have justified the progressive confidence of the authorities and their advisers in this comparatively young but promising application of gas turbines. From the date the first set was commissioned until December 31st 1959 the two sets had run for 9107 and 6333 hours, respectively, with total outputs of 35 540 900 and 21 193 600 kWh. A third, identical machine is at present being erected in Manama, while a fourth is under construction in Baden.

The installation costs of the new gas-turbine extension to the station, which was drawn up and supervised by Ewbank and Partners, the London firm of consulting engineers, amounts to about S.Fr. 600.– per installed kW, referred to maximum rated output.

The extension to Manama power station brings the number of Brown Boveri gas turbines in operation in the Persian Gulf area up to fourteen with a combined output of 74 200 kW. Eight more sets with a total rated capacity of 51 400 kW are at present under construction or being erected.

(H) W. P. AUER

THE WORLD'S LARGEST GAS-TURBINE POWER STATION PORT MANN IN CANADA

621.311.23:621.438 (71)

This article contains a description of the remote-controlled Port Mann power station and indicates the important role this thermal plant will play in a predominantly hydro-electric system.

ON THE 25th September, 1959, the world's largest gas-turbine power station was inaugurated. This station contains four two-shaft Brown Boveri gas turbosets each rated at 25 MW [1].[1] These machines belong to the British Columbia Electric Company, Vancouver, Canada, and are installed in the Port Mann power station located about 25 km east of the city of Vancouver (Fig. 1).

It is of interest to note that the power station will be remote controlled from the load despatching centre in the new B.C. Electric headquarters building located in the centre of downtown Vancouver. The gas turbosets will be started up, loaded, unloaded and shut down from this despatch centre without operating personnel having to be present at the plant site.

Conditions that Led to the Construction of the Gas-Turbine Power Station

The electrical system of the B.C. Electric Co. supplies power to the south-western area of the British Columbia mainland, including the cities of Vancouver and Victoria. Prior to the construction of the gas-turbine power station, the installed capacity of the company was made up exclusively of hydro-electric power plants totalling 780 MW. The majority of the hydro-electric plants were located far from the districts in which the power was utilized, thus necessitating long transmission lines. Therefore, in order to guarantee the continuous supply of energy in an emergency, namely transmission line outages,

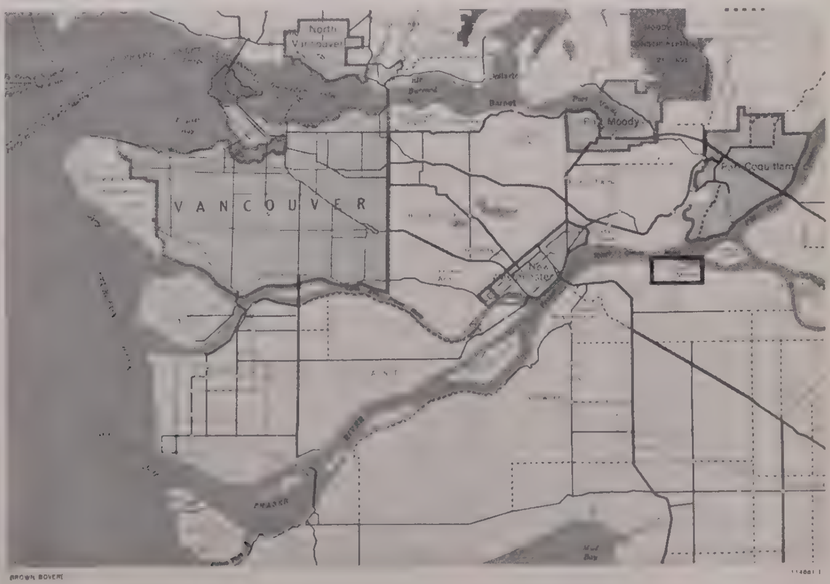

Fig. 1. – Map of Vancouver and surrounding area
showing the location of the Port Mann power station

---

[1] The figures in brackets refer to the bibliography on p. 72.

failure of a hydraulic plant due to breakdown or water shortage, and at the same time to meet the rapid rise in demand, it was decided that the B.C. Electric power system should be augmented by the construction of a thermal plant close to Vancouver. In times of water shortage this thermal plant could operate on base load thus "firming up" the hydro-electric system, that is, it would increase the dependable energy available to a level which would lie midway between the extreme capabilities of the hydro-electric system occurring during minimum and maximum water conditions [2].

Due to a gas turbine plant's low capital cost, extremely short start-up time, and fewer operating personnel, it was decided that a gas-turbine station of 100 MW capacity should be purchased. Other factors which led to this selection were: in contrast to steam turbosets, gas turbosets operate on a relatively simple thermodynamic cycle and thus lend themselves more easily to remote control; the gas turbine's efficiency, while somewhat lower than a steam turbine, is not so important when the plant is utilized during only a small part of the year (B.C. Electric have estimated an average annual utilization of 1200 hours), and finally, the rapid run-up to full load in 30 minutes from cold make the gas turbine ideal for use during emergency conditions.

Description of the Plant

Port Mann was selected as the location of the plant as it lay in the district of Vancouver and was near existing natural gas and crude-oil pipelines. Furthermore, this plant site is located on the Fraser River which provides ample cooling water for the air intercoolers and also affords facilities for delivery of heavy fuel oil by ship. Finally, a high-voltage transmission line, to which the gas turbosets could be connected, crosses the river at this point.

The four gas turbosets are arranged in a long, windowless building, 140 m long, 25 m wide (including an adjoining annex where the switchgear and control gear is located) and 18 m high. The building is laid out parallel to and about 300 m from the Fraser River. The axis of the turbosets run lengthwise to the building as this layout best suited the local terrain and gave the best arrangement of the large air intake ducts (Fig. 2, 3 and 4). A 50-t crane in the turbine room provides lifting capacity for the heavy turboset components. The air intake ducts and exhaust gas stacks are situated on the side of the building facing the river. The air inlet ducts are not fitted with filters as the surrounding air is of good quality. The ducts were nevertheless prepared for installation of filters should operating experience prove them necessary. The airblast circuit-breakers and the two main transformers, which step the generator voltage up from 13·8 kV to the transmission voltage of 230 kV, are also located outdoors on this side of the building.

Since the power station is located in a residential area, the air intake ducts and exhaust gas stacks were fitted with silencers containing a sound-absorbent material. The resultant noise level with the machines in operation has proved very satisfactory and noise is only audible in the immediate vicinity of the station.

The power needed during start-up is normally drawn from the system. The turbosets, however, must be completely independent of the system during emergency conditions. Therefore two diesel generating sets are provided, one of 1500 kW capacity to supply the starting motors and gas-turbine auxiliaries during run-up and one of 350 kW capacity to supply the motor-driven cooling-water pumps. Thus, with the aid of the diesel generating sets, the turbosets can be started singly and put on line successively until all four are running.

The pumping station by the river contains four cooling-water pumps driven by 200-h.p. motors. Each pump supplies the 1600 m^3/h of cooling water needed by its turboset. A fifth smaller pump of 160 m^3/h capacity was installed to keep the long cooling-water supply pipe (with a diameter of more than 1 m) full of water during periods when the power station is shut down, thus enabling the plant to start up at a moment's notice.

The gas turbines normally operate on natural gas taken direct from a high-pressure gas pipeline existing near the station. Should the supply of natural gas be interrupted, provision is made for the gas turbines to operate on crude oil. This is stored in a large tank with a capacity of 16 000 m³, which is sufficient to allow all four turbines to operate at full load for a period of two weeks.

The gas turbines are already equipped with the necessary apparatus for operation on heavy fuel oils, such as bunker C, should heavy fuels prove economical in the future; then the station will only have to be equipped with the necessary piping from the landing stage on the river to the storage tank and minor additional equipment such as heating elements, filters, etc., provided. At present the owners can obtain crude oil more cheaply; moreover, the gas turbines operate more satisfactorily on crude oil as it generally contains fewer ingredients likely to form blade deposits and requires little or no preheating prior to being fed to the combustion chamber.

The 13·8-kV and 2·3-kV switchgear, which was supplied by Brown Boveri (Canada) Ltd., is housed in an annex on the opposite side of the turbine room from the air inlet ducts and exhaust-gas stacks. This also includes the low-voltage switchgear, thermal control panel, contactor cubicle, generator switchboard, and cubicles for the automatic control, recording and telemetering devices and station service transformers, with the exception of the 5000-kVA auxiliary transformer located outdoors.

Automatic and Remote Control

The remote control of a thermal plant of this size represents a pioneering undertaking, so it may be of interest to outline the important features. As far as Brown Boveri are aware, the only previous plant of this type to be automatically controlled is the El Convento gas-turbine station of the C.A. La Electricidad de Caracas, Venezuela, which commenced commercial operation in August 1958 and gave Brown Boveri a wealth of experience in this field [3].

As stated earlier, the B.C. Electric power system previously relied solely on hydro-electric plants. Due to the high wage rates, most of these are remote controlled in order to reduce the number of operating personnel. Particularly for a peak-load thermal station with a low load factor, the personnel costs would have been high in relation to other costs, thus explaining why the client stipulated that this plant should also be equipped for remote control.

The gas-turbine station can be operated in four ways, namely:

Local control by hand with push-buttons and no master *controller.*

Semi-automatic local control with a master controller which can be turned from stage to stage by push-button control. The sequence of operations during run-up and shut-down is determined by the master controller; merely the time interval between stages is fixed by the operating personnel.

Automatic local control. Following a command "Start" or "Stop" the whole sequence is performed automatically; the master controller, once in motion, carries out the necessary operations in the correct sequence and at the right moment. An interlocking system is provided to ensure that the turboset can only be started up and loaded when everything is functioning correctly.

Automatic remote control. As described above, except that the commands are given by the load-despatching centre in Vancouver.

Of course, the gas-turbine station is normally operated by remote control. Fig. 5 and 6 show the control board at the load-despatching centre in Vancouver from which the gas-turbine station is controlled. Remote-control and telemetering signals are transmitted by carrier over the power line between the power station and Ingledow sub-station; and from this sub-station to the Vancouver load-despatching centre over an existing microwave link. The remote-control system employs coded pulse trains, each command having its own current-time characteristic. The coded programme is transmitted

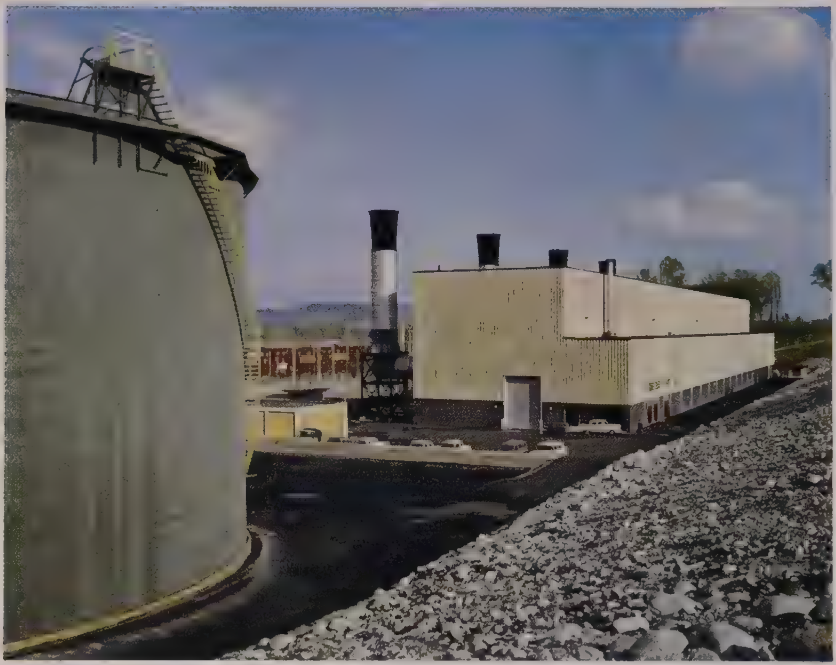

Fig. 2. – View showing the world's largest gas-turbine power station, Port Mann, owned by the British Columbia Electric Co., Vancouver, Canada

On the left is the crude-oil storage tank holding 16 000 m^3.

by means of a frequency-shift channel [4] which is insensitive to external disturbances and therefore very reliable.

The following operations can be carried out utilizing the system described above:

Start up/shut down turbine

Generator breaker on/off after synchronizing

Synchronizer bypass on/off when at zero system voltage

Increase/decrease load

Increase/decrease voltage or reactive power

Fuel selection gas/oil

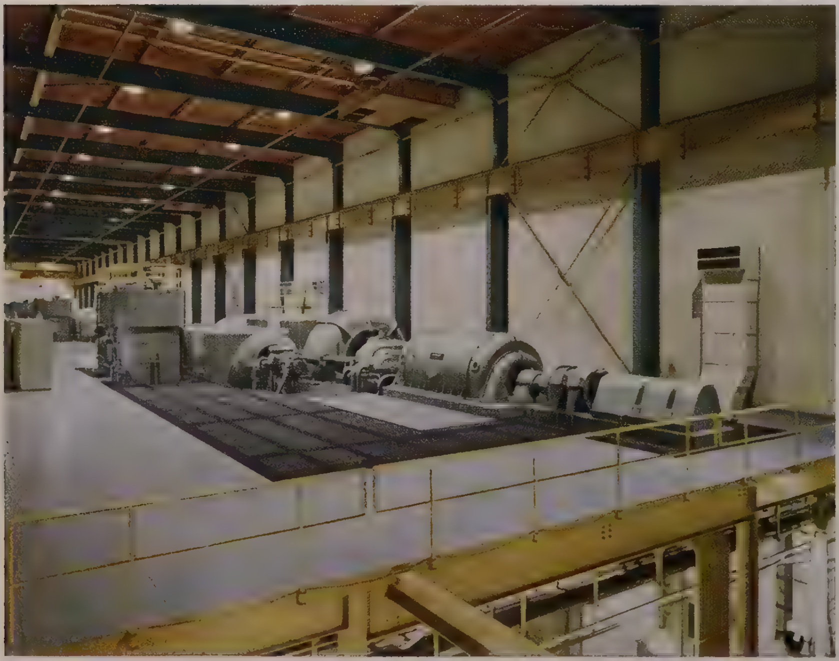

Fig. 3. – View of the turbine room in the Port Mann power station

One of the four gas turbosets with its combustion chamber (see detailed view in Fig. 4) can be seen in the foreground. A similar set can be seen in the background.

Fig. 4. – The high-pressure and low-pressure combustion chambers of one of the four gas turbines

The switchboard can be seen in the right foreground. In the background are the controls for local start-up and shut-down.

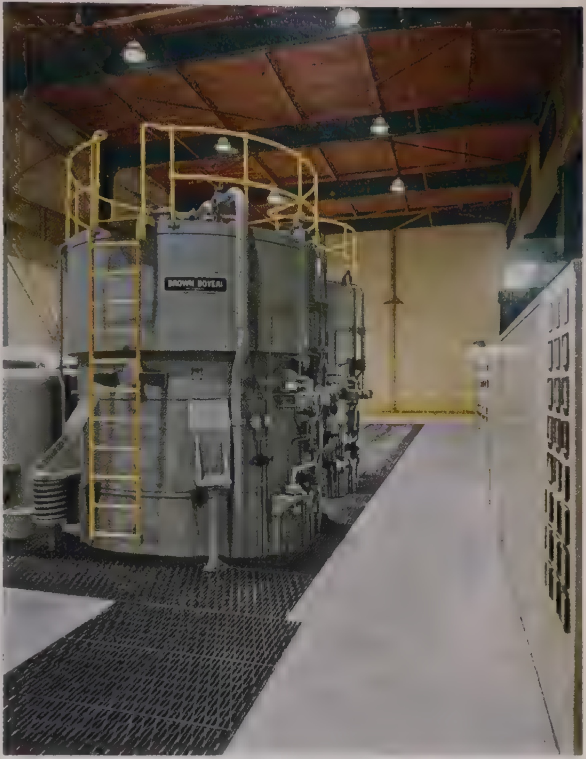

It is also possible to start up or shut down the diesel generating sets and to operate the two 230-kV breakers and transformer isolating switches by remote control. From the clearly arranged position indicators and alarm lamps on the control board the operational state of the gas-turbine station can be seen at a glance. The most important station measurands, such as load, reactive load, frequency

Fig. 5. – Load-despatching centre in Vancouver

This is located in central Vancouver about 25 km from the power station. The power station is remote-controlled from the board on the right.

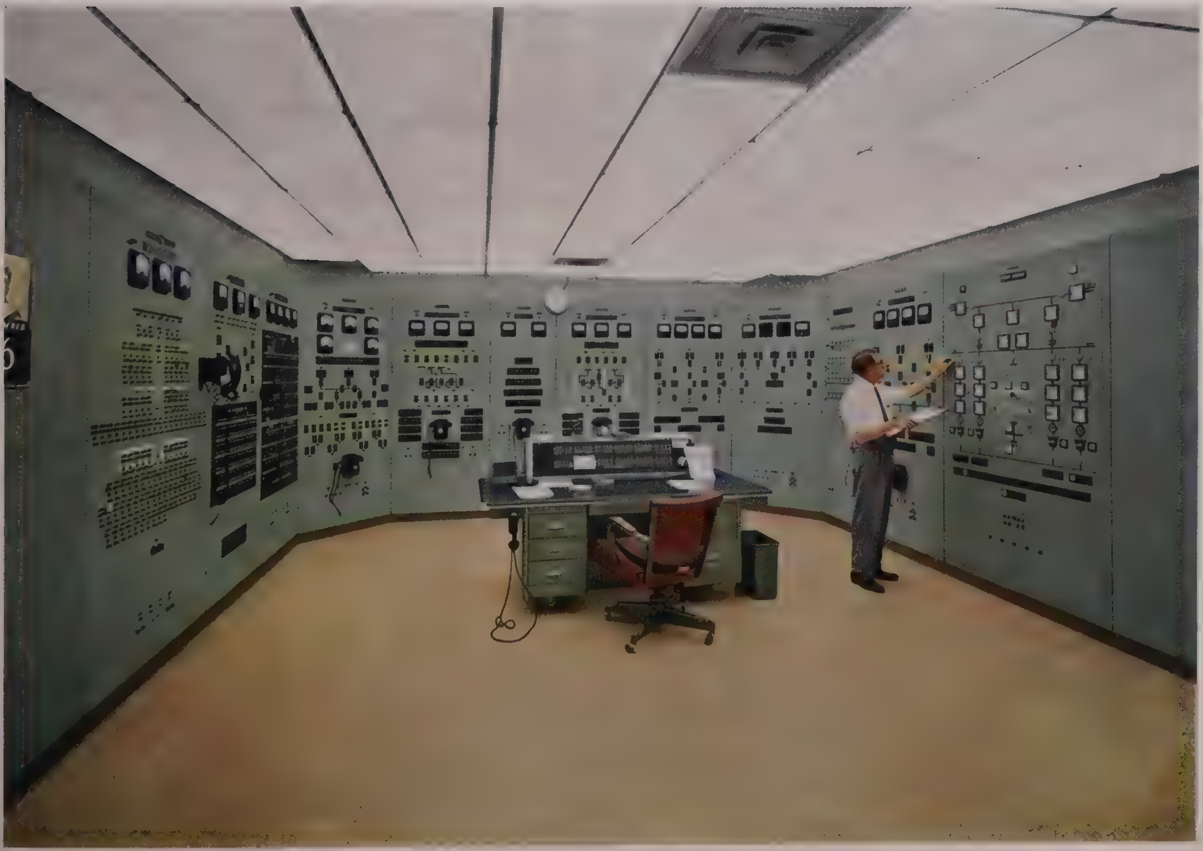

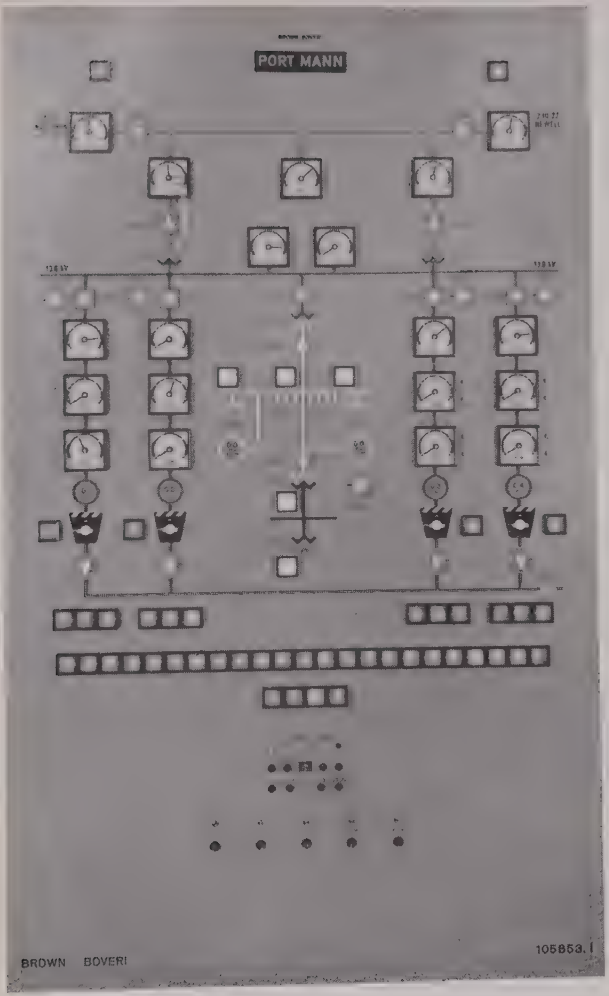

Fig. 6. – Detailed view of the control board in the Vancouver load-despatching centre

The control switches, measuring instruments and signal lamps are shown on the mimic diagram.

and voltage are transmitted by rapid-cyclic telemetering equipment operating on the frequency variation principle [5].

Since the plant has no operating personnel a reliable and comprehensive automatic supervisory system is essential. It comprises a number of multipoint recording devices with limit contacts on which all the important technical data such as currents, fuel quantities, speeds, vibrations, pressures and temperatures are recorded continuously. In the event of a breakdown in the plant four fault recorders indicate the variation of gas turbine inlet temperature, control oil pressure, safety oil and air pressures and movement of the fuel admission valves. This facilitates location of faults.

Conclusion

A month before the Port Mann power station was officially inaugurated, one of the gas turbines underwent an acceptance test which showed that the guarantees were met and that the guranteed maximum output was in fact considerably exceeded. Operation by remote control has also proved excellent.

The construction of this large gas-turbine power station has once again proved the important role gas-turbine stations can play as emergency reserve or peak-load capacity in hydro-electric systems. Indeed, this is also true in those areas where the cost of thermal power for base-load operation is greater than hydraulic power. Finally, this power station has proved that, where economic conditions demand, gas-turbine power plants can be built with advantage as unattended remote-controlled stations.

(T) R. SCHMIED

Bibliography

[1] H. PFENNINGER: Brown Boveri Gas Turbines. Brown Boveri Rev. 1957, Vol. 44, No. 4/5, p. 200–17, especially Fig. 28 on p. 215.

[2] T. INGLEDOW: Integration of Gas Turbines in Hydroelectric Systems. World Power Conference, Montreal 1958, Section A 1, Paper 31 A 1/2.

[3] J. HOGNESTAD: Operational Experience with an Automatically Controlled Gas-Turbine Plant in Venezuela. Brown Boveri Rev. 1959, Vol. 46, No. 7, p. 419–20.

[4] F. JAGGI: Remote Control of Power Plant and Substations. Brown Boveri Rev. 1955, Vol. 42, No. 7/8, p. 274–82.

[5] G. F. PIAZZA: Electronic Rapid-Cyclic Telemetering. Brown Boveri Rev. 1959, Vol. 46, No. 4, p. 260–70.

INVESTIGATIONS INTO THE EXHAUST PROCESS OF PRESSURE-CHARGED TWO-STROKE DIESEL ENGINES

621.436.052

When the pulse system is employed to pressure charge two-stroke diesel engines it is necessary to pay special attention to the exhaust-gas pipework. By means of calculations, the present article shows how to assess the influence of the shape of the pipework on the energy available at the turbine of an exhaust-gas pressure charger.

THERE is a noteworthy difference between the pressure charging of two- and four-stroke diesel engines. This difference lies in the procurement of the energy needed to provide air for combustion and scavenging. In the case of four-stroke diesel engines, this duty is always fulfilled by the exhaust-gas pressure charger alone, since the work performed by the piston in expelling the exhaust gases provides the means for varying within wide limits the energy which these gases contain. With two-stroke engines, however, apart from other considerations, it has so far only been possible to run over the entire load range with exhaust-gas turbochargers alone by employing the pulse system.

By means of correct timing, however, it is also possible here to exert an influence on the exhaust-gas energy from the engine, but only to a limited extent. By opening the exhaust ports early, the gases leave the cylinder at a higher pressure and higher temperature, and therefore contain more energy. But expansion work on the piston is lost since the pressure in the cylinder begins to drop earlier. Fuel is needed to regain this energy. Moreover, it is assumed that the higher gas temperature at the instant the exhaust ports open causes higher material temperature around the exhaust ports. The aim therefore is to strike a well-balanced compromise between the gain in exhaust-gas energy, increased thermal load and favourable fuel consumption.

Of considerable influence from an energy point of view is the good adaptation of the pressure charger to the engine. Further prerequisites are the correct assembly of the exhaust pipework, the choice of cross-sectional area and the clean arrangement of all pipework.

The following relates to two-stroke pressure-charged diesel engines which operate with the pulse system. Various arrangements of exhaust-gas pipework were investigated by means of calculation and experiment.

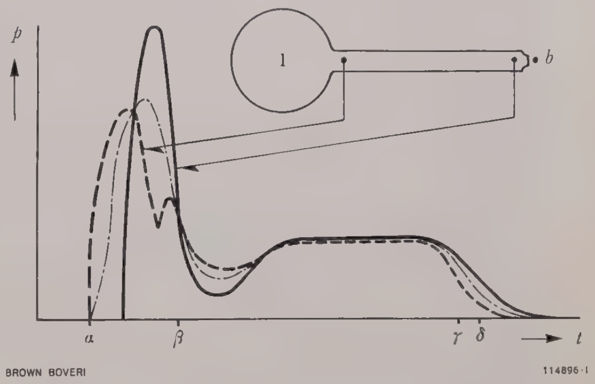

Fig. 1. – *Curves representing pressures in exhaust pipework without branches*

- - - - = Curve depicting pressure after cylinder No. 1
—— = Curve depicting pressure ahead of turbine b
-·-·- = Curve depicting pressure according to the step-by-step calculation

α = Exhaust port opens
β = Inlet port opens
γ = Inlet port closes
δ = Exhaust port closes
p = Pressure
t = Time

The pressure curve at the commencement of the line differs considerably from that in front of the turbine. The step-by-step calculation does not reveal this difference, but yields a mean curve.

1. Methods of Calculation

To be able to calculate the useful exhaust-gas energy it is first necessary to determine the pressure and temperature distribution ahead of the turbine. There are several processes available for this purpose:

Step-by-step method[1]

The principle of filling and evacuating is involved with these calculations, so that it is not possible to follow the pressure waves. The results are therefore most satisfactory with exhaust systems having comparatively short pipework. All the connections are regarded as a single compact volume. Thus, as Fig. 1 shows, the same pressure must necessarily obtain at all points at any instant. This does not also apply essentially with respect to temperature. By means of appropriate functions it is possible to introduce into and follow through the pipework gas layers having different initial conditions, similar to those which form during the scavenge period.

The work of calculation and evaluation is comparatively modest. The step-by-step method can be most easily evaluated with electronic computers; such equipment enables extensive investigations involving, for instance, the influence of individual parameters, to be performed within a reasonable time.

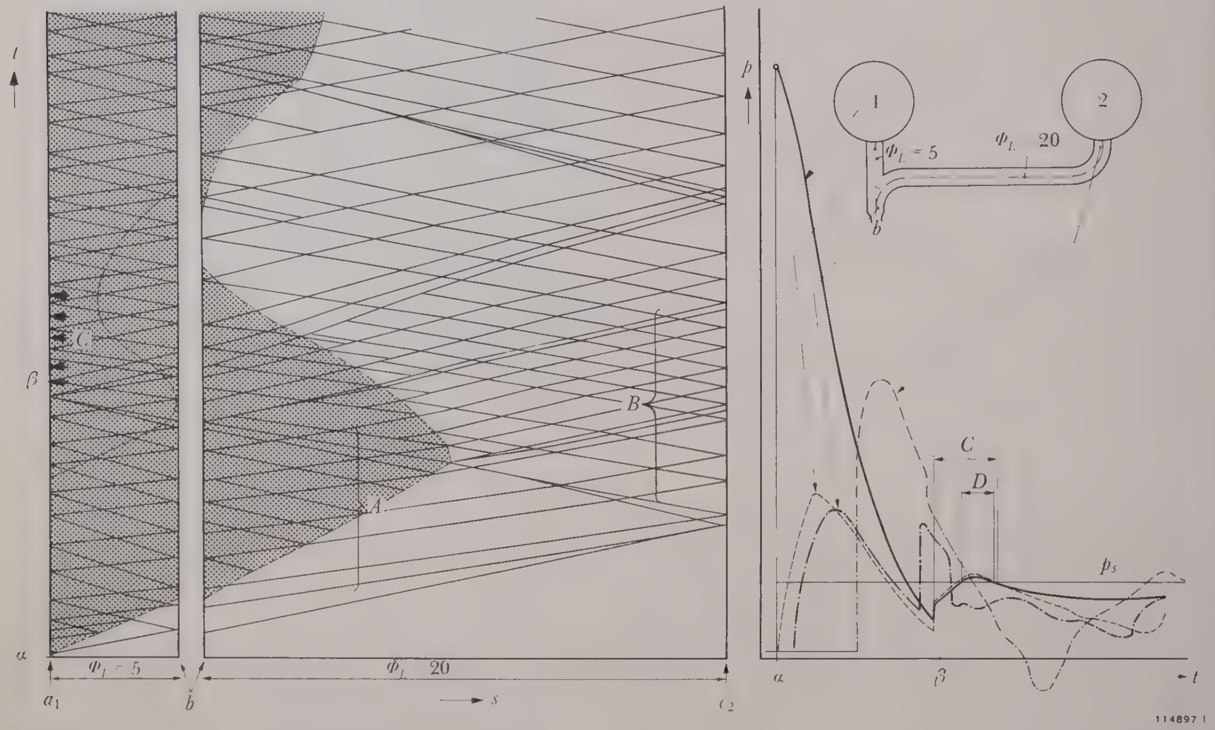

BROWN BOVERI

Fig. 2. – Characteristics calculation. Wave plan and pressure curves for the exhaust impulse in a line having branches

1 = Exhausting cylinder
2 = Cylinder 2 with closed exhaust port
Φ_L = Designation for the length of the line: time, expressed in degrees crank angle, required by a pressure wave to flow and return in a line
p_s = Scavenge pressure

Grey areas = Hot exhaust gases
A = Exhaust pulse
B = Reflected waves

C = Return of hot gases to the cylinder
D = Return of hot gases to the scavenge-air receiver
a_1 = Cylinder 1 exhaust
b = Turbine
c_2 = Closed end of pipework, cylinder 2
α = Exhaust opens
β = Inlet port opens
p = Pressure
s = Distance
t = Time

---

[1] For instance, according to Eichelberg.

Fig. 3. – Replacement of gas in a cylinder with uniflow scavenging

Left cylinder, right pipework

⟍⟍⟍⟍ = Hot gases
XXX = Mixed gases
//////// = Air
═══ = Mixing phase

σ = Separating layer
α = Exhaust port opens
β = Inlet port opens
γ = Inlet port closes
δ = Exhaust port closes
τ = Lower dead centre
e = Inlet
a = Exhaust
b = Turbine
s = Distance
t = Time

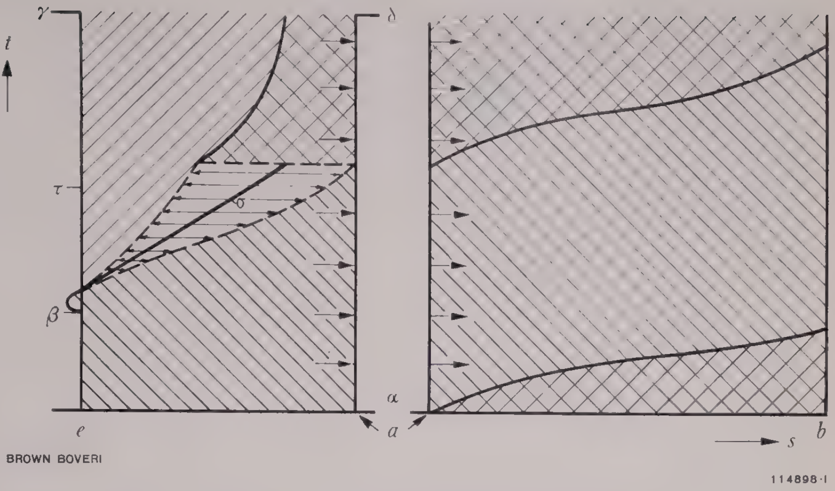

It is assumed that the entering scavenge air mixes in the separating layer with the hot cylinder gases in the ratio of 2:1. The mixture ratio results from non-steady temperature readings. The quantities forming the mixture are determined by the degree of purity of the cylinder contents at the end of the gas-replacement process.

Characteristics method

With this method of treating non-steady gas flow, pressure and temperature behaviour can be determined at any point, with the desired accuracy, depending on the time one is prepared to spend on the work. The method provides an extensive insight into the phenomena taking place in the exhaust pipework during the exhaust and scavenging period, and enables pressure waves to be followed, as well as the path of any desired particle of gas [1].[2]

In Fig. 2 the exhaust pipework from two cylinders is conducted to a common turbine inlet. The exhaust pulse from cylinder 1 expands not only in the pipe leading to the turbine, but also in the long branch line, where the pressure waves are reflected by the closed exhaust elements of cylinder 2, and travel back again. As the wave diagram shows, this causes hot gases to flow into cylinder 1.

The characteristics method is dealt with in detail in articles [2] and [3] and will therefore not be dealt with further. On the other hand, it might be of interest to dwell upon a few questions pertaining to the procedure with respect to the gas-replacement process.[3]

Calculations have shown that even in the cylinders of long-stroke, uniflow-scavenged engines there are no pressure waves and reflections which noticeably influence the gas change.[4] It is therefore only admissible to apply the characteristics process to the exhaust pipework; in the cylinder the far simpler step-by-step calculation suffices.

If in the characteristics calculation allowance is made for the wall friction, the work to be performed is increased by a multiple. The slope of the state characteristics would have to be determined anew at every step of the calculation (see also Fig. 4) and the prospect of dealing with several cases in a useful period of time would not be very encouraging. As will be demonstrated later, it is therefore advantageous to make an approximate allowance for friction in the boundary conditions. Similar considerations deter us from allowing for the heat input and output involved with the flow of gases into the exhaust pipework.

It would represent a considerable simplification if the entire calculation could be based on a medium

---

[2] The figures in square brackets refer to the bibliography at the end of the article.

[3] Those readers not acquainted with the characteristics method may disregard these references; the following comparisons and results will not suffer thereby.

[4] Gas change, or replacement, covers the exhaust and scavenging periods, i.e. the change from hot gas to fresh air.

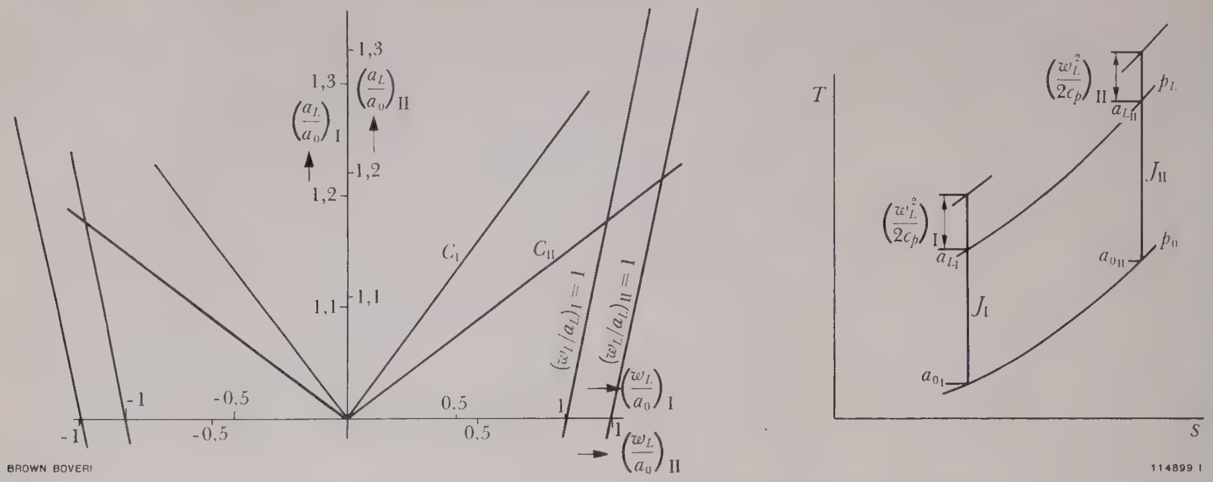
1,3
1,2
1,1
1,3
1,2
1,1
$\left(\frac{a_L}{a_0}\right)_I$
$\left(\frac{a_L}{a_0}\right)_{II}$
C_I
C_{II}
$(w_L/a_L)_I = 1$
$(w_L/a_L)_{II} = 1$
-1
-0,5
0,5
1
-1
-0,5
0,5
1
$\left(\frac{w_L}{a_0}\right)_I$
$\left(\frac{w_L}{a_0}\right)_{II}$
BROWN BOVERI
T
S
$\left(\frac{w_L^2}{2c_p}\right)_{II}$
$\left(\frac{w_L^2}{2c_p}\right)_I$
p_L
p_0
$a_{L_{II}}$
a_{L_I}
$a_{0_{II}}$
a_{0_I}
J_{II}
J_I
114899 I

Fig. 4. – Characteristics calculation: left, state diagram; right, entropy diagram

C = State characteristics (slopes) I = Isentropes

a_0 = Sonic speed at reference pressure p_0
a_L = Sonic speed at pressure p_L
w_L = Velocity of gas in the exhaust pipework
$\frac{w^2_L}{2\,c_p}$ = Pulsating pressure

T = Temperature
S = Entropy

Suffixes: I = Applies to gas mixture
II = Applies to hot gases

The scales and in particular the slopes of the characteristics in the state diagram are established by the position of the isentropes and by means of the isentrope exponents. Scale displacements similar to the one shown here for the layer-change from hot to mixed gas are obtained for all non-isentropic state changes, e.g. in the case of throttling, gas flow taking wall friction into consideration or the heat being supplied or taken away.

having a reference state which remained constant. It would then be possible to conduct every change of state on one and the same isentrope. But this simplification proves to be inadmissible since it leads to extremely wide errors; particularly when determining the energy. Consequently it is essential to introduce layers of gas which are followed during the change of gas. Thus pure air must be reckoned with on the inlet side; hot gases at the outlet, at the instant the ports open and, later, during the scavenging period, with a mixture of cool air and hot gas (Fig. 3). This process of partial mixture enables the gas-changing procedure to be described far more accurately than if the calculation were carried out in accordance with the known principles of the pure mixture or the displacement of gas layers.

Boundary Conditions

The considerations upon which the boundary conditions are based will now be explained.

If a pressure-wave process is calculated by means of the characteristics method, it is necessary each time to establish the isentrope upon which the gas particles change their state, since the scale of the state diagram and, particularly, the slope of the characteristics depend upon this. The position of an isentrope is described by the sonic speed a_0 at the reference pressure p_0 (Fig. 4).

Inlet

The test engine has outlet ports all round the periphery of the cylinder. A belt joins all the ports and serves to collect the gases for delivery to the exhaust pipework. It is assumed that, owing to turbulence, the kinetic energy is completely dissipated during expansion through the ports. The foregoing expansion is followed by a further expansion as the gases flow into the exhaust pipework. The results of throttling in the exhaust ports is that the states of the gases in the cylinder, on the one hand,

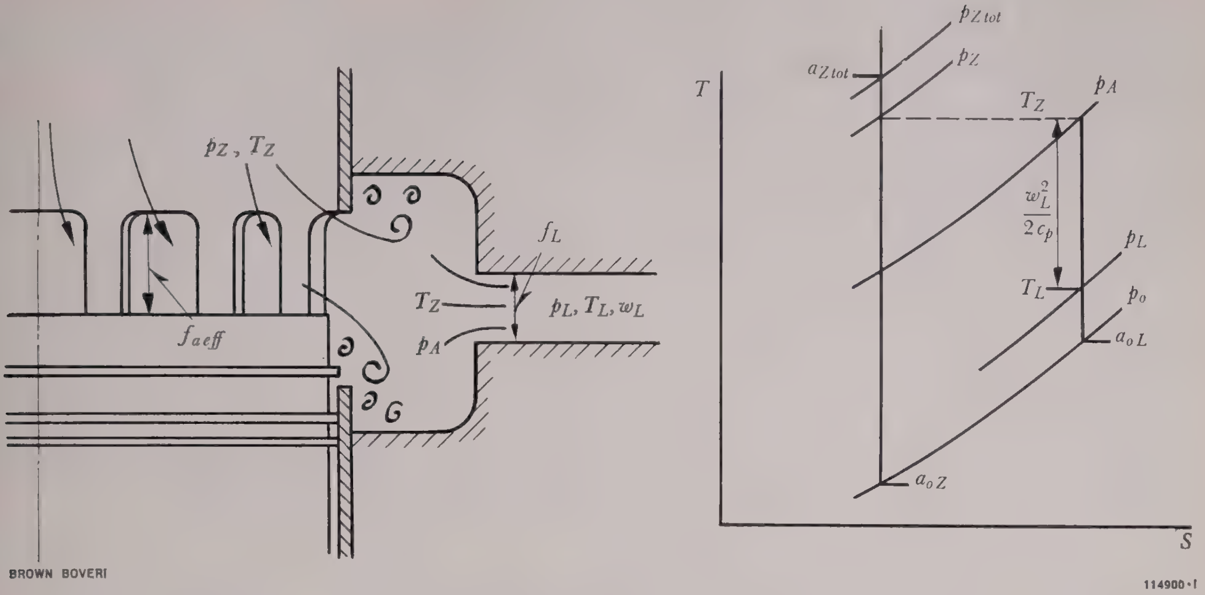

Fig. 5. – Boundary conditions in the exhaust belt

Suffixes:

Z = Cylinder
A = Exhaust belt
L = Pipework
tot = Condition with constant-pressure flow
0 = Reference state

$f_{a\,eff}$ = Instantaneous cross-section of all exhaust ports
f_L = Cross-section of pipework
T = Temperature
S = Entropy
p = Pressure
a = Sonic speed
w = Velocity of gas

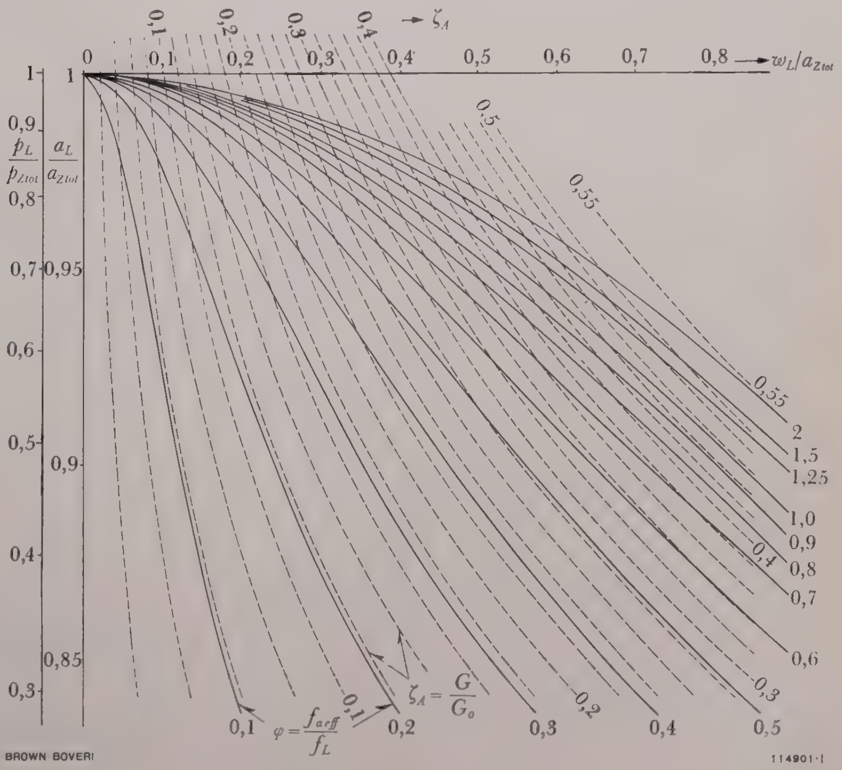

Fig. 6. – Boundary condition diagram for the emission from the cylinder via the exhaust chamber

φ = Surface ratio
ζ_A = Designation for the quantity being exhausted
G = Quantity being exhausted
G_0 = Reference magnitude: Quantity which would flow in the pipework at sonic speed if the stagnation pressure conditions of the cylinder obtained here.

The remaining designations are furnished in Fig. 5.

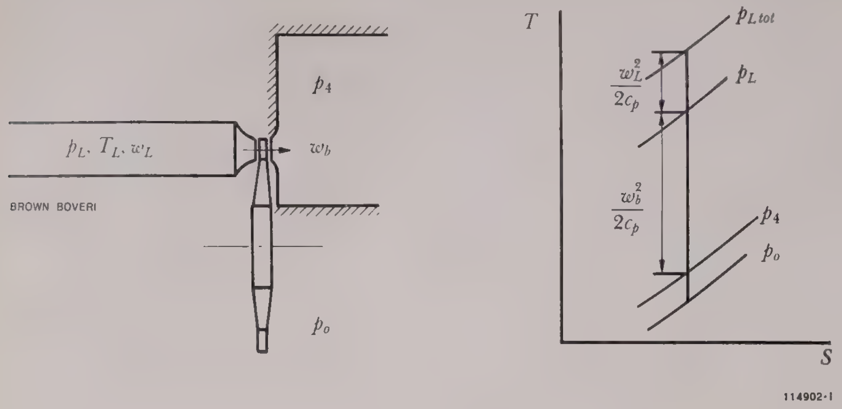

Fig. 7. – Boundary condition at the turbine; exhaust pipework without branches

w_L = Gas velocity in the pipework
w_b = Gas velocity in the turbine
p_4 = Back pressure after the turbine

Fig. 5 furnishes the remaining designations.

The stagnation pressure $\frac{w^2_L}{2\,c_p}$ is regarded as lost.

and in the exhaust pipework, on the other, are located on different isentropes. The greater the ratio of the cylinder pressure to the pressure in the pipework, and the less the exhaust ports are opened, the greater are the losses due to throttling. For this reason all engine builders strive to make the exhaust ports of their engines open as quickly as possible. But as regards the calculation this means that the slope of the characteristics would have to be determined afresh for each step. In order to evade this very considerable amount of extra work, a mean throttling value can be laid down, for instance, for the blow-down and for the scavenging period (Fig. 5 and 6).

Turbine (Fig. 7)

In the boundary conditions, the turbine of the exhaust-gas turbocharger is replaced by an orifice. A variable back pressure is not compensated for because the pressure fluctuations after the turbine are usually slight; moreover, they depend upon the pipework arrangement, and this varies from engine to engine. The total effect of friction is taken into account approximately by inserting the static instead of the total head for determining the useful gradient at the turbine. This general assumption seems appropriate when it is considered that an exhaust pipework system usually has two 90° bends and that a grille is fitted at the turbine inlet to catch pieces of piston ring. The resultant resistance to flow is of the order of magnitude of a stagnation pressure (Fig. 7).

Making use of the following assumptions, it is comparatively simple to evaluate branched pipework:

The pressure assumed at the junction represents the boundary condition for the individual pipes meeting at this point. This enables all the inflowing and outflowing quantities to be determined. The quantity balance provides a check for the assumed pressure.

The volume at the junction has no storage capacity.

The turbine is located directly at the junction. This assumption enables the flow from the turbine to be evaluated at the same place and at the same time as the in- or outflow from the connected branches.

In accordance with Fig. 8, the gases emanating from the cylinder being exhausted not only flow into the turbine, but also, initially, fill the branch line. The flow into the latter is accompanied by losses which are caused by separation at the edges of the branch. In practice, these entry losses are increased by the acute angle at the point where the pipes join. The friction is again taken care of by considering the stagnation pressure at the point of intersection as lost.

At the commencement of the scavenging period the branch line empties again. The flow towards the point of intersection should take place as far as possible without throttling; the sharp angle where the pipes converge assists to this end. The state of the gases flowing through the turbine at this instant

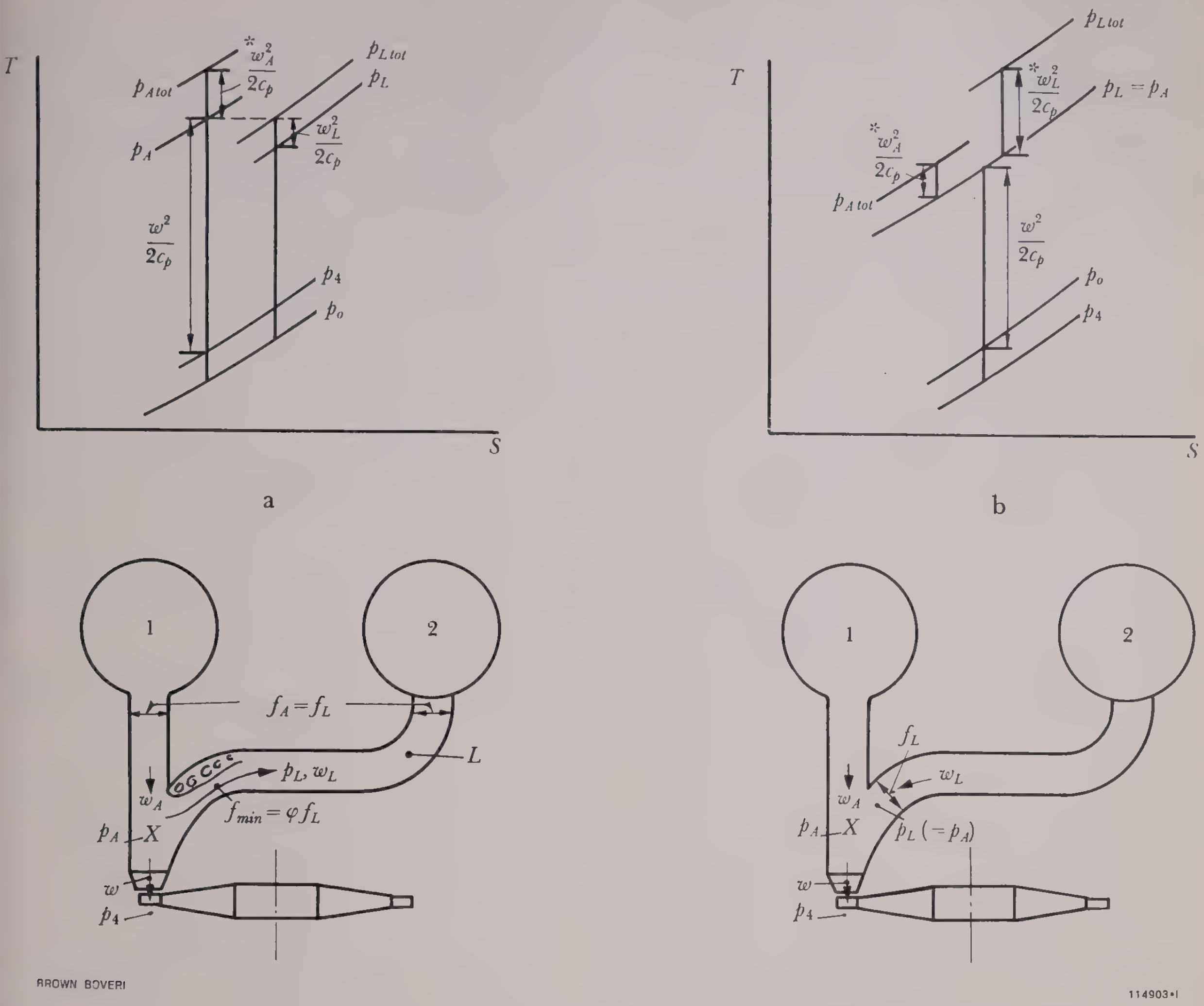

Fig. 8. – Boundary condition at the junction

a = Entry into the branch line

b = Exit from the branch line

1 = Cylinder exhausting
2 = Cylinder 2 with closed exhaust elements
L = Branch line
X = Junction
φ = Coefficient of flow for the entry into the branch line

Suffixes:
A = Applies for the pipework connection to the cylinder which is exhausting
L = Applies for the branch line
For the rest of the notation see Fig. 5.

The stagnation pressures (marked with *) of the gases flowing towards the junction are regarded as lost. The pressure at the end of the pipework attached to cylinder 1 is the same as that at the junction.

is located on an isentrope which lies—according to the mass flows—between the exhaust and the branch line isentropes.

2. Comparison between Calculation and Measurement

In order to judge the success of pressure charging it is necessary for engine builders to take test-bed readings. In the main, these are static readings of pressures, temperatures and air quantity.

The efficiency with which the pressure charger converts the exhaust-gas energy cannot be measured when operating with the pulse system. However, by taking comparative readings on one engine, it is possible to determine the turbine dimensions which yield the best results. But in order to get an idea

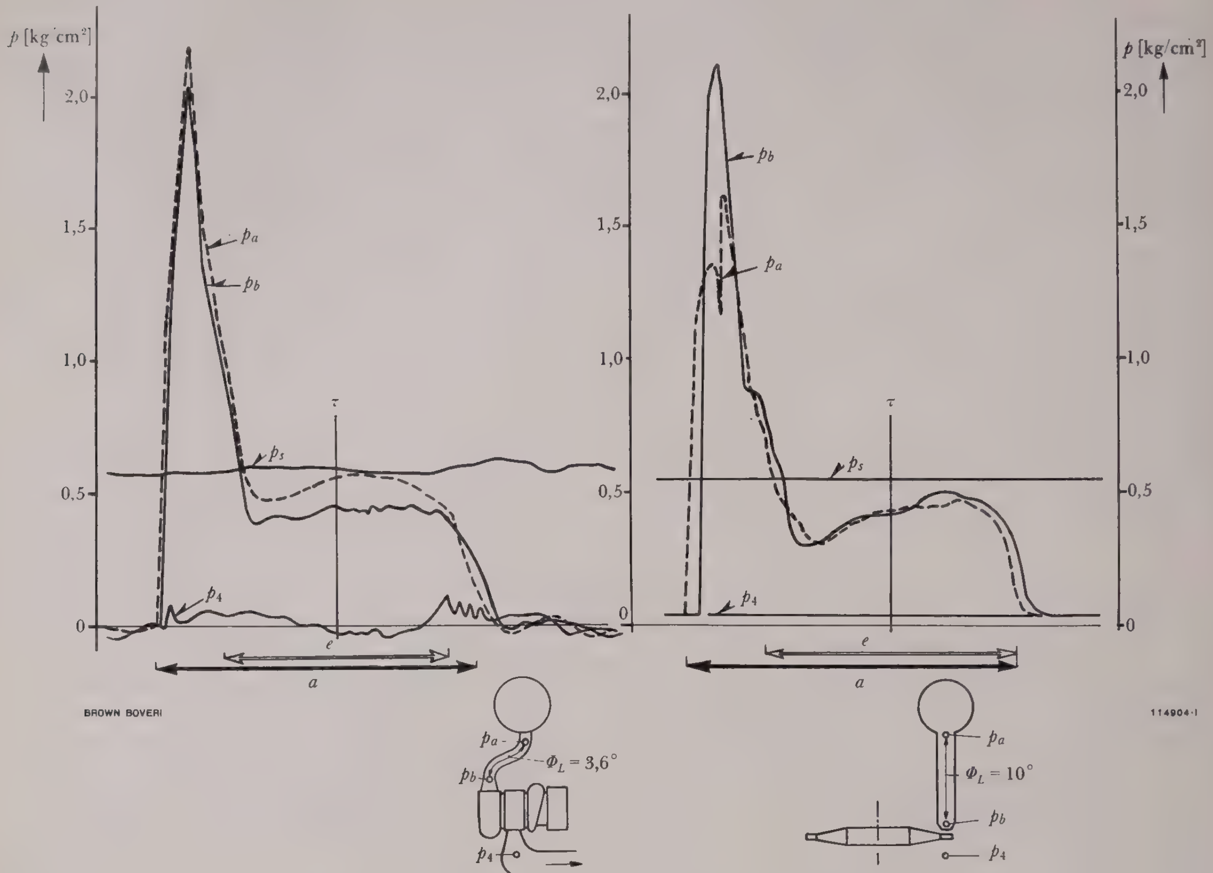

*Fig. 9. – Exhaust impulse in a line without branches**

Left: Measurement—engine data:

Bore = 600 mm
Stroke = 2000 mm
$p_{me} = 7{\cdot}45$ kg/cm²
$n = 139$ rev/min

Right: Calculation—engine data:

Bore = 750 mm
Stroke = 2500 mm
$p_{me} = 7$ kg/cm²
$n = 110$ rev/min

Φ_L = Characteristic magnitude for the length of the pipework; see also Fig. 2
p_s = Scavenge pressure
p_a = Pressure after the cylinder
p_b = Pressure in front of the turbine
p_4 = Pressure after the turbine
τ = Lower dead centre
e = Inlet ports open
a = Outlet ports open

of what takes place during a change of gas in the exhaust pipework, it is essential to take dynamic pressure readings. Such readings enable the quality of the pipework system to be assessed. In this way, for instance, pressure waves and their reflections can be followed; undesired resonance phenomena are traceable; the blow-back of hot cylinder gases in the scavenging-air receiver at the beginning of the scavenging period can be assessed, etc. Nevertheless, these readings are not sufficient to determine the energy available at the turbine and thereby the efficiency of the pressure charger. Furthermore, non-steady temperature and mass-flow readings would have to be taken immediately ahead of the turbine. There are known methods for recording variable temperatures in a gas stream [4], but a process is lacking which enables the mass-flow or—what amounts to the same thing—the velocity of the gas to be

---

* The company Chantiers et Ateliers de Provence, Marseilles, kindly permitted us to test several pressure-charged two-stroke diesel engines (type Doxford). The readings here are from a type 60 SBD 4 S engine, while those in Fig. 10 are from a type 60 SBD 6 S.

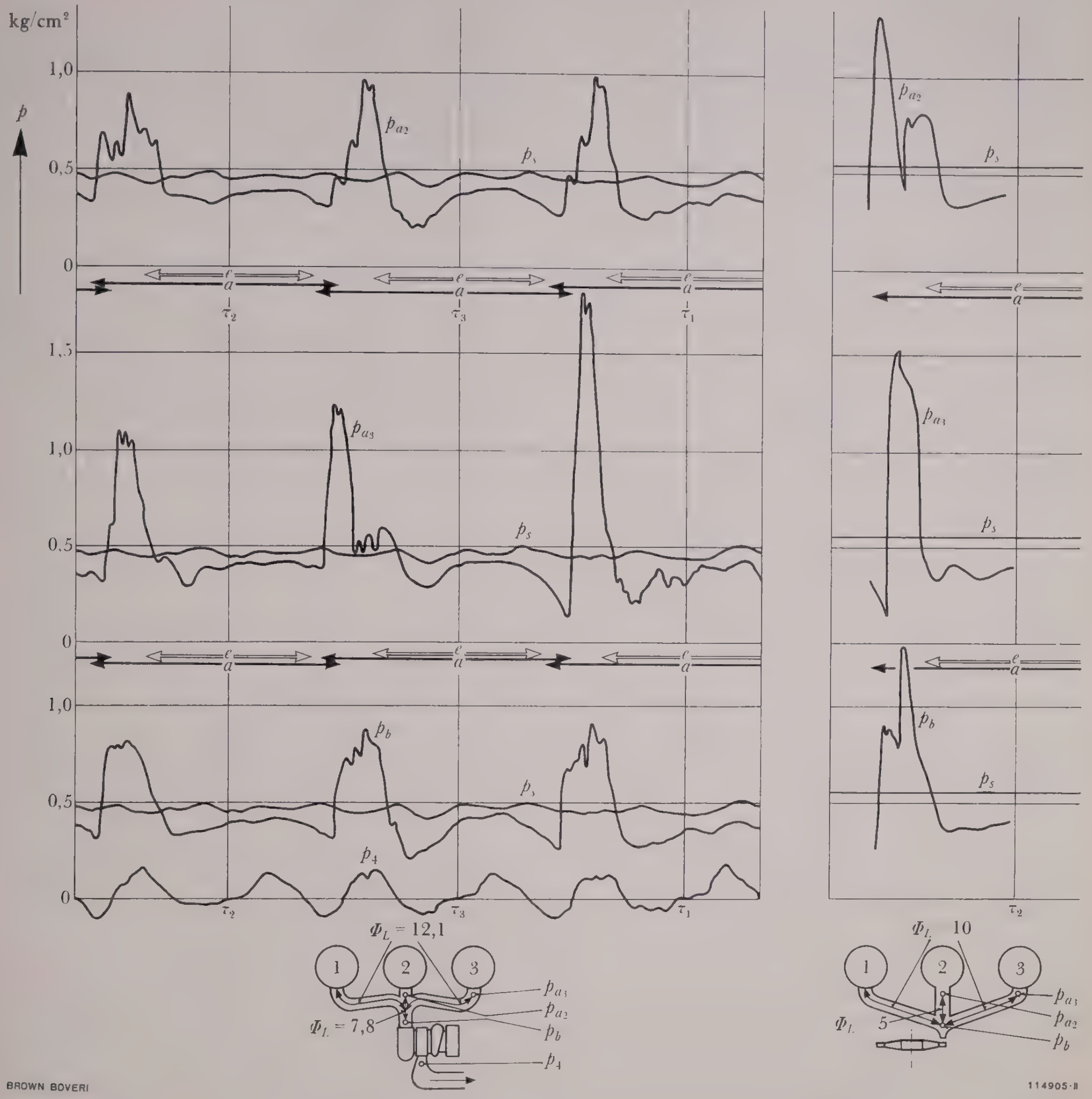

Fig. 10. – Three-cylinder case; exhaust pulses in a double-branch line

Left: Measurements—engine data:
Bore = 600 mm
Stroke = 2000 mm
$p_{me} = 6 \cdot 9$ kg/cm²
$n = 137$ rev/min

Right: Measurements—engine data:
Bore = 750 mm
Stroke = 2500 mm
$p_{me} = 7$ kg/cm²
$n = 110$ rev/min

Φ_L = Characteristic magnitude for the length of the pipework
p_s = Scavenge pressure
p_{a2} = Pressure after cylinder 2
p_{a3} = Pressure after cylinder 3
p_b = Pressure in front of the turbine
p_4 = Pressure after the turbine
τ_1, τ_2, τ_3 = Lower dead centre of cylinders 1, 2 and 3
e = Inlet ports open
a = Outlet ports open

The pressure curves are drawn beneath each other so that the outer left measurement enables the pulse from cylinder 2 to be followed; that in the centre, the pulse from cylinder 3; and the one on the right, the pulse from cylinder 1. The upper curve is for the measuring point after cylinder 2; that in the centre for the measuring point after cylinder 3, and the lower one for the measuring point in front of the turbine. The calculation shows the pulse from cylinder 2 at the appropriate points.

measured with adequate accuracy when the temperature changes rapidly and the pressure varies.

With the aid of two examples it is now proposed to compare results from the characteristics calculation with dynamic pressure measurements.

Fig. 9 shows the typical curve associated with the expulsion of gas into a line without branches, similar to the arrangement encountered occasionally with five-, seven- and also four-cylinder engines. The pressure in the line rises sharply during the blow-down period. At the instant the inlet ports open, the pressure has not yet dropped below the scavenging pressure. This indicates that the cylinder is not completely empty and that a slight rebound of hot gases into the scavenge-air vessel must be reckoned with. In other respects the scavenge period proceeds undisturbed; no other noteworthy reflections are noticeable.

The engine used for the readings did not conform precisely to the calculation assumptions. This is the reason why the calculated pressure curve does not coincide in every detail with the one obtained by measurements.

In this regard we wish to make the following observation: A somewhat higher pressure peak was measured after the turbine than in front of the turbine; actually, the reverse would have been expected from the calculation. The different behaviour can be explained by the fact that the engine used in the test had considerably shorter pipework than was assumed in the calculation. The reflections from the turbine are thus superimposed on the initial exhaust impulse at an earlier stage, when the line pressure has hardly dropped. Consequently, altogether, the pressure at the beginning of the line rises higher. Moreover, the turbine measuring point had to be placed in a part of the line having a larger cross-sectional area; but this causes the pressure curve to be slightly lowered. Furthermore, increased wall friction caused by two acute bends on the test engine might have conduced to the lowered pressure ahead of the turbine.

Fig. 10 shows pressure curves for a six-cylinder engine whose cylinders are assembled in two groups of three and led to a common turbine inlet. This pipework arrangement provides the ideal case for pressure charging with the pulse system. The pressure ahead of the turbine is composed of a constant-pressure and a pulse component. The three impulses from the exhausting cylinders are superimposed on the constant-pressure component. The pressure in the pipework never drops to that of the surrounding state: thus only a small amount of energy is lost until the line is full. Since the turbine always operates with full admission, windage losses do not occur. The essential phenomena can be followed unambiguously, with the calculation as well as with the measurements. A detailed comparison of the pressure curves is not necessary here, since the tested engine did not conform to the assumptions made for the calculation.

Unlike the conditions obtaining in a pipework system without branches, the pressure peaks at the commencement of the blow-down period are comparatively low. This is explained by the fact that once these exhaust pulses reach the branch they can expand towards three pipework connections, so that the pressure is reduced. This also applies to the reflections which, moreover, spaced with respect to time, return from the ends of the branch lines. The enormous build-up of gases in front of the turbine, as encountered in pipework without branches, is not observed here. Sooner or later, depending on the geometry of the pipework, the reflections are superimposed on the initial exhaust impulse. Altogether, therefore, the pressure in front of the turbine rises less than the calculation would infer, because in the case of the measured engine, the reflections did not manifest themselves until later and were, moreover, less intense.

It is also desirable to refer to the following, which the calculation already revealed: at the commencement of the gas-changing process, with respect to cylinder 1, for instance, the exhaust impulse from this cylinder advances towards the branch, where it diminishes and divides. Part of the gases enter the branch line of cylinder 3. The comparatively low pressure peak now reaches the closed exhaust ports;

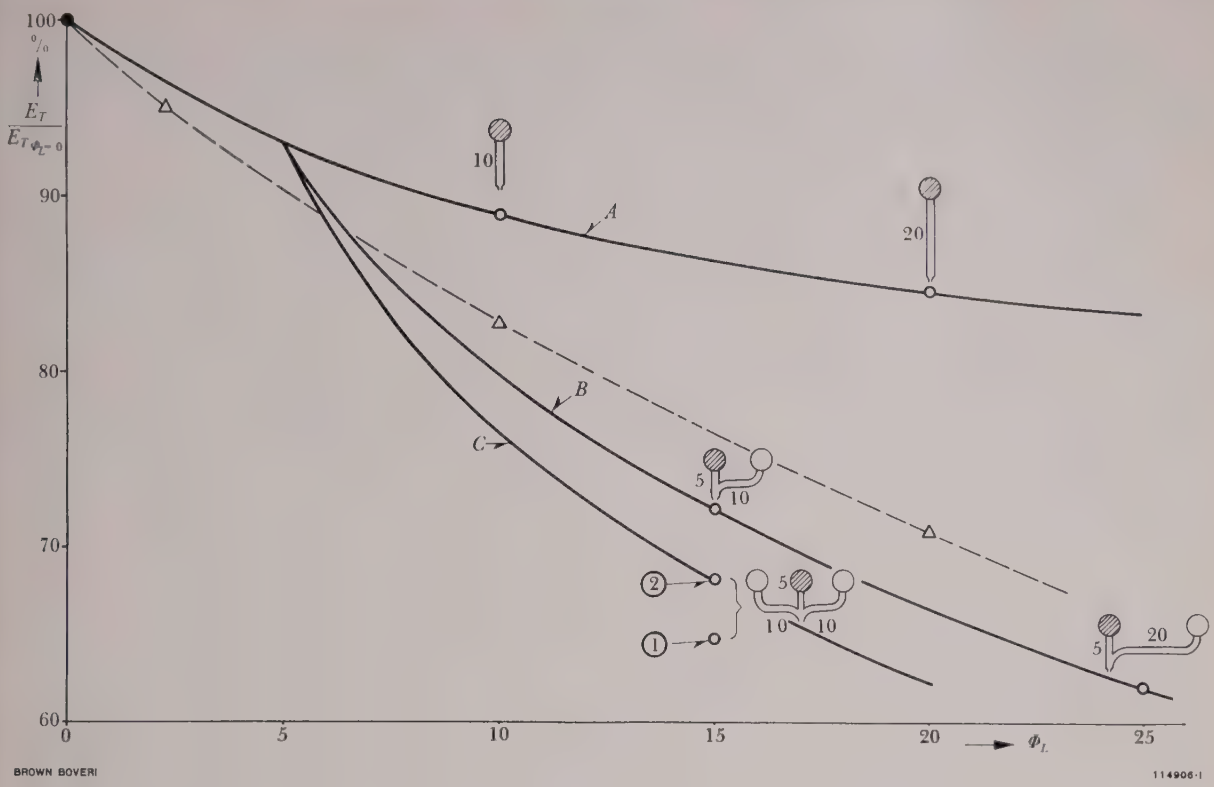

Fig. 11. – Useful exhaust-gas energy—calculated results assembled

—○— = Characteristics calculation
A = Curve for pipework without branches
B = Curve for pipework with single branch
C = Curve for pipework with double branch
---△--- = Step-by-step calculation

E_T = Useful exhaust-gas energy in the turbine
$E_{T\Phi L=0}$ = Useful exhaust gas energy with infinitely short pipework
Φ_L = Characteristic magnitude for the length of the pipework; see also Fig. 2

The cylinders exhausting are shown hatched, the figures next to the pipework arrangements give the Φ_L values. With the calculation for the double-branched line, two assumptions are encountered:

① = Between two pulses the line pressure drops right down to the surrounding pressure.
② = Between two pulses the line pressure does not drop to the surrounding pressure.

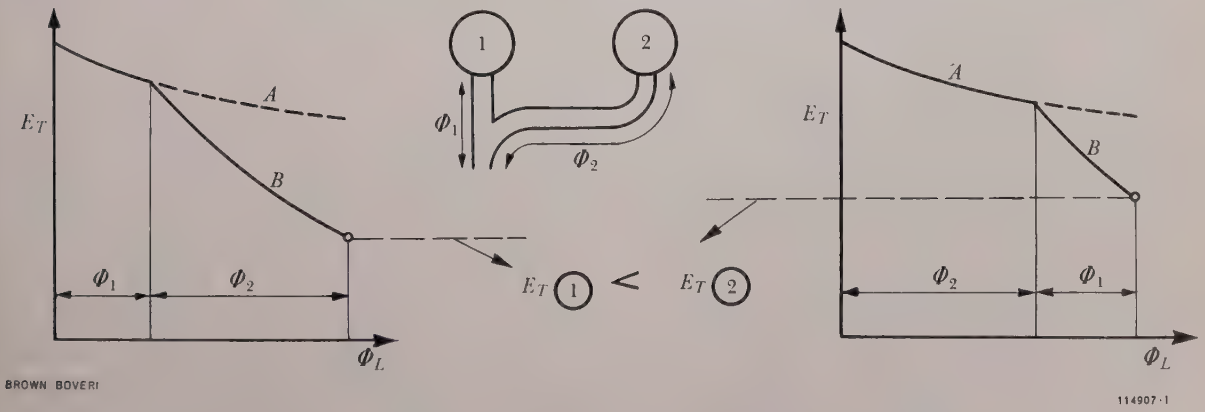

Fig. 12. – Distribution of the exhaust-gas energy according to its origin

Left: Procedure when exhausting cylinder 1 Right: Procedure when exhausting cylinder 2

Notation as Fig. 11.

here the gases are dammed by the advancing contents of the pipework and the pressure increases quite considerably. The same effect can be observed during the gas-changing process of cylinder 2.

3. Evaluation of the Calculated Results

Measurements [5] and calculations show that the energy available at the turbine is dependent on the form of the pipework. It is also known that most exhaust gas energy is available when the pipework volume is smallest. Fig. 11 shows how this energy can be represented in relationship to the pipework arrangement. In the case of pipework without branches, the length of the exhaust system exerts only a slight influence. A flat curve is the result. With pipework having branches the energy drops heavily. Since for all the calculated cases a length corresponding to $\Phi_L = 5$ was assumed for the pipework connected to the exhausting cylinder, the curve only starts to fall at this value. This infers that the exhaust impulse advances in a line without branches as far as the branch junction and diminishes at this point, according to the length of the laterally connected branches. This effect is particularly pronounced in a system having double branches.

For short lines and also for those having simple branches, the results obtained from the step-by-step calculation compare very well with those obtained from the characteristics calculation. For an infinitely short line they must coincide. Agreement is also obtained for lines with double branches; although this cannot be seen unhesitatingly with this representation. In the characteristics calculation double branches are treated like single ones, except that double the cross-sectional area is taken. In Fig. 11 this leads to the calculated three-cylinder arrangement being drawn above $\Phi_L = 15$. Since now with the step-by-step calculation it is only possible to evaluate the influence of the pipework volume, a comparison can only be made when the volumes are the same. This requirement is fulfilled in the present case when the result for the three-cylinder arrangement is shifted further to the right, so that $\Phi_L = 25$. By this means, good agreement is recognized also for the double branch system.

It must be particularly emphasized that Fig. 11 does not illustrate how the turbine assimilates the energy supplied. Thus the representation should not create the impression that the employment of exhaust-gas turbochargers is fundamentally better in conjunction with pipework devoid of branches than when these are present. It is realized, for example, that extremely good results are achieved with the three-cylinder case, although with this arrangement less energy is available at the turbine. But because here the turbine always operates with full admission, there are no windage losses; the exhaust-gas energy is used efficiently. If, on the other hand, these three cylinders were individually connected to the turbine, about three times as much turbine surface would be needed than if the pipework were combined. For economic reasons alone this is not efficacious. Furthermore, it must be taken into consideration that, due to the comparatively wide fluctuations of the gradient in the case of an exhaust impulse in the pipework without branches, a lower mean peripheral efficiency obtains at the turbine than with the three-cylinder arrangement. Then the turbine operates with only one-third admission at any one time, so that quite considerable windage losses occur. By and large, the exhaust-gas energy is used with little success.

If in an exhaust system in which a number of cylinders are combined the energy available at the cylinder is divided up according to its origin, it will be observed that in the majority of cases the cylinders involved make unequal contributions. Fig. 12 shows, with the aid of Fig. 11, how these contributions can be determined in the case of two cylinders connected to a common pipe. The exhaust gases of cylinder 2 contain more useful energy than those of cylinder 1. This proves that the shorter lateral branch conduces to the larger delivery of energy to the turbine.

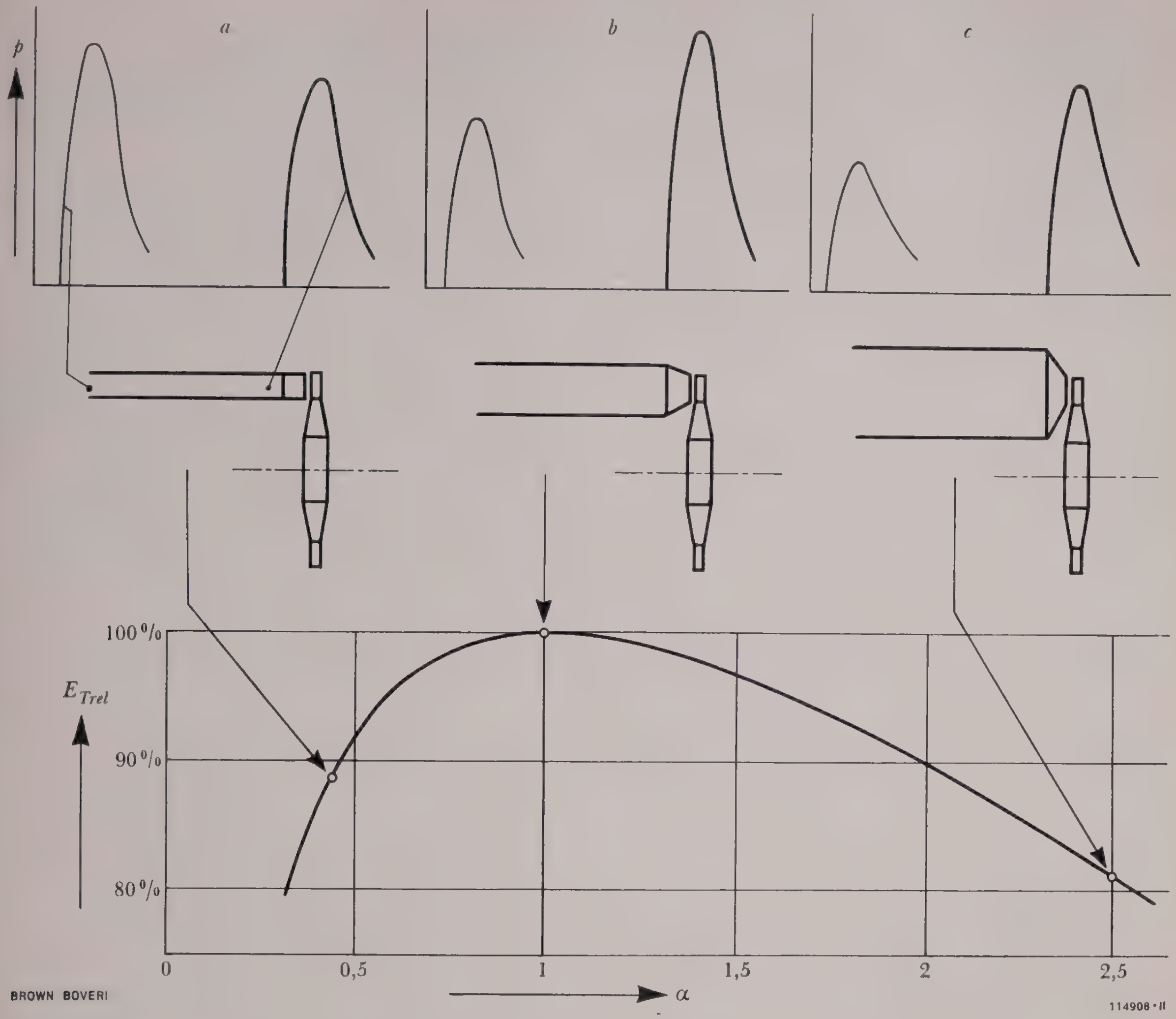

Fig. 13. – Selection of the cross-sectional area of the pipework

a = Pipework too narrow
b = Optimum pipework cross-section
c = Pipework too wide
p = Pressure
$E_{T_{rel}}$ = % energy arriving at the turbine

$$\alpha = \frac{\text{Cross-sectional area of pipework}}{\text{Optimum cross-sectional area of pipework}}$$

Apart from the arrangement, the cross-section of the exhaust pipework has a significant influence on the energy available at the turbine. In an installation in which everything but the cross-section is determined, in particular the effective turbine surface, the pipework must be dimensioned so that the pressure in front of the turbine rises as much as possible, because in this way the useful energy attains a maximum value. This is demonstrated by Fig. 13. If the selected pipework is too narrow, the wall friction, on the one hand, is considerable, and the gases at the turbine, on the other, are only very slightly dammed, or not at all. Decisive for the desired damming is the ratio: effective turbine surface to pipework cross-section. If the latter area is too large, the throttling losses at the commencement of the blow-down period are so great that the highest possible pressure is no longer obtainable, in spite of a small surface ratio at the turbine. The characteristics calculation enables the optimum pipework cross-section to be determined.

Conclusions

The significance has been emphasized of the layout of exhaust pipework belonging to pressure-charged two-stroke diesel engines which operate with the pulse system. Since at the moment there are no sufficiently accurate methods of measurement, the energy available at the turbine of exhaust-gas pressure chargers can only be determined by calculation. Of the calculation methods described, the characteristics process is most suitable for assessing exhaust pipework systems. The results of such calculations have been assembled. They demonstrate the relationship of the useful exhaust-gas energy to the form and cross-section of the pipework.

(FJH) G. GYSSLER

Bibliography

[1] H. HERGER and E. JENNY: Turbo-charging of diesel engines, present state and future developments. Congrès international des machines à combustion (CIMAC) 1957, final report, p. 129.

[2] E. JENNY: Unidimensional Transient Flow with Consideration of Friction, Heat Transfer, and Change of Section. Brown Boveri Rev. 1950, Vol. 37, No. 11, p. 447–61.

[3] R. SAUER: Charakteristikenverfahren für die eindimensionale instationäre Gasströmung. Ing. Arch. 1942, Vol. 13, p. 79.

[4] S. AFTALION: The Determination of Rapidly Changing Exhaust-Gas Temperatures in Internal Combustion Engines. Sulzer Tech. Rev. 1958, Vol. 40, No. 2, p. 67–74.

[5] W. KILCHENMANN: Contributions to the development of the supercharged two-stroke diesel engine. Congrès international des machines à combustion (CIMAC) 1957, final report, p. 567.

BROWN BOVERI AND ATOMIC ENERGY

621.039

EXPERIENCE gained over the last few years has proved that, to obtain energy economically from nuclear fission, it is not only important for the physical phenomena inside a reactor to be mastered, but also for solutions to be found to a host of problems of a conventional nature. Since maximum reliability and effectiveness are demanded of all components of such installations, advantage can be taken of the wealth of knowledge of the design and construction of such items as containers, pumps, heat exchangers, turbo-machines, control equipment, and so on, and an attempt made to adapt such components to the special requirements of atomic power plants. To do this it is necessary to study the atomic plant as a whole. Brown Boveri began to consider the problems associated with harnessing atomic energy at an early stage. At the beginning, in 1946, there was no clear indication of where this would lead the Company. The only fact which was then obvious was that, to gain some practical knowledge of the subject, it would be necessary to study reactors and finally to build one. Thus, as a result of close collaboration with other Swiss firms, the organization known as *Reactor Ltd.* was established, with the primary task of building a research reactor.

Later it was decided that the Company itself would not build reactors, at least for the time being, but rather would concentrate on certain important ancillary components such as the electrical machines and switchgear, circulating blowers, heat exchangers and, above all, the thermal machines involved. They regarded it as their special duty to undertake the overall planning of atomic power stations, to study safety problems and questions of economics and the like, in order to be in a position to give customers specialist advice on such problems.

In view of the many different reactor systems which have been developed, Brown Boveri could not confine their attention to a *single* type because, after all, their steam turbines are not designed to operate only *one* kind of boiler. On the contrary, they had to retain maximum flexibility. But to uphold this principle it was essential for them to retain full freedom in the development of their products.

Some of the Company's licencees and associates, however, adopted a different approach. *Brown Boveri, Mannheim*, collaborated with *Friedrich Krupp, Essen*, and offered the German authorities a gas-cooled, high-temperature reactor conceived by Dr. Schulten, which has since been ordered. *Richardsons Westgarth, Wallsend*, joined with a number of other British firms to found *Atomic Power Construction Ltd.*, who developed a reactor in accordance with British practice. They were entrusted with the contract to build a complete 500-MW station at Trawsfynydd.

The success of these allied companies enables Brown Boveri to study the special aspects of their reactors and to exploit the knowledge so gained in accordance with the aims set out above. Therefore the first two articles which follow describe these reactors and allow readers to compare their features; the third article is a further continuation of a series of studies into certain aspects of the design of atomic power stations.

(KME) C. SEIPPEL

THE BROWN BOVERI-KRUPP HIGH-TEMPERATURE GAS-COOLED REACTOR

621.039.52.034.3

In August 1959 the contract was placed with Brown Boveri, Mannheim, and Friedrich Krupp, Essen, for construction of a prototype high-temperature gas-cooled nuclear reactor developed by them in collaboration. This prototype, with a net electrical output of 15 MW, will be installed at Jülich, Germany, and operated by AVR (Arbeitsgemeinschaft Versuchsreaktor). With the construction of this plant the Brown Boveri concern has a major share in the realization of the first German project for a nuclear power reactor.

Fundamental Considerations and Aims

THE DEVELOPMENT of economic nuclear power plants with reactors of well-known types which have been tried in service—mainly pressurized-water reactors, boiling-water reactors, and gas-cooled reactors of the Calder Hall type—is limited by several technical factors. First mention in this respect goes to the restrictions on temperature imposed by the high system pressures in water-cooled reactors, and by the use of metallic uranium in the Calder Hall type of reactors; consequently, the *steam conditions* that can be reached compare rather unfavourably with those in modern conventional steam power plants. For boiling-water reactors, therefore, it was quite natural that development should proceed in the direction of nuclear superheating. However, the problem of improving the thermal efficiency of nuclear power plants is not as decisive as is often stated. The gains to be expected are relatively low, due to the increased cost of the plant as a whole.

More serious is the effect of the restrictions on the *power density* imposed by the temperature limitations in the fuel elements. This is a problem of finding an optimum compromise between the number and dimensions of fuel elements on the one hand and costs on the other. Even for ceramic fuel elements (oxides and carbides) the cautious stipulation that central melting should be avoided is still followed. This stipulation generally limits the feasible power densities far more rigorously than the need for sufficient heat transfer.

However, the most important factor with respect to the economic characteristics of nuclear power plants is the problem of the attainable fuel burn-up. Here one has to discriminate between two quite different limiting factors: the mechanical strength of the elements and the reactivity needed to maintain the chain reaction. With reactors built so far, the exhaustion of the reactivity reserves (compensated by the control rods and "burnable poison") is normally decisive for the attainable burn-up, but little is known about the mechanical strength of the elements in terms of burn-up. Mostly figures in the neighbourhood of 3000 MWd/t (megawatt days per ton) for metallic natural uranium elements and 10 000 MWd/t for slightly enriched ceramic elements are quoted nowadays; these figures, however, are generally based on reactivity calculations which only take certain zone loading schemes into consideration. However, if a new reactor conception can attain a high conversion rate of fertile to fissile material and can always keep the reactivity as high as necessary (by providing facilities for the continuous addition of new fissile material, for example) or if the reactor is even a breeder (conversion rate > 1), the output limit from the mechanical and material aspects becomes the decisive factor. If suitable elements can be developed, this opens a way to substantially lowering fuel costs and to achieve economical nuclear power plants by combining principles which so far have not been exploited to a very large extent.

The development of a high-temperature gas-cooled reactor taken up in 1956 by a study group formed by Brown Boveri and Krupp tries to approach such a solution by the use of an optimum fuel cycle (the Th^{232}-U^{233} cycle), by using a high-temperature steam turbine cycle, by new ideas in the design of the reactor (jointly with DEGUSSA), and by the development of a new type of fuel element. Above all, the design work for the prototype was guided by *safety* considerations. At the same time, however, every possible effort was made to realize the further aims of *low capital investment, low fuel costs and simple construction* in this prototype.

The station, construction work on which will start in the spring of 1960, is considered as a pilot plant with which experience will be gained for the design of larger units. In particular, the characteristics of the fuel elements will be tested and the possibility of higher loading in a small part of the core investigated. Therefore this first reactor should be regarded as a prototype serving technical development, and not as a mature, commercial type. Experience gained with this reactor and power costs cannot therefore be taken as characteristic for larger plants to be built later. However, it will be possible to gain valuable results by extrapolation.

The basic conception and the high expectations for reactors of this type seem to be justified by the parallel developments which are taking place in other countries. The most advanced programmes are those of General Atomic for the Peach Bottom, Pennsylvania, USA, plant and the "Dragon" project of the OEEC nations.[1]

Main Features of the Brown Boveri–Krupp Reactor

The completely new basic principle of this reactor, with spherical fuel elements in a "pebble bed" freely (statistically) heaped was chosen to meet the demands for simple construction, low susceptibility to disturbance and low fuel costs with, at first sight, a rather bold but universally applicable concept. In the reactor the fuel elements move by gravity only and the lines of flow of the spheres can be influenced by additional devices, so that the power density profile over the core can be regulated to a certain extent. Extensive experiments were carried out to prove the applicability of this concept. With the exception of four absorption elements which can be lowered in graphite sleeves into the core and which are only used for fast reactor shut-down and for lowering the temperature after the reactor has been shut down, the core contains no mechanically moved parts at all. Above all, there are no movable control devices, the safe functioning of which would impose considerable problems in view of the high temperatures in the core. A further feature of the reactor is that its output is controlled merely by varying the speed of the blowers; this control principle is based mainly on the effect of the negative temperature coefficient. The ability to add or subtract fuel at any time with the reactor in full operation, and furthermore to influence the spatial distribution in the core, makes it unnecessary for a reactivity reserve for fuel burn-up to be incorporated and controlled.

With the "pebble bed" concept a limitation of the possible power density due to the relatively high void volume in the core (39%) has been accepted because of the predominant advantages of simplicity and low costs. On the other hand, the fuel element design with the porous, sintered fuel graphite cylinder inserted into the graphite sphere, makes it possible to allow high temperatures or even central melting and therefore to increase the load capacity of the elements and the power density in the core. In this respect the core of the prototype reactor has been designed very cautiously—the maximum temperature in the fuel inserts is still about 1000 °C below the melting point—but one of the major objects of operating the prototype reactor will be to test single, more heavily loaded elements to destruction in order to establish the true capability of elements of this new type. Fuel dispersions or impregnation of the graphite spheres with fissile material are further possible fuel element designs which may be tested in the prototype.

---

[1] L. R. Shepherd: The possibilities of achieving high temperatures in a gas-cooled reactor. Report P/314 of the Second Geneva Conference on the Peaceful Uses of Atomic Energy, Sept. 1958.

The use of graphite as canning material for the fuel—which is also an advantage in view of the identity of the moderator and the canning, the neutron economics, and the ability to attain high temperatures—makes it possible for the burn-up limits imposed by mechanical and material considerations to be substantially raised compared with fuel elements of conventional design with metal canning. By choosing suitable graphite (with low permeability) the pressure of gaseous fission products inside the element can still be kept sufficiently low to prevent it from "bursting" but, on the other hand, the diffusion of fission products can be slowed down so that radioactivity released to the coolant stream can be limited. Thermal stresses can be kept within permissible limits. Since radiation damage to graphite is very low at elevated temperatures, the limitation in the load capacity of the elements is mainly governed by a slow contamination of the graphite by fission products and daughter products, producing a slow change in the physical properties of the graphite, and by mechanical abrasion. For reactors with high conversion rates, for which a burn-up of 100 000 MWd/t or more is possible and feasible from the point of view of the neutron balance, the above qualities of the fuel elements assume considerable importance.

On account of the very good neutron economy of the reactor design—there are no absorbent metals in the core, used for canning or control purposes—the conversion factor, which is determined to a large extent by resonance captures in fertile material, can be made very high in larger reactors of this type (the precise extent is largely determined by the optimum compromise attainable between the contradictory conditions of high conversion rate and long core life, as long as the conversion rate stays < 1. The choice of thorium as the fertile material, and a core design ensuring a high share of the Th^{232}-U^{233} conversion was therefore a natural choice in view of the optimum neutron yield of U^{233} in thermal reactors. After an initial period with U^{235} as fissile material the cycle will mostly maintain itself with bred U^{233} as fissile material, resulting in improved neutron economy and a further increase in the conversion rate. From present knowledge of the complicated and competing effects of resonance fission and resonance conversion, as well as the neutron yields in such cycles, it is very likely that thermal breeding (conversion rate $\geqslant 1$) can be achieved with graphite moderation on this basis.[2] The achievement of a conversion rate of 1, however, does not imply that a "magic line" has to be crossed as is so often assumed, and only changes the characteristics of the reactor very slightly. The conception of the pebble bed reactor permits continuous addition of new fuel and correction of the neutron balance at any time with the reactor running at full power. High conversion rates, however, are still important because of the overall economics of the reactor.

In the first phase of operation the prototype will be run at a lower power level without thorium, to facilitate the investigation of its general characteristics and the output capacity of the fuel elements. The core will be charged with twenty-percent enriched uranium only and will be overmoderated to compensate for the lack of absorbing material. The fertile material in this phase is U^{238} alone, with the U^{238}-Pu^{239} conversion cycle employed in all reactors using only partially enriched uranium. Also in the second phase (with thorium as fertile material) part of the U^{238}-Pu^{239} cycle remains because the uranium at present obtainable has a maximum enrichment of twenty per cent. It is hoped that this undesirable mixture of different conversion cycles—the nuclear properties of Pu^{239} in thermal reactors are far inferior to those of U^{233}—will only be a temporary solution and that fully enriched uranium will be available for this project, as it was for similar projects in the USA and Britain. It would then be possible to dispense with the segregation of uranium and thorium, as is necessary when only twenty-

---

[2] J. CHERNICK and S. O. MOORE: Breeding potential of thermal reactors. Nucl. Sci. & Engng 1959, Vol. 6, p. 537–44.

Principal Data of the Prototype Plant

	1st phase (without thorium)	2nd phase (with thorium)
Reactor heat output	25 MW	49 MW
Net electrical output	< 7 MW	15 MW
Coolant gas		
Type	He or He-Ne	
Reactor inlet temperature	200 °C	
Reactor outlet temperature	850 °C	
Pressure	10 kg/cm^2 abs	
Steam		
Temperature	505 °C	505 °C
Pressure	75 kg/cm^2	75 kg/cm^2
Mass flow		60 t/h
Feedwater temperature		110 °C
Reactor core		
Diameter	3·0 m	3·0 m
Height	1·96 m	2·22 m
Average power density in core	1·81 kW/l	3·12 kW/l
Average specific power	1·44 MW/kg U^{235}	1·52 MW/kg U^{235}
Fuel elements (uniform diameter 6 cm)		
Uranium-carbide graphite spheres, number	25 100	46 500
Thorium-carbide graphite spheres, number	—	22 900
Graphite spheres, number	34 700	—
Weight of materials in reactor core		
U^{235}	17·4 kg	32·3 kg
U^{238}	69·6 kg	129·2 kg
Th^{232}	—	235·5 kg
Graphite	14 200 kg	16 500 kg
Atomic ratio of materials in reactor core (normalized to U^{235})		
U^{235}	1	1
U^{238}	4	4
Th^{232}	—	7·2
Graphite (C)	16 000	10 000
Graphite reflector		
Thickness on all sides	0·5 m	
Weight	46 000 kg	
Average thermal neutron flux	$6{\cdot}5 \times 10^{13}\ cm^{-2}\ s^{-1}$	$7{\cdot}0 \times 10^{13}\ cm^{-2}\ s^{-1}$
Total temperature coefficient	$-6 \times 10^{-5}\ \Delta k_{eff}/°C$	$-6 \times 10^{-5}\ \Delta k_{eff}/°C$
Average heat flow on the surface of the uranium-carbide graphite spheres (for phase 2 initial condition)	8·8 W/cm^2	9·4 W/cm^2
Temperatures in the reactor core		
Fuel element surface (average)	700 °C	
Sintered cylinder surface (average)	1 000 °C	
Centre of sintered cylinder (maximum)	1 500 °C	
Reactor container		
Outside diameter	7·54 m	
Height	25·6 m	

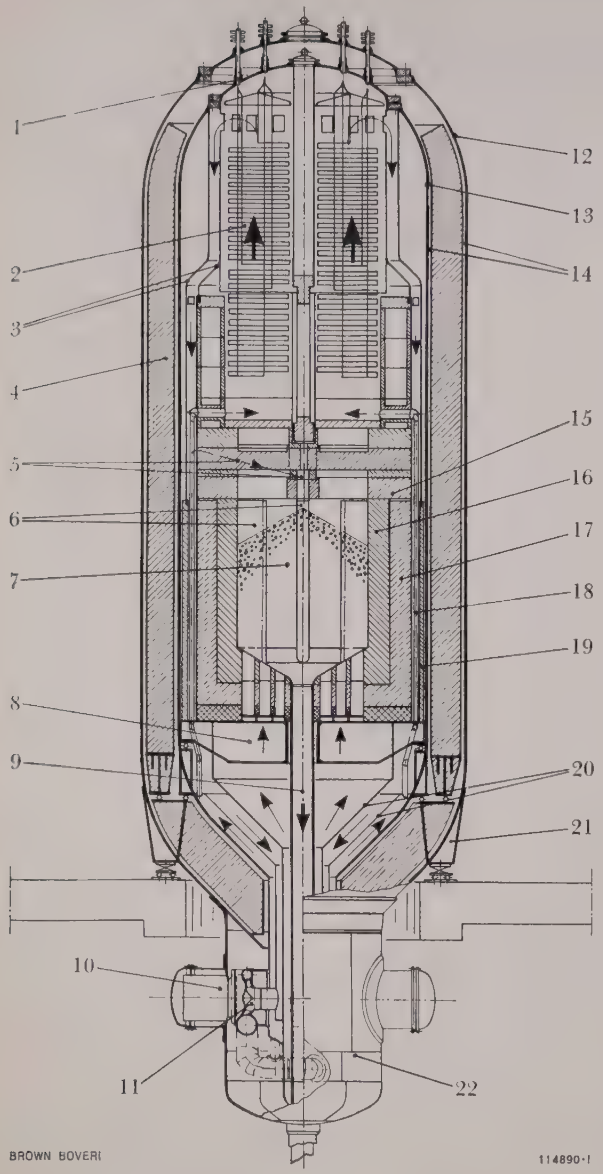

Fig. 1. – Section through the reactor

1 = Steam-raising unit pipe bushing
2 = Steam-raising unit
3 = Coolant gas guide vanes
4 = Biological shield
5 = Fuel element charging
6 = "Noses" for shut-down devices
7 = Reactor core
8 = Grid plate
9 = Withdrawal of fuel elements
10 = Blower motor
11 = Blower
12 = Reactor container II
13 = Reactor container I
14 = Isolation gaps I and II
15 = Bridge of coal-dust bricks
16 = Graphite reflector
17 = Jacket of coal-dust bricks
18 = By-pass piping
19 = Thermal shield
20 = Coolant gas
21 = Foot construction
22 = Blower dome

percent enriched uranium is used—isotope separation during chemical reprocessing of the spent fuel elements would be too expensive.

To preserve the simplicity of the design, every effort has been made to use only conventional elements for the reactor, as far as possible. In view of the reduced thermal stresses and the higher safety of the installation the choice fell upon the design with a single container in which reactor core, primary coolant circuit, coolant blowers, and steam-raising unit are arranged in the same container. Although the steam-raising unit has to be made as compact as possible, steam conditions of 505 °C and 75 kg/cm^2 can be reached, approximately corresponding to the steam conditions usual in modern steam power plants of the conventional pattern.

The choice of the coolant gas is not only influenced by technical considerations. Provided the USA agree to supply it, pure helium will be used. When sufficiently pure, helium does not absorb neutrons, remains chemically inert even at high temperatures, and has good thermodynamic properties. However, the reactor will be designed to employ a mixture of helium and neon in the natural ratio in which they occur in air (22% by volume of helium and 78% neon) as coolant, as well as pure helium. Both coolant gases considered are also suitable for a later development in the direction of a gas-turbine process which, with the high temperatures considered, promises a further increase in efficiency and economy.

Description of the Plant

Reactor and Fuel Elements

The sectional drawing (Fig. 1) shows the reactor and the primary coolant system and their arrangement in one double-shelled container. The concept of an inner and an outer container, with two gas-filled isolating gaps at a slightly higher pressure than the coolant gas in the inner container, serves the two purposes of preventing radioactive leakage and relieving the pressure on the inner (hot) container wall. The space between the two container walls is filled with barite concrete bricks and acts as an inner biological shield.

The fuel element (or "blanket" element if filled with fertile material), as shown in Fig. 2, consists of a graphite sphere with cylindrical bore in which the fissile or fertile material is inserted in the form of a porous sintered cylinder. Fissile and fertile material in the sintered cylinder are mixed with graphite in a ratio U:C = 1:50, or Th:C = 1:7, respectively. A thermally stabilized graphite screw closes the bore. The mechanical load limit of the sphere, which increases slightly with rising temperature, was studied in comprehensive fall tests. The thermal stresses in the sphere are relatively small since the temperature gradient always lies between 100 and 150 °C/cm, even allowing for irradiation damage, due to the good thermal conductivity of graphite. Since most of the fuel elements are operated at temperatures above 300 °C only very small Wigner energy build-up is to be expected. Periodic heating of the graphite by temperature balancing is, however, planned on account of a potential Wigner energy storage in the reflector graphite.

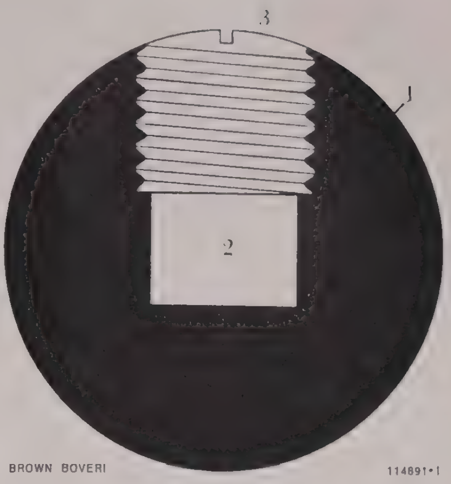

BROWN BOVERI 114891·1

Fig. 2. – Heterogeneous fuel element in natural size

1 = Graphite canning
2 = Porous sintered fuel cylinder
3 = Graphite screw

Four graphite "noses", spaced at intervals of 90°, which act as guiding sleeves for the shut-down elements, penetrate the reactor core. When the reactor

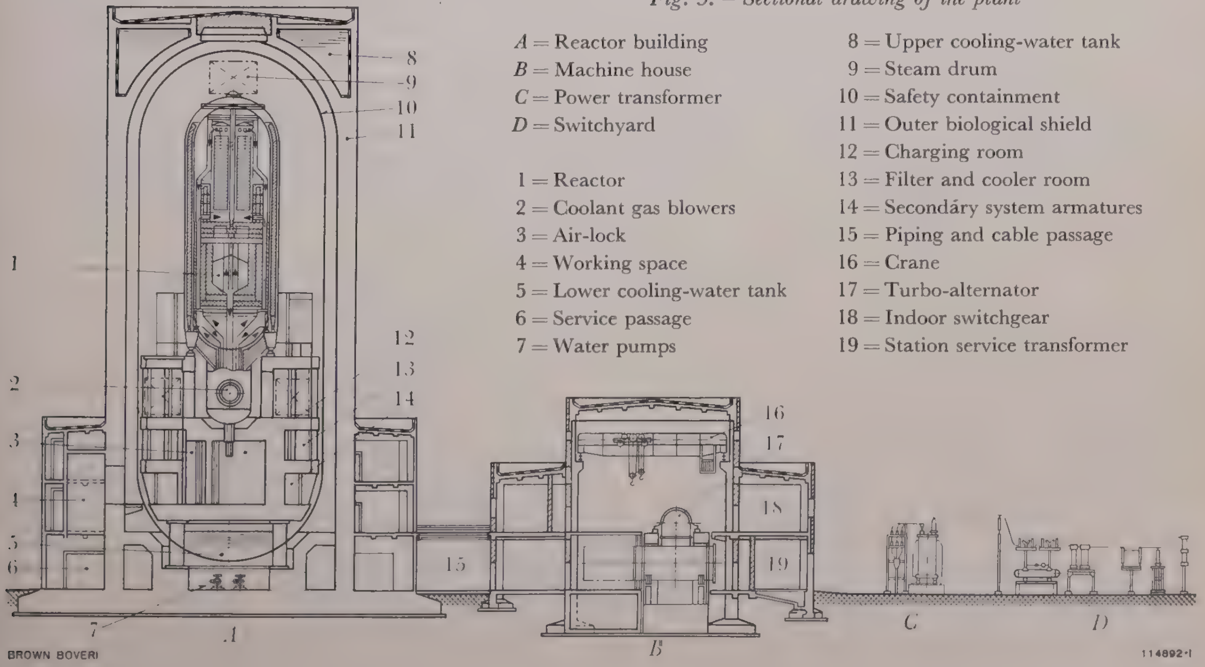

BROWN BOVERI 114892·1

Fig. 3. – Sectional drawing of the plant

A = Reactor building
B = Machine house
C = Power transformer
D = Switchyard

1 = Reactor
2 = Coolant gas blowers
3 = Air-lock
4 = Working space
5 = Lower cooling-water tank
6 = Service passage
7 = Water pumps
8 = Upper cooling-water tank
9 = Steam drum
10 = Safety containment
11 = Outer biological shield
12 = Charging room
13 = Filter and cooler room
14 = Secondary system armatures
15 = Piping and cable passage
16 = Crane
17 = Turbo-alternator
18 = Indoor switchgear
19 = Station service transformer

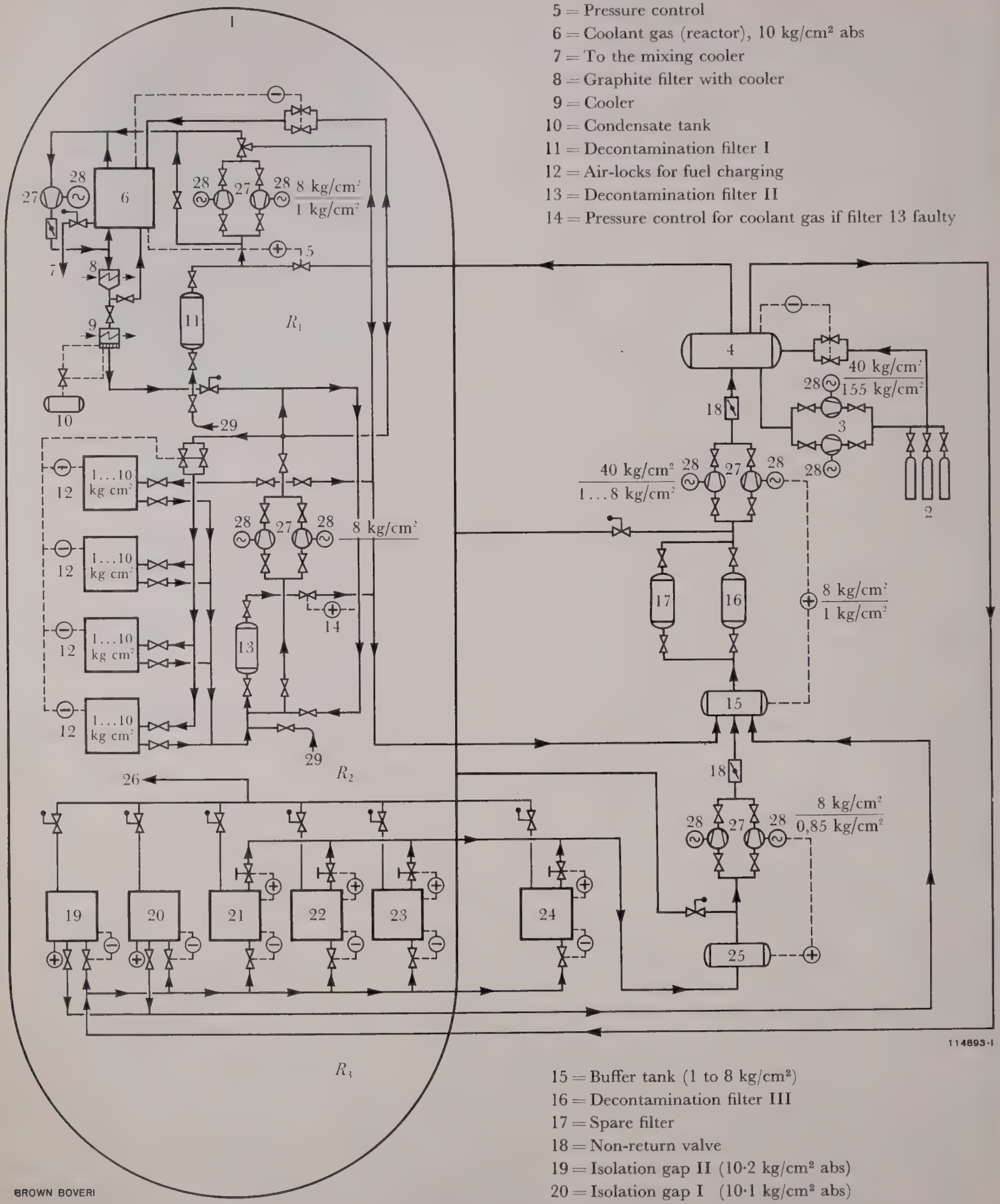

Fig. 4. – Flow diagram of the gas purification and decontamination system

R_1 = Purification loop 1 R_2 = Purification loop 2
R_3 = Purification loop 3

1 = Safety containment
2 = Ne-He or He cylinders
3 = Return blowers to gas cylinders
4 = 40 kg/cm² clean-gas tank
5 = Pressure control
6 = Coolant gas (reactor), 10 kg/cm² abs
7 = To the mixing cooler
8 = Graphite filter with cooler
9 = Cooler
10 = Condensate tank
11 = Decontamination filter I
12 = Air-locks for fuel charging
13 = Decontamination filter II
14 = Pressure control for coolant gas if filter 13 faulty
15 = Buffer tank (1 to 8 kg/cm²)
16 = Decontamination filter III
17 = Spare filter
18 = Non-return valve
19 = Isolation gap II (10·2 kg/cm² abs)
20 = Isolation gap I (10·1 kg/cm² abs)
21 = Fuel charging room (< 1 kg/cm² abs)
22 = Control room (< 1 kg/cm² abs)
23 = Air-lock of fuel charging room (< 1 kg/cm² abs)
24 = Hot cell (< 1 kg/cm² abs)
25 = Buffer tank (0·85 kg/cm² abs)
26 = To the mixing cooler
27 = Blower
28 = Blower motor
29 = From the coolers

is in operation these shut-down elements are located above the core. New fuel elements are introduced into the core by a simple loading device, from which they roll down a graphite groove to the middle of the bridge of coal-dust bricks shown in Fig. 1, and there they fall down into the pile in the core. The fuel elements can be withdrawn from the core at the bottom outlet through the funnel of graphite and coal-dust bricks. Spent fuel elements are removed in welded containers through an air-lock while elements that can still be used are returned to the loading device, also through an air-lock.

For safety reasons the reactor is located in its own building (Fig. 3), comprising the safety containment, the reactor and a number of auxiliary systems directly concerned with the reactor, and the outer biological shielding with various auxiliary rooms for the reactor. The steel containment is designed for an excess pressure of 1·7 kg/cm², calculated for the "worst conceivable accident" with ruptures in the primary and secondary systems.

Coolant Gas System and Radioactivity in the Plant

The coolant gas enters the core from below, is heated to 850 °C, and conveyed to the steam-raising unit through narrow channels in the graphite ceiling above the core. In the steam-raising unit it is cooled down to 180 °C and returns to the blowers via an annular gap around steam-raising unit and reactor core.

In the event of a breakdown, for example a fractured tube in the steam-raising unit, the circulating gas stream is switched to a by-pass following the two parallel blowers. In this circuit the gas bypasses the reactor core and is blown in radially from all sides below the steam-raising unit, thus assuring continued cooling of the steam-raising unit without the reactor core being exposed to harm from the hot steam. (Such a partial or complete reduction of cooling in the reactor is perfectly permissible in view of the enormous heat storage capacity of the graphite and coal-dust bricks.) The by-pass gas stream returns to the blowers by the same annular gap as during normal operation.

With fuel elements of the type described, having graphite as the canning material, radioactive contamination of the coolant-gas system is to be expected. Experiments to ascertain the extent and the kind of contamination are being carried out in a test reactor at Mol (Belgium), also using graphite of the best and latest qualities, having a very low permeability. However, it would be wrong to presume that wholly impermeable graphite would be an ideal canning material since destruction of the fuel elements by the inner pressure of the accumulating fission product gases has to be avoided in order to achieve a high burn-up. It will be one of the main tasks of the prototype reactor to find the best compromise between the life of the fuel elements and radioactivity in the cooling system.

The cooling system, the two isolating gas systems, the air-locks, the loading rooms, control room, and hot cell are connected to purification and decontamination systems (Fig. 3). For decontamination purposes multi-stage charcoal filter systems, working at different temperatures, are used. Because of the high coolant temperature high purity of the gas is essential for chemical reasons. Graphite dust, water vapour, and carbon monoxide and dioxide are continuously removed in a purification by-pass. Pre-purification by dust filters and gas coolers with water separation removes the graphite dust and the larger part of the water vapour. In the more complicated post-purification system the gas stream passes through copper oxide contacts, pre-coolers and molecular sieves.

Steam-Raising Unit and Secondary System

The steam-raising unit is located in the upper part of the reactor container in a steel cylinder, shielded from the reactor core by a graphite and coal-dust brick ceiling, and is of the forced-circulation counterflow type. To reduce the consequences of tube breakage the unit is divided into four equal and independent systems which are controlled and shut off individually. Each of these systems has automatic emergency isolation valves, as well as normal remote-controlled stop valves on the feedwater side and on the steam side, to shut off a defective system in the event of a breakdown. Emergency cooling is then carried out by the three unaffected systems.

With the exception of special isolation valves to prevent radioactive leakage into the secondary circuit due to a breakdown, the secondary system is designed in accordance with normal practice.

Plant Control

The transient behaviour of the reactor is mainly determined by the high and always negative temperature coefficient of the reactivity, and by the high heat storage capacity of the large graphite and coal-dust brick masses in and around the reactor core. The negative temperature coefficient creates an inherent tendency to maintain a constant mean reactor temperature, independent of reactor output, and the available heat storage capacity reduces temperature transients during power transients. The nearly homogeneous mixture of fuel and moderator improves these characteristics. By a combination of these effects it is possible to control reactor power, without special control devices, merely by varying the flow of gas from the blowers. This simplest method of control, impossible with most other known reactor types, is one of the main features of this reactor concept. A certain inter-dependence of the temperature of the coolant and the power taken off at the steam-raising unit (caused by the growing temperature difference between the fuel insert and the graphite canning with growing specific output) remains in limits which are by no means likely to impair the safe operation of the steam-raising unit.

The influence of delayed neutrons and the time constant of the temperature change from the fuel to the surface of the sphere and to the coolant gas give rise to temperature transients following fast power transients. As detailed investigation has shown, even a full-load throw-off only results in a temperature transient of about 70 °C, which is quite harmless.

Because of fuel burn-up and the "poisoning" effect of the fission products, the mean reactor temperature slowly decreases as time goes by. This slow change is counteracted by periodically adding fresh fuel elements and withdrawing spent elements without affecting the operation of the reactor.

For the steam-raising unit the forced-circulation system with moving evaporation point has been chosen, because the heat transfer from the coolant gas stream to the tube walls of the steam-raising unit is a non-linear function. This flexibility in the size of the heat transfer area of the superheater and the additional help of a controlled spray cooler before the final superheater bank, allow the most important factor in the secondary system to be controlled, i.e. the steam temperature. To keep the flow of spray water always within the control range, the ratio of feedwater to spray is transmitted as a signal to the blower control. For the prototype plant the control will be designed in such a way that the designed value for power output of the steam-raising unit can be set by hand.

Control of the other parts of the secondary system is in accordance with conventional standards.

R. SCHULTEN
E. JANTSCH

THE TRAWSFYNYDD NUCLEAR POWER STATION FROM THE TECHNICAL POINT OF VIEW

621.311.25:621.039 (420)

A general review of the plant and some details on the turbo-generator sets which are to be supplied by the Company's British licencees, Richardsons Westgarth & Co. Ltd., was given in the Brown Boveri Review last year [1].[1] The main purpose of the present article is to give a description of the reactors. A comparison with the other Calder Hall-type reactors shows the progress in the development of graphite-moderated, gas-cooled, natural-uranium reactors.

THE TRAWSFYNYDD nuclear power station in North Wales, ordered by the Central Electricity Generating Board (CEGB) and being built by Atomic Power Constructions Ltd. (APC), will have an installed gross electric output of 580 MW and is the world's largest nuclear power station in construction. Seventh in the series of large British nuclear power stations with graphite-moderated, gas-cooled, natural-uranium reactors, it incorporates the results of a consistent development of this successful type of reactor, realized for the first time at Calder Hall. The principal data of Trawsfynydd are listed in Table I.

Description of the Plant

Layout

Fig. 1 shows the site by Lake Trawsfynydd and the division into two reactor buildings, one turbine house, and the buildings for the storage of fresh and spent fuel elements. To improve the circulation of cooling water in the relatively small lake, a dam will be built between the pump-house and the cooling-water outfall.

Fig. 2 shows the characteristic arrangement of the cooling circuit for each of the twelve boilers and gas circulators (6 to each reactor). The reactor and primary system are shielded to the outside as well as to the fuel-handling machine control room above the reactor. The concrete shield is air-cooled near the reactor. The radiation dose received by reactor operating personnel is kept below 2·5 rem per year.

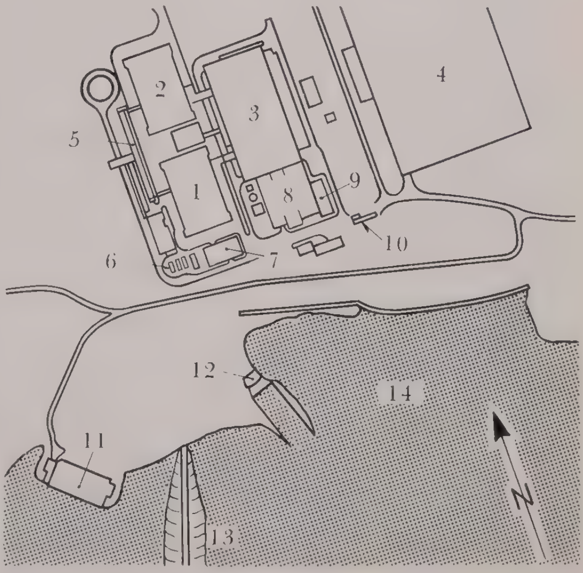

Fig. 1. – Plan of the power station site at Trawsfynydd

1 = No. 1 reactor building
2 = No. 2 reactor building
3 = Machine house
4 = Outdoor switchgear
5 = Cooling pond
6 = CO_2 store
7 = New fuel store
8 = Workshop
9 = Office block
10 = Main entrance
11 = Cooling-water pumphouse
12 = Cooling-water outfall
13 = Dam
14 = Trawsfynydd lake

---

[1] The figures in square brackets refer to the bibliography at the end of the article.

TABLE I

Principal station data for Trawsfynydd

Guaranteed net electrical output	500 MW
Installed gross electrical output	580 MW
Number of reactors	2
Reactor heat output	870 MW
Coolant gas	
Type	carbon dioxide
Reactor inlet temperature	200 °C
Reactor outlet temperature	399 °C
Pressure at reactor inlet	17·9 kg/cm²
Flow rate per reactor	4080 kg/s
Core	
Equivalent diameter of active core	13·65 m
Height of active core	7·31 m
Equivalent diameter including reflector	14·60 m
Height including reflector	8·40 m
Number of coolant channels	3720
Number of control rod channels	241
Lattice pitch (square)	0·197 m
Total weight of graphite per reactor	1900 t
Fuel elements	
Material	natural uranium rods
Rod diameter	28·6 mm
Rod length	715 mm
Canning material	Magnox A 12
Number of rods per channel	9
Number of rods per reactor	33 480
Weight of uranium per reactor	280 t
Control rods	
Material	boron steel
Number per reactor	185
Diameter	63·6 mm
Length	7·93 m
Weight	97 kg
Temperature in the core	
Fuel element can (maximum)	440 °C
Fuel centre (maximum)	585 °C
Graphite moderator (average)	360 °C
Pressure vessel (spherical)	
Diameter	18·59 m
Wall thickness	89 mm
Main gas circulators	
Type	single-stage axial
Number per reactor	6
Power per circulator	4500 kW
Running speed	2950 rev/min
Main gas ducts	
Number per reactor	6
Diameter	1·67 m
Wall thickness	23·8 mm
Boilers	
Number per reactor	6
Diameter	5·48 m
Height	35·3 m
Turbo-generators	
Total number for station	4
Maximum continuous rating for each turbo-generator	145 MW
Running speed	3000 rev/min
Steam conditions at turbine stop valve	
High-pressure steam	379 °C; 66·1 kg/cm²
Low-pressure steam	363 °C; 21·4 kg/cm²
Steam flow for each turbine	
High-pressure steam	393 t/h
Low-pressure steam	211 t/h
Flow ratio h.p. steam/l.p. steam	65/35
Condenser back pressure	0·040 kg/cm²
Feedwater end temperature	105 °C

Fig. 2. – Section through a reactor building, showing one of the cooling-gas circuits

Each reactor supplies heat to six exchangers.

1 = Reactor core
2 = Support for the reactor core
3 = Standpipes
4 = Pressure container
5 = Thermal column
6 = Ion chamber handling room
7 = Charge machine
8 = Portable service trolley
9 = 450-t overhead crane
10 = CO_2 outlet from reactor
11 = Air-cooled bushing through concrete
12 = Hanger failure emergency support
13 = Containment valve
14 = Removable access openings
15 = Expansion joint
16 = CO_2 safety valve
17 = CO_2 safety filter
18 = Hinge bellows unit
19 = Boiler (heat exchanger)
20 = H.P. superheater
21 = L.P. superheater
22 = H.P. evaporator
23 = H.P. economizer
24 = L.P. evaporator
25 = Mixed h.p./l.p. economizer
26 = Auxiliary bypass valve
27 = Main bypass valve
28 = Gas circulator
29 = Circulator drive
30 = Throttle valve
31 = Gas inlet to reactor
32 = Valve motor room
33 = Live-steam pipes

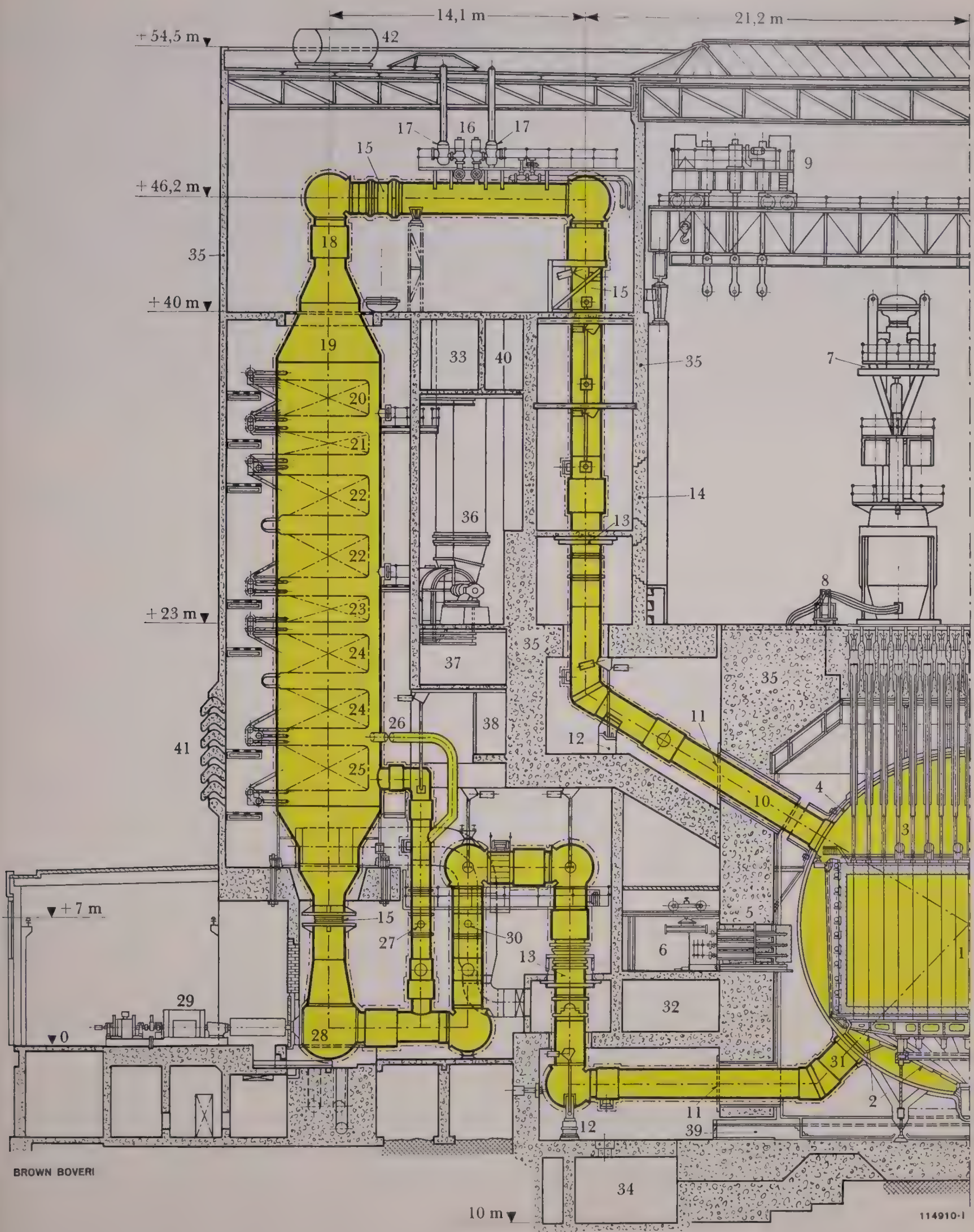

34 = Active waste storage
35 = Concrete biological shield
36 = Blower for air cooling shield
37 = Plenum chamber for cooling air
38 = Filter chamber for cooling air
39 = Air intake
40 = Air outlet
41 = Louvre for ventilation of boiler room
42 = Air extractor from boiler room

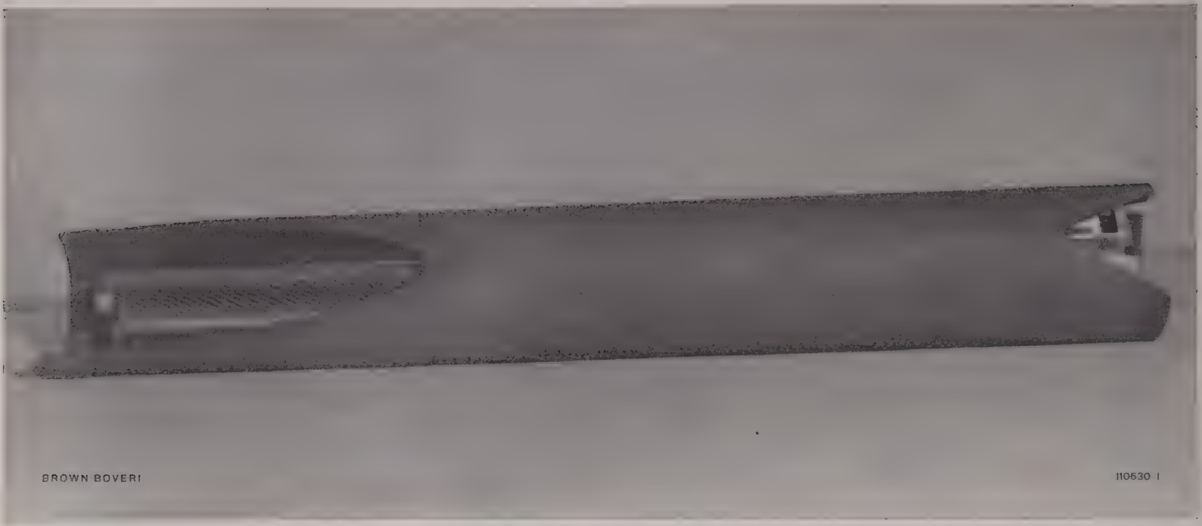

Fig. 3. – Fuel element with part of the graphite sleeve cut away

The surface of the Magnox A 12 canning is provided with multi-start helical fins to improve heat transfer. Four ongitudinal vanes divide the flow of cooling gas into four quadrants.

Reactor and Fuel Elements

The active core, built of nine layers of graphite blocks, forms a twentyfour-sided regular polygon in horizontal cross-section. It is penetrated by 3720 vertical coolant channels and 241 control-rod channels, arranged in a square lattice. The coolant channels, in which the fuel elements are placed, are formed by graphite sleeves separated from the moderator blocks by an insulating gap. Thus, in combination with the relatively high gas inlet temperature, the moderator is kept at a temperature sufficiently high to substantially reduce the undesired effect of Wigner energy storage (displacement of atoms in the crystal lattice by fast neutrons) and the need for periodically heating up the moderator. The graphite sleeves, which are cooled on their inner surface and are thereby kept at lower temperatures on the gas inlet side, can be replaced without affecting reactor operation.

The fuel elements—nine per channel placed one above the other—consist of solid uranium metal rods canned in magnesium alloy. Fig. 3 shows the way in which the surface of the can is extended, the outcome of extensive tests regarding heat transfer and pressure loss: impact-extruded, longitudinally finned tubes are twisted so that the fins form a multi-start helix; four longitudinal straight splitter vanes, extending almost to the internal diameter of the graphite sleeve divide the flow passage into four quadrants, increasing turbulence and heat transfer as well as keeping the fuel rods central in the channel. Fuel elements of a similar design will also be used in the nuclear power stations at Bradwell, Berkeley, Hinkley Point, and Latina (Italy). It has therefore been decided not to await the completion of a development programme in tubular fuel elements—which at equal maximum fuel temperature would allow higher surface temperatures—but to take advantage of this well-known, reliable design. The choice of a solid rod, combined with the limit on the centre-line uranium temperature as imposed by the allotropic alpha-beta phase transition of uranium metal, results in practice in an approximate maximum heat output per channel. The obvious possibility of increasing the channel heat output by lowering the gas inlet temperature is no longer significant in view of the desired steam cycle. It would also adversely affect the problems of Wigner energy storage, mentioned above.

Some of the coolant channels are gagged to attain maximum possible heat production in the given temperature limits and to approach as closely as possible to the design value of 440 °C for the maximum can surface temperature in each channel [2]. The principle used in Calder Hall for reducing gas circulator power, namely the division of coolant channels into radial zones and the reduction of channel diameters in the outer zones, has been abandoned because of the complicated radial neutron flux and heat production distribution which changes with core life and control rod programme and no longer bears any resemblance to the well-known Bessel distribution. The radial ratio of maximum to average flux with a value of 1·20 is low anyway. The gagging devices are installed so that they can be easily exchanged. The ability to obtain optimum conditions for the reactor itself and not to accept restrictions resulting from theoretical approximations, which may be more rigorous than necessary, is one of the main features of this reactor.

To flatten the radial neutron flux distribution as much as possible the 185 control rods can be inserted in different arrangements in a total of 241 control rod channels. In addition, the excess reactivity of a fresh fuel loading is compensated by a maximum of 24 stainless-steel rods inserted in control rod channels in the outer regions of the core. These stainless-steel rods, in contrast to the normal control rods, have no drive mechanisms, but can be removed or rearranged by the charge machine while the reactor is in operation.

Pressure Vessel and Charging Machine

Decisive for the design of the reactor pressure vessel was the present limit of 3·5 in. wall thickness (89 mm) for on-site welding. The sphere has already been accepted as the most advantageous shape for earlier Calder Hall-type designs. The next step was to reduce the diameter by making the layout of the core compact and by developing a new design for the core support, which uses pillars and thus saves space. The 241 standpipes, penetrating the sphere wall from above for insertion of control rods, as well as for charging and discharging the fuel elements, have also been arranged to save space. The smaller diameter of the pressure vessel in combination with the maximum possible wall thickness then made it possible to set the coolant pressure at 17·9 kg/cm^2 (254 psia), which in turn conduced to a compact core design.

The two charging machines per reactor, which are moved by a 450-ton crane above the reactor, consist primarily of shielded pressure vessels. They are connected to the standpipes by means of a pneumatically operated telescopic joint, allowing the fuel elements to be lowered into any one of the 16 coolant channels served by the standpipe, or removed from the channels.

Gas Flow

A schematic flow diagram for each of the two reactors is shown in Fig. 4. In contrast to all the other nuclear power plants of the Calder Hall type, constant-speed gas circulators have been chosen here to improve reliability and lower the cost. Since Britain has an extensive interconnected grid system, and the first nuclear power stations in the country are planned for base-load operation, no difficulties are to be expected from this solution. To avoid changes in gas temperatures following changes in reactor output, a gas by-pass with gas recirculation through the low boiler stages is provided after each of the main gas circulators. The by-pass valves are of simple and robust design and coupled in antiphase to the throttle valves in the main gas circuit. The throttle valves are so designed that the gas flow is not completely shut off when the valves are closed, and adequate decay heat cooling is obtainable by natural circulation after the reactor and gas circulators have been completely shut down.

Fig. 5 is a cross-section through one of the single-stage axial gas circulators. The circulators are driven by induction motors, while flywheels ensure that the gas continues to flow for approximately 20 minutes after a gas circulator is shut down.

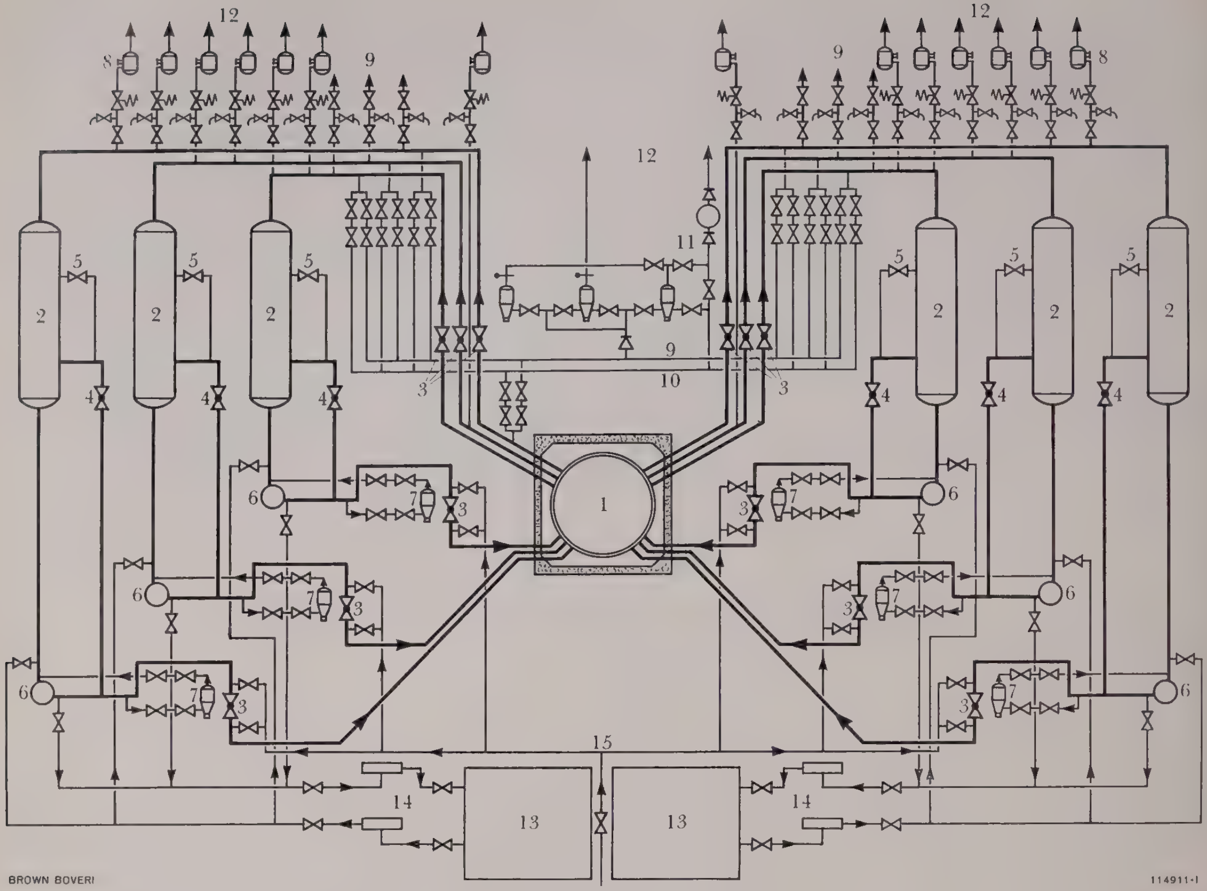

Fig. 4. – Simplified flow diagram of the CO_2 coolant system for one of the two reactors

Since the circulators run at constant speed the flow of gas is controlled by a combination of throttle valves in the main circuits and bypass valves. The flow of gas is recirculated in the bypass through the economizer stages in the boilers.

1 = Reactor
2 = Boiler
3 = Containment valve
4 = Main bypass valve
5 = Auxiliary bypass valve
6 = Gas circulator
7 = Bypass filter
8 = Safety valve and filter
9 = Vent line
10 = Vacuum line
11 = Vent and vacuum plant
12 = To atmosphere
13 = CO_2 drying plant
14 = Gas filter
15 = CO_2 supply to main circuits

Station Control

The station is controlled through two independent automatic systems: the by-pass valves after the main gas circulators receive signals from the generator frequency and from the steam pressure, and the somewhat slower correction of reactor power after a load change follows the gas outlet temperature and is automatically effected by a group of 9 control rods.

The control rods, boron steel rods canned in stainless steel, are hung by a cable from a drum. A permanent-magnet motor, driving the drum, controls the rate of insertion of the rod into the reactor core. In addition to this, 24 standpipes are occupied by special emergency shut-down rods. These are intended for operation only in an extreme emergency and are sufficient to shut down the reactor, even if all the control rods remain out of the core.

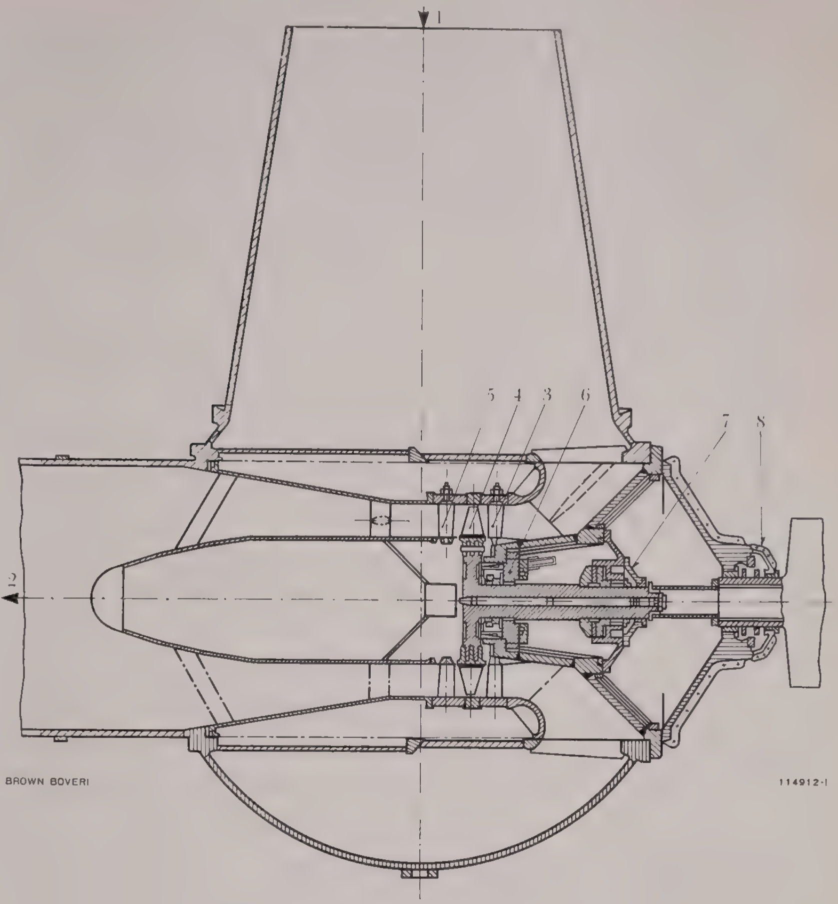

Fig. 5. – Section through one of the single-stage gas circulators

with two sets of fixed blade rings, rigidly coupled with the motor, for constant speed.

1 = Gas inlet
2 = Gas outlet
3 = Pre-stator blades
4 = Rotor blades
5 = Post-stator blades
6 = Gas seal and inner bearing assembly
7 = Thrust bearing assembly
8 = Anti-reversing device

Thorough investigations have been carried out to determine the values of the temperature coefficients of the reactivity, which, in reactors of this type, always become positive after a certain core life, and to predict the effects on reactor performance. The moderator temperature coefficient for the Trawsfynydd reactor after equilibrium in the fuel cycle is $+12\times 10^{-5}\,\Delta k_{eff}/^{\circ}\mathrm{C}$ at the operating temperature, while the prompt fuel temperature coefficient is $-2\times 10^{-5}\,\Delta k_{eff}/^{\circ}\mathrm{C}$. Therefore, while slow radial power oscillations could be initiated in the core, axial oscillations are not to be expected. To meet this effect, the core has been divided into zones which, due to the size of the whole reactor and the much smaller mean free neutron path, behave like small independent reactors; in each of these zones automatic steering is provided for one control rod with the special purpose of damping possible spatial instabilities.

Advances in the Design of the Trawsfynydd Station

Economic Advances

The Calder Hall type is today perhaps the best-known reactor type, incorporating the results of a most consistent development. But it is also the type whose limitations are best known, whether they be fixed or whether they vary with engineering progress. Each advance, and here the word "advance" mainly means reduction in energy production costs, is therefore based on improved understanding of the characteristics of this reactor type, on a slow approach to feasible limits without decrease in safety, and on obtaining optimum values for all station data in relation to running and capital costs. Fundamentally new concepts have played a relatively minor role in the development of this reactor type so far.

TABLE II

Comparison of temperatures and steam conditions

	Gas temperature at reactor outlet	High-pressure steam at turbine stop valve		Low-pressure steam at turbine stop valve		Flow ratio h.p. steam/l.p. steam	Overall efficiency of station (based on guaranteed net electrical output)
	°C	°C	kg/cm²	°C	kg/cm²		%
Calder Hall	336	311	14·0	177	4·6	77/23	18·9
Bradwell	390	371	52·3	371	13·7	66/34	28·3
Berkeley	345	319	21·8	316	5·1	68/32	24·8
Hunterston	394·5	369	39·7	346	10·7	67/33	28·0
Hinkley Point	373	360	44·2	346	11·5	64/36	26·0
Latina	390	373	52·8	373	14·4	66/34	28·4
Trawsfynydd	399	379	66·1	363	21·4	65/35	28·8

For a comparison with the Trawsfynydd station the data of the following stations will be considered in this chapter: Calder Hall, the first reactor of which came into operation in May 1956, the station being completed in February 1959; Bradwell, Berkeley, Hunterston, Hinkley Point, and Latina (Italy), at present under construction. Chapel Cross, which has been in partial operation since February, 1959, is mostly a replica of the Calder Hall station, while the station planned for Kai-tokai-maru (Japan) is very similar to Hunterston.

If we examine the specific costs of these stations, in chronological order of placing the definite contract, we observe a striking reduction in these specific costs and a corresponding effect on the fixed energy production costs, which dominate in nuclear power stations:

Calder Hall	2200 S.Fr./kW
Bradwell	1750 S.Fr./kW
Berkeley	1730 S.Fr./kW
Hunterston	1630 S.Fr./kW
Hinkley Point	1460 S.Fr./kW
Latina	1540 S.Fr./kW
Trawsfynydd	1350 S.Fr./kW

Today a modern coal-fired steam power station in Britain would cost approximately 550 to 600 S.Fr. per kW. In spite of the considerable difference remaining, the production of atomic energy in Britain has come quite close to economical production: the Trawsfynydd station is expected to produce electricity for approximately 3·5 S.cts./kWh (on the basis of a 75% load factor, depreciation over twenty years, and 5½% p.a. interest). This cost of generation is only about 10% more than that of coal-fired power stations in the same region.

Temperature in the Reactor and Steam Conditions

For uranium metal rods in a reactor, the temperature of 662 °C, the transition point from the allotropic alpha to the beta phase, forms an absolute upper temperature limit, since in such a transition the changed characteristics of the crystal lattice can lead to the destruction of the element. Similarly, there is an upper temperature limit for the canning, as long as magnesium alloys with their good neutron economy and heat transmission are used. For Magnox A 12, for example, a design temperature of 440 °C, which takes into consideration possible temperature transients during load and power transients, can hardly be exceeded.

The possible advance here can be found in a reduction of the temperature differential, or the insulating gap between uranium rod and can. The

TABLE III

Comparison of power output, gas pressure and power density

	Net electrical output per reactor MW	Reactor heat output MW	Gas pressure at reactor inlet kg/cm²	Power density in core kW/m³	Specific power, based on weight of uranium MW/t	Percentage of space in pressure vessel occupied by core and reflector %	Power density in pressure vessel kW/m³
Calder Hall	38	201	8·0	445	1·58	36·5	94
Bradwell	150	531	10·3	579	2·23	30·2	116
Berkeley	138	557·4	9·8	563	2·20	34·5	125
Hunterston	150	535	11·5	530	2·13	31·6	105
Hinkley Point	250	960	14·0	725	2·55	39·0	216
Latina	200	705	14·7	713	2·68	33·9	159
Trawsfynydd	250	870	17·9	823	3·11	41·5	260

Trawsfynydd reactor has been designed on the basis of a value of 0·5 °C/W/cm², but still further reduction of this value seems possible. Thus the temperature limit of the Magnox can, not of the uranium metal, has become the limiting factor for this reactor. The use of new canning materials and new fuel element designs, such as tubular fuel elements, may permit further improvements in the future.

A new feature in the development of the Trawsfynydd reactor is that the specified design condition is the irradiated state of fuel-cycle equilibrium, not the virgin charge condition. This has been made possible by the use of large digital computers. Because of the axial temperature differentials in the coolant channels there are some deviations for the axial burn-up compared with the cosine curve to be expected at uniform temperature, and for the point of maximum can temperature in the channel compared with that calculated by Ginn's equation [3]. Because of the exact prediction of these data for the irradiated condition, it was no longer necessary to include safety margins for uncertainty in this respect.

Steam conditions can be substantially improved for high gas outlet temperatures, as shown in Table II. The net station efficiency is affected by other factors, too, such as the necessary gas circulator power.

Pressure Vessel and Power Density

From the beginning of the development it was clear that Calder Hall-type reactors can only be economical if they have a very high power output. Accordingly, there are two ways of reaching that goal: The first is to improve power densities in the core by better command of the temperature problems in the core, as well by increasing the gas pressure and correspondingly improving heat transfer. The second is to make the best possible use of the space inside the pressure vessel. The basic limitation here is given by the wall thickness of the pressure vessel for on-site welding. This limitation was set at 2 in. for Calder Hall, and has been increased to 3·5 in. for Latina and Trawsfynydd. The spherical shape has been chosen for most Calder Hall-type stations, the exceptions being Calder Hall itself, Chapel Cross and Berkeley.

By developing new space-saving core support constructions and at the same time reducing the space needed for the standpipes and the charging and discharging mechanisms above the core, it has been possible to increase the percentage space in the vessel occupied by the core and reflector to 41·5%. The reduction in vessel size, in combination with the given wall thickness, has made possible a rise in the gas pressure and a remarkable increase in power density, in spite of a simultaneous increase in gas temperatures. It has not only been possible to build reactors of large power but also, as can be seen from a comparison of Hinkley Point and Trawsfynydd, to reduce the size of the vessel (and therefore also the size of the building) for reactors of equal net electrical output. Table III gives an illustrative comparison to show this development.

Since lattice pitch and fuel rod diameter in natural-uranium, graphite-moderated reactors can vary only in a very small range because of the nuclear characteristics, further progress in power density would necessitate a higher channel heat rating only obtainable with enriched uranium (as already planned for the advanced gas-cooled reactor).

Finally it should be mentioned that substantial reductions of the specific costs of the stations have been achieved by compact designs of the boilers, by the use of larger turbines, and—so far only in the case of Trawsfynydd—by the use of constant-speed gas circulators.

E. Jantsch

Literature References:

[1] E. A. Kerez: Trawsfynydd Atomic Power Station in North-Wales. Brown Boveri Rev. 1959, Vol. 46, No. 7, p. 381–4.

[2] L. S. Dzung: Thermal Problems in Atomic Power Stations III: Pressure Losses and Flow Distribution in a Gas-Cooled Reactor. Brown Boveri Rev. 1958, Vol. 45, No. 1, p. 14–20.

[3] S. A. Young: Trawsfynydd—Technical Calculations. Nuclear Power 1959, Vol. 4, No. 43, p. 95.

THERMAL PROBLEMS OF ATOMIC POWER STATIONS (IV)[1]

Design Criteria for the Containment of Water-Cooled and Water-Moderated Reactors[2]

621.311.25:621.039:536

In the design of nuclear power plants, the new branch of Brown Boveri activities, a most important consideration is the question of protection against the consequences of all conceivable accidents, chiefly the prevention of radioactive fission product release to the environment. Above all, the design of reactor containments for the highest pressures to be expected after an accident imposes a number of problems, including prediction of the variation of the pressure with time. Using considerations and calculations for actual projects, the present article presents a comparison between different types of containment with respect to their pressure-time behaviour and the "inherent" pressure-tightness.

IN THE PRESENT phase where experience in power reactor operation is relatively small and safety requirements enhanced, it has become common practice in the United States and in Europe to provide pressure-tight containments, especially for water-cooled and water-moderated reactors. Such containments, in addition to enclosing the reactor, may also contain the entire primary system or the whole plant without the control room. Typical containments are:

1. Steel containments, above ground or partially buried, usually of spherical or cylindrical shape,
   (a) biological shielding inside the steel container,
   (b) biological shielding outside the steel container.
2. Underground caverns, with or without pressure-tight lining.

Generally, the design pressure of the containment is calculated from a postulated accident involving a breach in the primary system and possibly also the secondary system or part of it, assuming instantaneous release of the total energy stored in the hot pressurized water. With the further assumption of ideal and instantaneous mixing of air and vapour, the resulting pressure inside the containment and the fraction of water flashed can be easily determined (Fig. 1). However, it will be shown in this article that the variation of the pressure with time following the accident is also important for the design of the containment and, especially, the "inherent" pressure-tightness of the containment—here defined as the pressure-tightness in case of failure of all installed artificial cooling systems—can be quite different.

---

[1] Continued from the series "Thermal Problems of Atomic Power Stations I – III", Brown Boveri Rev. 1956, Vol. 43, No. 1, p. 7 – 15; No. 12, p. 515 – 24, and 1958, Vol. 45, No. 1, p. 14 – 20.

[2] Extract from a paper presented at the symposium on reactor safety of the "VI Rassegna Internazionale Elettronica e Nucleare", Rome, June 1959.

The Pressure-Time Function Following an Accident

Once thermodynamic equilibrium has been reached in the water-vapour-air system—which is normally assumed to be at the moment of the accident, without considering time-dependent flow-out of water and vapour, and is therefore on the safe side—comparatively slow energy changes of the spatially closed system will be accomplished by the competition of several major effects:

Heat production of the reactor core—as long as sufficient water is present in the core for moderation—and decay heat production in the fuel elements.

Heat transfer from hot parts of the plant.

Possible metal-water reactions.

These three effects all tend to increase the temperature and pressure inside the containment.

Vapour condensation on cooling surfaces.

Heat transfer from the water to cooling surfaces.

Pressure reduction by means of special systems, like spray cooling systems, cooling ponds, etc.

These three effects all tend to reduce the temperature and pressure inside the containment.

To get to know the "inherent" qualities of a chosen system, the artificial pressure suppression systems mentioned above must not be considered, although to reduce the consequences in any phase after the accident their availability will be of great importance.

In the first few minutes after the accident, when the heat input from the hot parts of the plant and from metal-water reactions is added to the decay heat production, which to begin with is several percent of the nominal reactor heat production, it is possible for the heat input to the system to exceed the heat flow that can be dissipated, mainly by vapour condensation, at the cooling surfaces. Whether there will be a temporary net heat gain in the system depends partly on the values of the heat transfer coefficients for condensation cooling. The pressure curves in Fig. 2 and 3 were calculated with heat transfer coefficients as derived from a general semi-empiric theory by J. Madejski for the condensation of vapours in the presence of non-condensible gases [1];[3] to use this theory it is necessary to estimate flow velocities along the cooling surfaces. It will be possible to prove the dependability of these theoretically determined values by comparison with the results of experiments in caverns with simulated reactor accident conditions, which have started in Italy [2, 3].

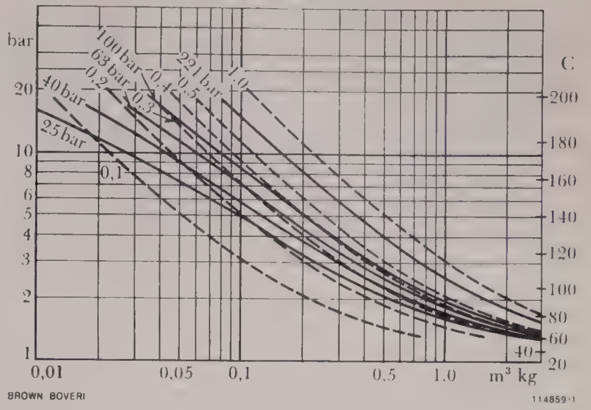

Fig. 1. – Pressure and temperature in the containment after instantaneous adiabatic coolant release for water at saturation pressure (full curves) and fraction of water flashed (dotted curves)

Initial air condition: 1 bar, 20 °C

Abscissa: Ratio $\frac{\text{Containment free volume}}{\text{Mass of water in system}}$ in m³/kg

Ordinate left: Equilibrium pressure in bar

Ordinate right: Equilibrium temperature in °C

Far more important as regards the dissipation of heat is the thermal diffusion from the cooling surfaces through the material layers behind. In most

---

[3] The figures in brackets refer to the bibliography at the end of this article.

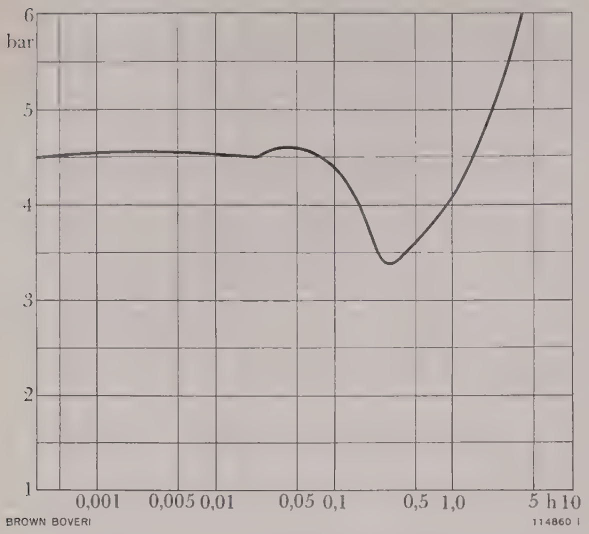

Fig. 2. – Example of the pressure variation after an accident in a containment above ground, with external concrete shielding, without any special pressure suppression systems

The discontinuity at 78 s marks the start of an assumed partial zirconium-water reaction

Abscissa: Time after accident in h
Ordinate: Containment pressure in bar

cases in practice relatively thin layers of steel or relatively thick layers of concrete are involved; the delaying effect of surface coatings can normally not be neglected. The temperature diffusion in steel walls is then approximately given by the formula for the infinitely wide plate of finite thickness:

$$\frac{T_s - T}{T_s - T_0} = \sum_{\nu=1}^{\infty} \frac{2\sin\Phi_\nu}{\Phi_\nu + \sin\Phi_\nu \cos\Phi_\nu} \cdot e^{-\frac{\Phi_\nu^2 a t}{s^2}} \cdot \cos\left(\Phi_\nu \cdot \frac{x}{s}\right) \quad (1)$$

where the coefficients Φ_ν are the solutions of the equation

$$\frac{ns}{bs} = \cot(ns) \quad (2)$$

and can be found in table 13–8 of [4], for example. In the same way the ratio of the absorbed heat to the available heat absorption capacity is given by

$$\frac{Q(T_s) - Q}{Q(T_s) - Q(T_0)} = 1 - \sum_{\nu=1}^{\infty} \frac{2\sin^2\Phi_\nu}{\Phi_\nu^2 + \Phi_\nu \sin\Phi_\nu \cos\Phi_\nu} \cdot \left(1 - e^{-\frac{\Phi_\nu^2 a t}{s^2}}\right) \quad (3)$$

In the above equations T_0 is the initial temperature of the material, which is assumed to be uniform, T_s the temperature of the environment, T the temperature at a depth x, a the thermal diffusivity, b the ratio of heat transfer to thermal conductivity, s the plate thickness for unilateral heat flow and half plate thickness for bilateral heat flow, and t the time. The surface temperature is determined by making $x = 0$, so that the last factor in equation (1) becomes unity. Equations (1) and (3) can be expressed as functions of the non-dimensional groups $\left(b\,s, \frac{a\,t}{s^2}, \frac{x}{s}\right)$ and in this form the solutions can be read directly from diagrams published under the names of their authors Hottel, Gurney-Lurie, Groeber and Heisler [4, 5].

Because of the high thermal diffusivity of steel, the temperature rise in steel walls of practical sizes takes place over the entire cross-section from the very beginning, so that a large amount of heat is absorbed in the first phase, but almost no heat absorption capacity is left when the surface temperature approaches the bulk temperature of the vapour-air mixture. In the containment this results in a sharply defined pressure minimum, followed by a relatively fast pressure rise (see Fig. 2—on account of the relatively small containment with a small cooling surface, as chosen in this example, an assumed zirconium-water reaction causes a temporary slight pressure rise during the first few minutes).

In concrete, temperature diffusion is so slow that in the first heating phase the surface temperature very quickly approaches the bulk temperature of the vapour-air mixture, while the material layers behind are heated only very slightly above initial temperature. For cavern walls backed by rock—insulating layers or gaps being avoided—and, for the first few hours, also for thick concrete structures inside the containment, after the first quick surface heating the heat flow per unit area at a depth x is given with very good approximation by the formula for the semi-infinite plate:

$$q'' = \frac{\lambda(T - T_0)}{\sqrt{\pi a t}} \cdot e^{-\frac{x^2}{4at}} \quad (4)$$

and for the heat flow through the surface ($x = 0$) the last factor becomes unity. λ is the thermal conductivity of the material. It can be seen from this equation that, for quasi-steady surface temperatures, the heat flow decreases according to a $t^{-0.5}$ law. Therefore, in caverns a flat pressure minimum followed by a slow pressure rise is to be expected (see Fig. 3). Curves *c* and *d* in Fig. 3 show the different effects with the two kinds of heat dissipation considered and the strong influence of the temperature diffusion of the material for concrete-lined caverns of equal volume in curve *d*, part of the cooling surface being provided by a steel sphere enclosing the reactor, with only slight increase of the total cooling surface area. The low thermal diffusivity of concrete, approximately a twentieth of that of steel, tends to raise the pressure slightly above its initial value in curves *a*, *b*, and *c* of Fig. 3, whereas the quick-acting heat sink of the steel sphere prevents such a pressure increase in curve *d*. Only in a case like that considered for curve *d* can the initial containment pressure following an instantaneous adiabatic hot-water release be used to determine a safe design pressure for the cavern, whereas in the other cases considered only the maximum pressure occurring a few minutes after the assumed accident gives the same safety with respect to its use for design pressure.

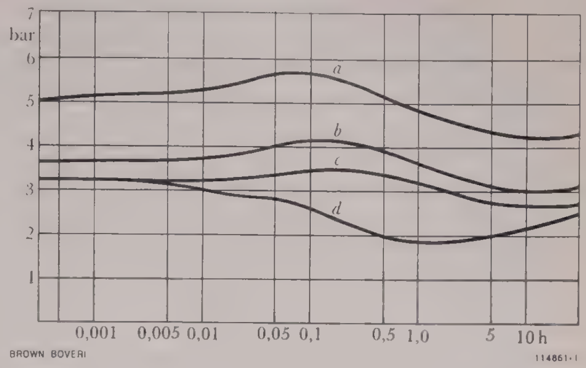

Fig. 3. – Example of the pressure variation after an accident in an underground cavern with concrete lining, without any special pressure suppression systems

After 70 s a partial zirconium-water reaction is assumed to start.

Curve *a*:	Containment free volume	2400 m³
	concrete cooling surface	1625 m²
Curve *b*:	Containment free volume	4000 m³
	concrete cooling surface	2025 m²
Curve *c*:	Containment free volume	5000 m³
	concrete cooling surface	2275 m²
Curve *d*:	Containment free volume	5000 m³
	concrete cooling surface	1950 m²
	plus steel cooling surface	450 m²

Abscissa: Time after accident in h
Ordinate: Containment pressure in bar

Time and Height of Second Pressure Maximum

After the rapid initial heating of the first layers of material behind the cooling surfaces, or the exhaustion of the immediately available heat absorption capacity, the pressure usually increases in containments dimensioned to the present standards. For containments above ground with no internal concrete lining this pressure rise in practice is limited only by the ability to equalize the decay heat production by radiation of heat from the hot containment walls to the environment. Cooling by natural air convection or by wind is quite insufficient. To limit the second pressure maximum to approximately 5 to 6 bar (58 to 73 psig) it would be necessary for the ratio of nominal reactor heat output to effective radiation surface to be 50 to 70 kW/m² at the most. The difficult problem of cooling the absorbing surfaces, especially those of a surrounding concrete shield, remains unsolved, however, and reduces the likelihood of achieving "inherent" safety in this way.

For an underground cavern or a containment largely buried in the ground, however, the second maximum is determined by the equality of decay heat production and heat dissipation through almost infinitely thick walls. The decay heat production can be approximated by the well-known Untermyer-Weills formula or, few hours after the accident, by the simpler Way-Wigner formula

$$q \approx 0{\cdot}00582\,P[t^{-0{\cdot}2}-(\tau+t)^{-0{\cdot}2}] \tag{5}$$

where P is the nominal reactor heat output, t is the time in days after the reactor became sub-critical, and τ the core exposure time in days. It can be seen from this formula that the decay heat production initially follows a $t^{-0{\cdot}2}$ law and, as can be shown by development into a binominal series, for $t \gg \tau$

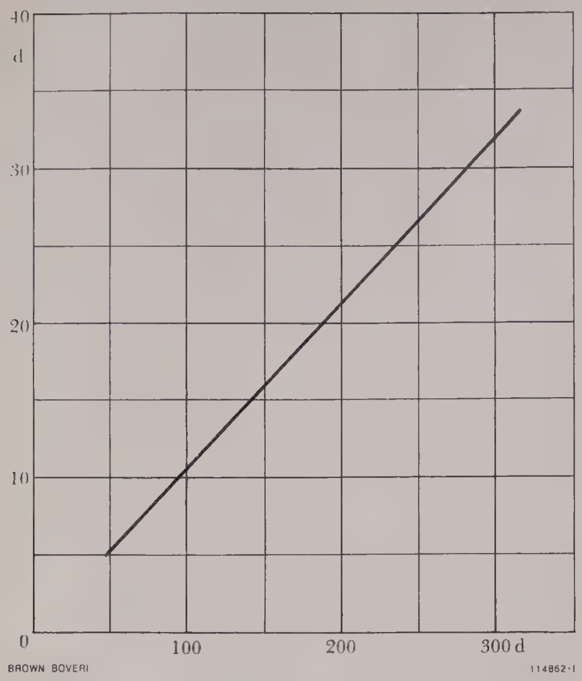

Fig. 4. – Time after the accident for the occurrence of the second temperature and pressure maximum in a containment with semi-infinite walls, for example in an underground cavern

Abscissa: Core exposure time in days
Ordinate: Time after the accident for the second maximum in days

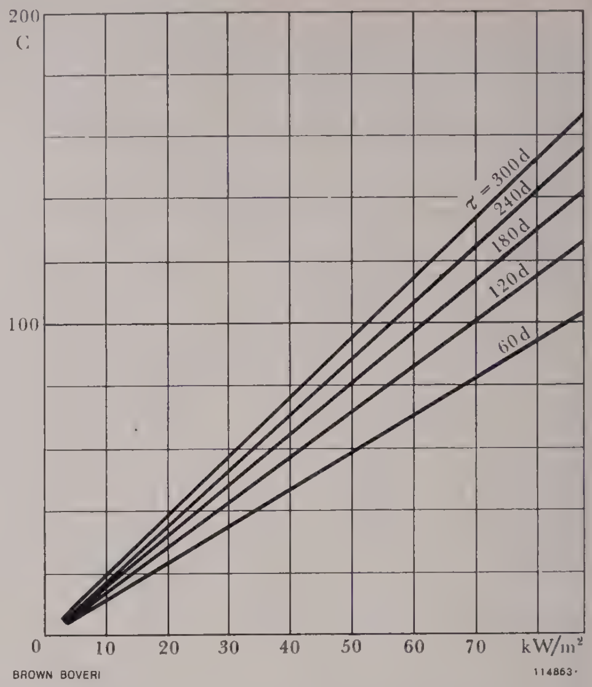

Fig. 5. – Height of the second temperature maximum in a containment with semi-infinite walls, for example in an underground cavern

Abscissa: Ratio $\dfrac{\text{Nominal reactor heat output}}{\text{Cooling surface}}$ in kW/m²
Ordinate: Surface temperature at second maximum minus initial uniform material temperature in °C

τ = Core exposure time in days

towards a $t^{-1\cdot2}$ law. The condition of equal heat input and heat dissipation at the second maximum leads to the following equation for the time t_{max} between accident and second maximum

$$0{\cdot}3\,\tau^{2\cdot2}\,t_{max}^{-0\cdot7} - 0{\cdot}5\,\tau^{2}\,t_{max}^{-0\cdot5} + {} + 0{\cdot}3\,\tau\,t_{max}^{0\cdot5} - 0{\cdot}3\,t_{max}^{1\cdot5} + \ldots = 0 \qquad (6)$$

Solutions of this equation are shown in Fig. 4. It will be seen that in caverns the second maximum (Fig. 5) is reached after a few days only and shows a very flat characteristic. Therefore, there is much more time available for human intervention than in containments above ground, especially those with concrete shielding outside.

By substitution in equation (4) the surface temperature at the second maximum can be determined and, assuming a heat transfer coefficient, the temperature and pressure of the vapour-air mixture also. "Inherently safe" designs for pressures of not more than 5 to 6 bar (58 to 73 psig) can be achieved in this way for ratios below 50 to 80 kW/m², but here in a completely natural manner, without difficulty from additional cooling on the outside. The curves *c* and *d* in Fig. 3, with 39 and 41 kW/m², respectively, are examples of designs in which the second pressure maximum never exceeds the first. Similar cases are the partially buried concrete-lined containments at Shippingport, with a ratio of 22·5 kW/m² for the total cooling surface, and a ratio of 37 kW/m² for the concrete cooling surface alone [6]. For Indian Point, with a partially buried steel containment and external concrete shielding (because of the more efficient shielding after an accident) and a ratio of 60 kW/m², a second pressure maximum results which slightly exceeds the first maximum. For the design originally considered with internal shielding, and a necessarily larger containment, however, the first maximum would not have been exceeded [7].

Conclusions

From the above considerations three important conclusions can be drawn regarding the design of containments for water-cooled and water-moderated reactors:

1. For containments characterized by slow-acting heat sinks of large heat absorption capacity, or by relatively small cooling surfaces, the first pressure maximum may appear only a few minutes after the accident and will then exceed the pressure resulting from an instantaneous adiabatic hot water release. A safe design of the containment must take into consideration this higher peak pressure.
2. In containments with walls that can be considered infinitely thick in respect to their thermal diffusion characteristics, the second pressure maximum will be very flat and will be reached only after several days. Even if it is higher than the first pressure maximum, and if the design pressure is determined by this figure, there is much more time available for human intervention than with containments having quick-acting heat sinks of relatively small heat absorption capacity.
3. For underground caverns and for containments above ground, especially those which are partly buried and those with internal concrete shielding, designs are possible which prevent the second pressure maximum from exceeding the first. If the first maximum forms the criterion for the design pressure, such a containment will remain "inherently" pressure-tight in all phases following the accident, without human intervention and without any special pressure suppression system being called upon to function.

Naturally, the choice of a suitable containment will be influenced by a number of further considerations, especially regarding the costs.

E. JANTSCH

Bibliography

[1] J. MADEJSKI: Über die Wärmeübertragung bei der Kondensation von Dämpfen in Anwesenheit inerter Gase. Chem.-Ing.-Techn. 1957, Vol. 29, No. 12, p. 801.

[2] T. LEARDINI: Considerazioni circa un problema particolare del contenimento in caverna. VI Rassegna Internazionale Elettronica e Nucleare, Rome, June 1959.

[3] T. LEARDINI: Sistemazione in caverna di centrali nucleari. LX Riunione Annuale A.E.I., Venice, Oct. 1959.

[4] M. JAKOB: Heat Transfer. Vol. I, New York, 1949.

[5] W. H. MCADAMS: Heat Transmission, 3rd Edn, New York, 1954.

[6] R. M. ROME, T. R. MOFFETTE: PWR Plant Container Sizing Criteria. WAPD-SC-549, Pittsburgh, 1957.

[7] S. ESLEECK: The Babcock & Wilcox Co., Atomic Energy Division, Lynchburg, Va. Private communication.

Publications by Brown Boveri Authors in Other Journals

EHRENBERG, W.: Frequenzsprünge und Zieherscheinungen an gekoppelten Kreisen. Bull. schweiz. elektrotech. Ver. 1959, No. 21, p. 1009–16.

HÜBNER, R.: Die Goubau-Leitung. Tech. Mitt. schweiz. Post-, Telegr.- u. Teleph.-Verw. 1959, No. 10, p. 453 to 458.

RIEDER, W., and SOKOB, P.: Probleme der Lichtbogendynamik. Sci. elect. 1959, Vol. 3, p. 93–112.

STARKERMANN, R.: Gegenseitige Beeinflussung der Regelgrössen in Mehrkreissystemen; ein Beispiel. Regelungstechnik 1959, No. 9, p. 301–6.

STEINER, G.: Moderne Lichtbogen-Schmelzofenanlagen. Tech. suppl. to Neue Zürcher Ztg of 21st Oct. 1959.

ZWAHLEN, R.: Elementare Biegeschwingungstheorie, entwickelt an Hand eines einfachen Beispiels. Tech. Rdsch. 16th Oct. 1959.

Our Thermal Products

Steam and Gas-Turbine Sets
for public and industrial supply

Complete Steam Power Stations

Complete Gas-Turbine Plants
stationary and mobile

Atomic Power Stations and Accessories

Velox and Electric Boilers

Boiler-House Auxiliaries

Exhaust-Gas Turbochargers
for all sizes of two and four-stroke diesel engines

Turbo-Compressors
centrifugal and axial, for use with all gaseous media, for propulsion by gas or steam turbine

Gears

Marine Material
especially marine propulsion turbines and gears

Supersonic Wind Tunnels

High-Altitude Test Plants for Aircraft Engines

Refrigeration Compressors (Frigiblocs)

Published by Brown, Boveri & Company, Limited, Baden, Switzerland. Printed by Kreis & Co. AG., Basle, Switzerland.
Obtainable direct from the publishers.